

CZECH TECHNICAL UNIVERSITY IN PRAGUE
Faculty of Electrical Engineering
Department of Control Engineering
K13135

Diploma Thesis
X35DP

Combustion Engine Model Identification



České vysoké učení technické v Praze
Fakulta elektrotechnická

Katedra řídicí techniky

ZADÁNÍ DIPLOMOVÉ PRÁCE

Student: **Bc. Libor Ptáček**

Studijní program: Elektrotechnika a informatika (magisterský), strukturovaný
Obor: Kybernetika a měření, blok KM1 - Řídicí technika

Název tématu: **Identifikace modelu spalovacího motoru**

Pokyny pro vypracování:

Seznamte se s fyzikálním popisem spalovacího motoru zejména s ohledem na proces spalování a emise. Najděte stupně zjednodušení vhodné pro tvorbu simulačních modelů použitelných pro návrhy řídicích systémů.

Na příkladu analyzujte numerické vlastnosti modelu a jeho řešitelnost. Srovnajte různé parametrizace z hlediska numerické stability a tuhosti (angl. stiffness) rovnic. Pokuste se nalézt nejlepší parametrizaci.

Vyzkoušejte numerické metody kalibrace modelu na základě změřených dat a ověřte věrnost takového modelu v ustáleném stavu i během přechodových dějů v celém pracovním rozsahu.

Seznam odborné literatury:

J. B. Heywood, Internal Combustion Engine Fundamentals, McGraw Hill, 1988 (několik reedic).

C. F. Taylor, Internal Combustion Engine in Theory and Practice, The MIT Press, 1985 (několik reedic).

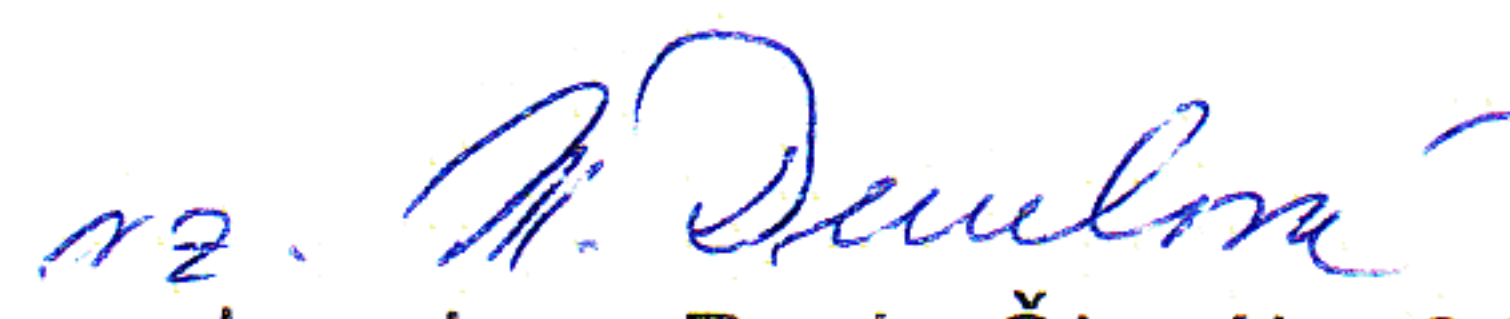
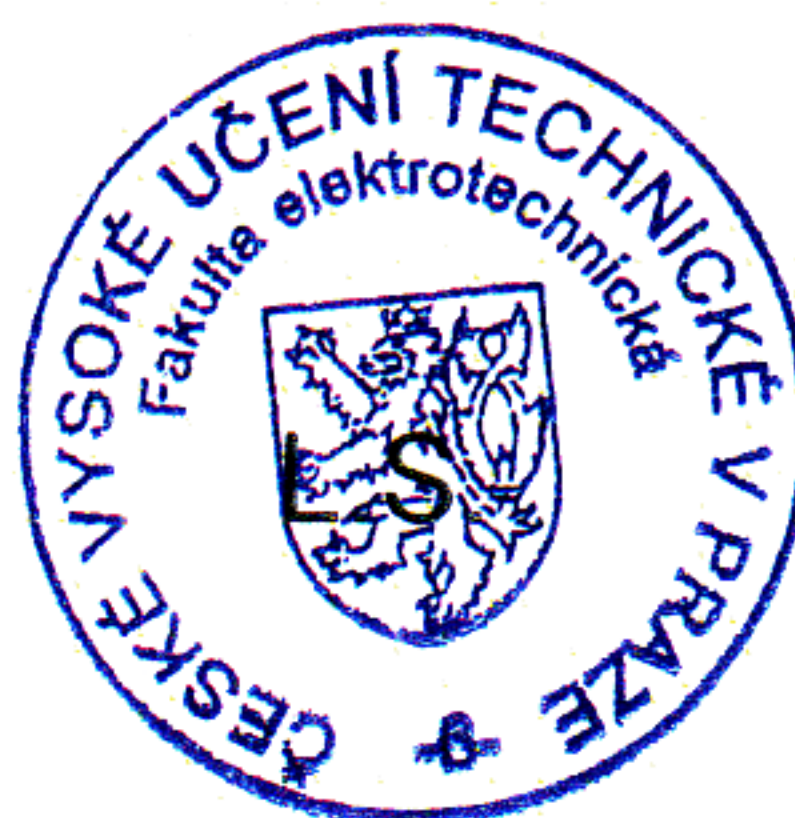
L. Guzzella, C. H. Onder, Introduction to modeling and control of internal combustion engine systems, Springer, 2004.

Vedoucí: Prof. Ing. Vladimír Havlena, CSc.

Platnost zadání: do konce letního semestru 2010/2011



prof. Ing. Michael Šebek, DrSc.
vedoucí katedry



doc. Ing. Boris Šimák, CSc.
děkan

V Praze dne 30. 10. 2009



Affidavit

I declare that this thesis is my own work and I used only the materials (literature, projects, SW, etc.) quoted in the attached reference list.

In Prague, 14th May, 2010

.....
Signature



Abstract

This diploma thesis will focus on the turbocharged combustion engine. Its aim is to verify and modify a computer model (a block library for model creation) of the specific combustion engine for the advanced controller design based on the models (MPC).

The combustion engine is a complicated system described by various physical laws and in order to develop its model it is necessary to find suitable ways of a simplification. The simplification must preserve important characteristics of the control and controlled quantities.

The block library of the engine simulation is based on the Matlab S-Function or more precisely on Matlab's simulation environment called Simulink. After connection of all blocks according to the technological scheme it is necessary to fit the parameters using data provided by an engine manufacturer.

There is a serious problem with numerical instability of the simulation caused by the nonlinear stiff equations describing the whole engine. Constrained state reduction is used to dealing with these problems.



Anotace

Tato práce je zaměřena na problematiku spalovacích přeplňovaných motorů. Jejím cílem je ověření a úprava počítačového modelu (knihovny bloků pro vytvoření modelu) spalovacího motoru pro konkrétní motory za účelem návrhu pokročilých regulátorů založených právě na modelech (MPC).

Spalovací motor je složitý systém popsáný různými fyzikálními zákony a pro vytvoření modelu je nutné nalézt vhodné způsoby zjednodušení. Zjednodušení však musí zachovat důležité vlastnosti týkající se regulačních a regulovaných veličin.

Knihovna bloků pro simulaci spalovacího motoru je vytvořena jako soubor S-funkcí v Matlabu, resp. v jeho simulačním prostředí Simulink. Je vytvořena tak, aby vytvořené simulační schéma motoru odpovídalo technologickému nákresu. Po zapojení jednotlivých bloků je nutné provést jejich kalibraci pomocí dat dodaných výrobcem motoru.

Velkým problémem při simulaci je numerická nestabilita způsobena nelineárními „tuhými“ rovnicemi popisující motor. Odstranění těchto problému je provedeno pomocí redukce stavů nalezeného modelu.



Acknowledgements

I would like to express my gratitude to my supervisor prof. Ing. Vladimír Havlena, CSc. for his patience and effective advice throughout the process of writing the thesis.

I would also like to thank my parents and my family for their support during my studies and my whole life.

Finally, my thanks go to my friends, schoolmates and colleagues who supported and encouraged me during my work on the thesis.



Contents:

1. INTRODUCTION.....	9
1.1. Electronic Control Unit.....	10
1.2. Spark Ignition (Petrol) Engine	11
1.3. Compression Ignition (Diesel) Engine	11
2. MAIN ENGINE PARTS	14
2.1. Compressor, Turbine (Turbocharger).....	14
2.1.1. Compressor	17
2.1.2. Turbine	19
2.2. Intercooler.....	20
2.3. Exhaust gas recirculation (EGR)	21
2.4. Wastegate	21
2.5. Cylinders and Combustion	21
3. ENGINE MODEL LIBRARY.....	23
3.1. Auxiliary blocks.....	26
3.1.1. Auxiliary manifold.....	26
3.1.2. Valve.....	26
3.1.3. Flow Restrictions	27
3.1.4. Mix	28
3.1.5. Flow Splitter	29
3.2. Engine	30
3.2.1. Intake Manifold	31
3.2.2. Exhaust Manifold	32
3.2.3. Volumetric Pump	33
3.2.4. Combustion.....	34
3.3. Turbocharger	35
3.3.1. Rotating shaft.....	35
3.3.2. Compressor	36
3.3.3. Turbine	37
3.4. Heat Exchanger.....	39
4. MODEL VERIFICATION	40
5. STIFFNESS AND NONLINEARITY.....	46
5.1. Singular Perturbation Theory	49
5.2. Constrained State Reduction	50
6. CONCLUSION	57
7. REFERENCES.....	59



8. APPENDIX	61
8.1. Six-cylinder Bi-turbocharged Engine – Gain and Time Constant.....	61
8.2. Four-cylinder Turbocharged Engine – Constrained State Reduction	81
8.3. Six-cylinder Bi-turbocharged Engine – Constrained State Reduction.....	84



1. Introduction

Nowadays, automotive industry invests a lot of money into research and development of new combustion engine types. The main goal is to lower fuel consumption and gas emissions. Engine manufacturers have to obey strict emission limits declared in European and American legislative. The time progress for emission limits of NO_x and particulate matter (PM) of heavy duty truck and bus engines is shown in Fig. 1.1. Limits for standard diesel and gas engines are even stricter. Exact limits for standard and for heavy duty diesel engines respectively are mentioned in [1].

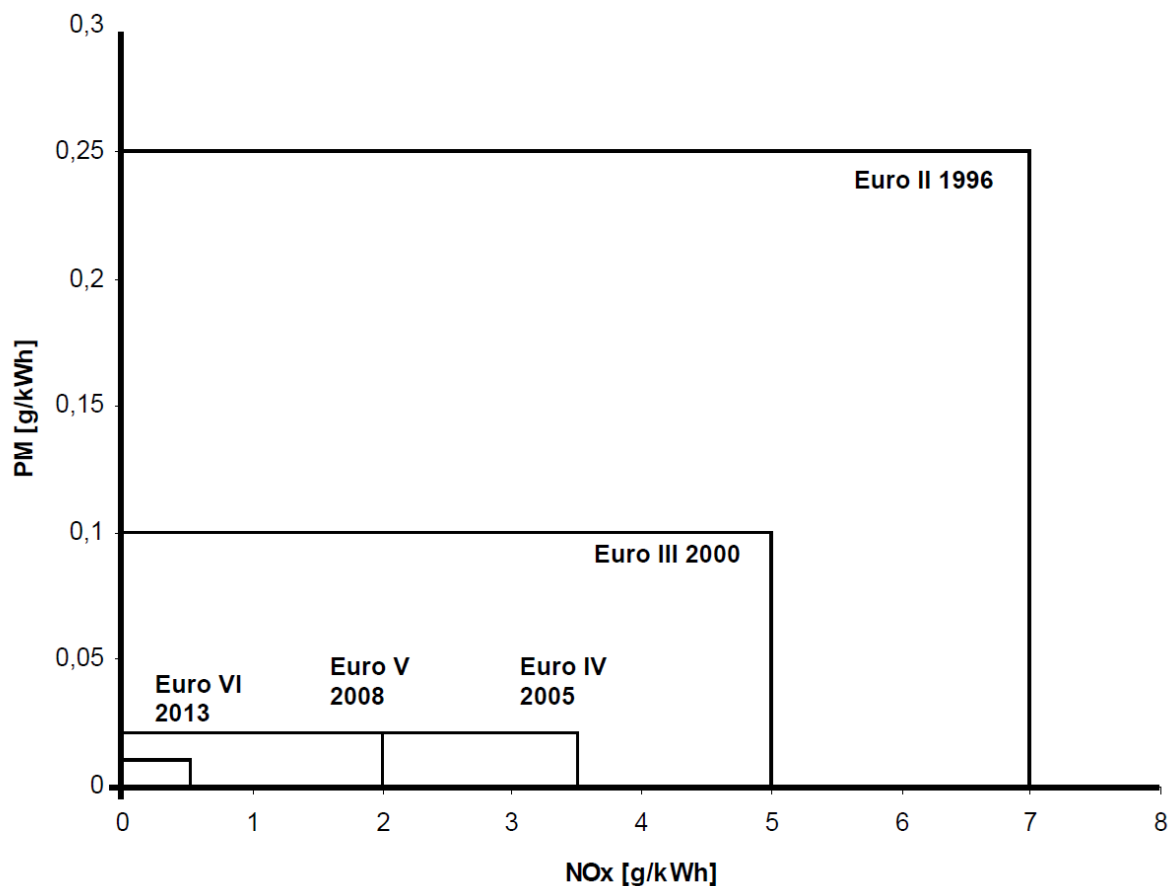


Fig. 1.1 – Emission limits for heavy duty diesel truck and bus engines

Euro III emission limits have been achieved by higher injection pressure. It is more difficult to reach the level of Euro IV and Euro V limits. To fulfill the limits, car producers use cooled exhaust gas recirculation (EGR), selective catalytic reduction



(SCR) or both methods. EGR also lowers fuel consumption in spark ignition engines. It has not been announced yet how to achieve the Euro VI stage for heavy duty (only a very few standard diesel engines conform to this standard) but car producers are close to announcing and producing an engine for Euro VI.

Use of the computer and mathematical engine models is a cheaper and more useful way when developing new engine types. Mathematical modelling lowers the price and the time spent on the development. Of course, it is not possible to produce a new engine without classical models and a lot of testing on the prototypes. By using computer modeling, engineers gather lots of test results in real-time without the necessity of building a fully working prototype. These models are based on the physical principles (mostly differential equations) of the engine combustion and the following exhaust flow. This thesis is concerned with control oriented models and their usage for controller design. New types of control methods (MPC, etc.) require process model.

There are differences between a spark ignition engine and a diesel engine that are described in more detail in section 1.3.

1.1. Electronic Control Unit

The classical mechanical parts are replaced by electronics in modern cars. The main part of the electronics is the electronic control unit (ECU). It does not matter whether a car has a spark ignition, a diesel or an electric engine. The ECU controls everything in the car, i. e. combustion, engine, wheels, brakes, ABS, air conditioning, etc.

Combustion is controlled by PID controllers with varying parameters that depend on the engine mode (engine speed, fuel injection quantity, NO_x concentration, acceleration, etc. Finding tables of PID parameters is very expensive and this way of control is not optimal. Model based control design is one of the ways how to improve control of the combustion and to lower emissions, fuel consumption and cost of the controller design.

1.2. Spark Ignition (Petrol) Engine

Spark ignition engines are mainly used in light-weight passenger cars. Otto's process permits purification of exhaust gases with high efficiency. Nowadays these engines use three-way catalytic converters and a direct injection as they produce very little particulate matter. Typical configuration of this engine type is in Fig. 1.2.

A torque of a stoichiometric spark ignition engine depends on the amount of the air/fuel mixture (air/fuel ratio remains constant) in the cylinders. This amount is changed by the intake pressure and the air/fuel density. New engines use electronic throttle control, variable valve timing, turbocharger etc. for better fuel efficiency and reduced emissions.

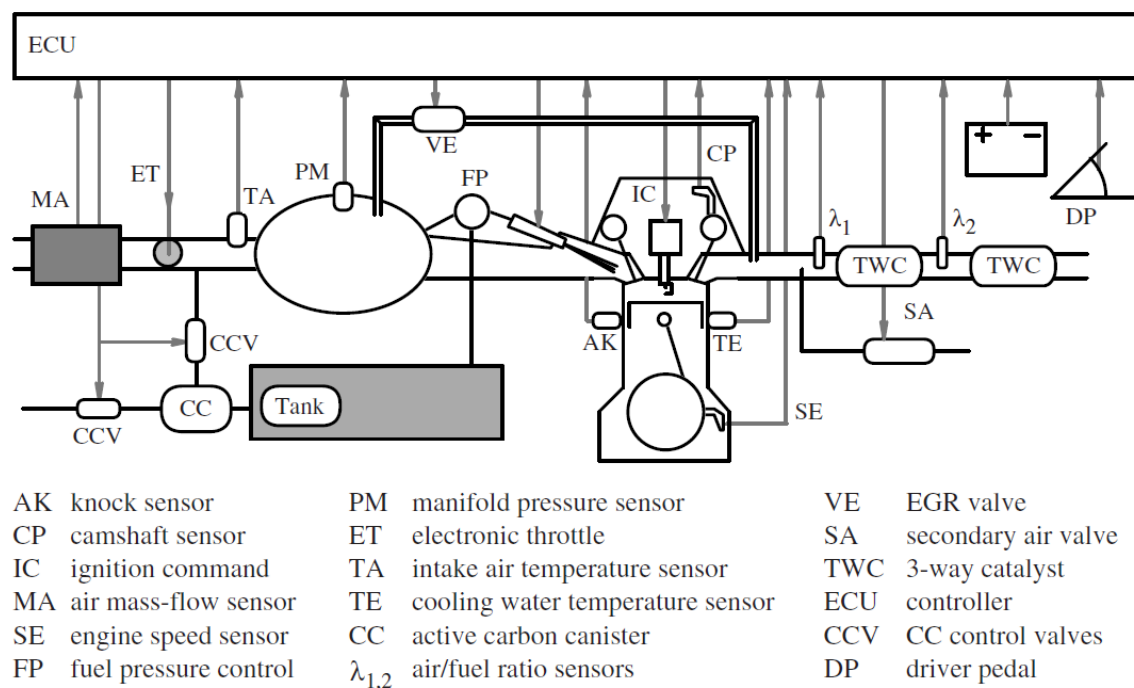
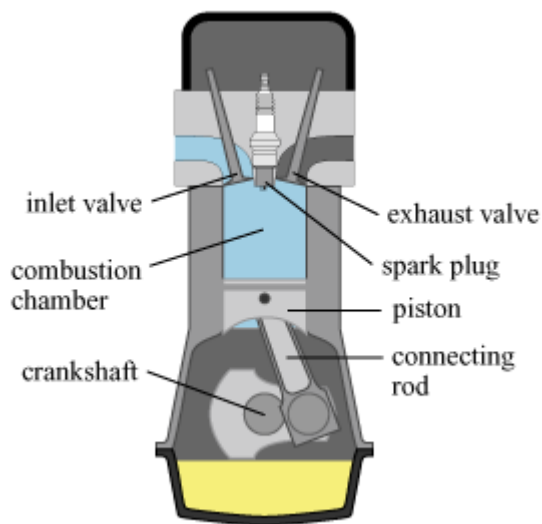


Fig. 1.2 – A typical configuration of a spark ignition engine (reprinted from [1])

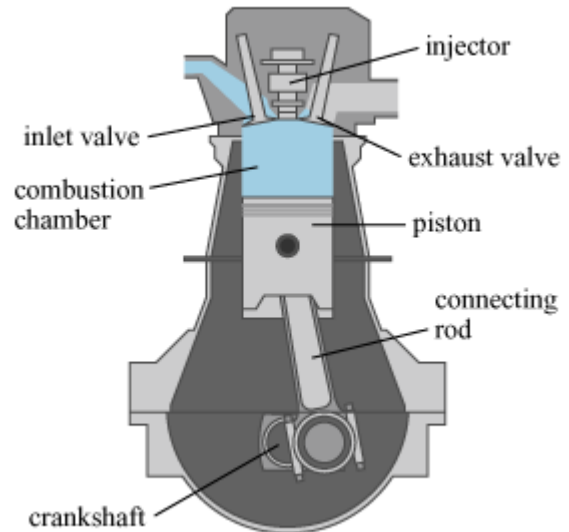
1.3. Compression Ignition (Diesel) Engine

The main difference between a diesel and a spark ignition engine is in the combustion process (Fig. 1.3). The diesel engine compresses the air in the combustion chamber and rather than using a spark plug, it injects the fuel to start the ignition to burn the fuel. Diesel engines have a better fuel efficiency than spark

ignition engines but they are more pollutant. Most of these engines are turbocharged with the direct injection (a replacement for a pre-chamber injection) or with the integrated pump injectors (common-rail system).



Spark Ignition Engine



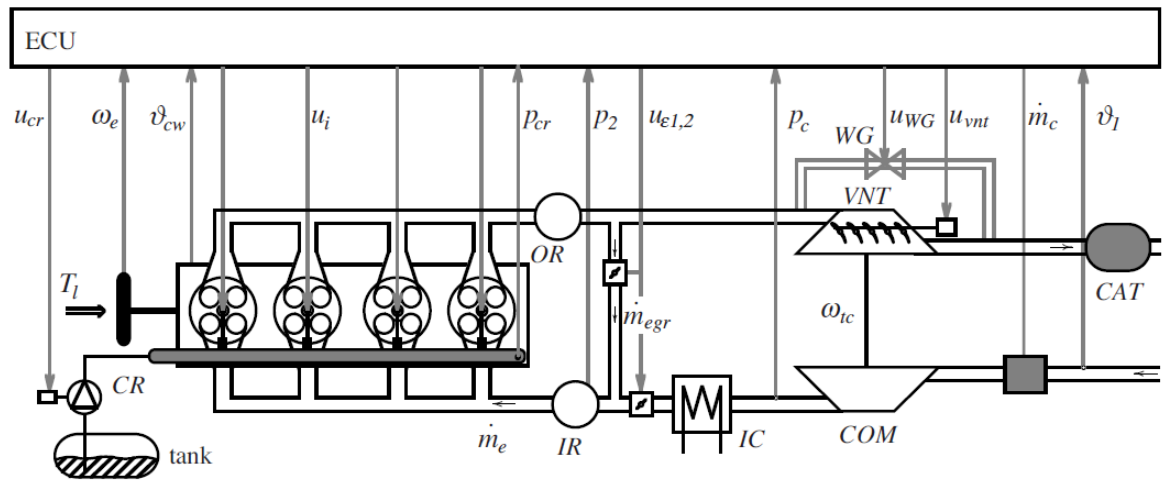
Diesel Engine

Fig. 1.3 – Differences between a spark ignition and a diesel engine (reprinted from [4])

An electronic control system of the diesel engine has to provide the required torque combined with a minimal fuel consumption and low emissions and noise. These requirements are achieved by using an exhaust gas recirculation, a turbocharger and an optimal injection control.

Application of new after treatment systems, e.g. selective catalytic reduction (SCR), particulate matter filters, exhaust gas recirculation (EGR) rates, etc. reduces the emissions.

A typical diesel engine configuration is shown in Fig. 1.4.



CAT	oxidation catalytic converter	$u_{\epsilon 1,2}$	EGR valve(s) command	p_c	pressure after COM
COM	compressor	u_{cr}	CR pump command	p_2	intake pressure
CR	common-rail system	u_i	injection command	p_{cr}	CR injection pressure
IR	intake receiver	u_{vnt}	turbine nozzle command	\dot{m}_c	intake air mass flow
OR	outlet receiver	u_{wg}	WG command	ϑ_I	intake air temperature
IC	intercooler	T_l	load torque at the flywheel	ϑ_{cw}	cooling water temperature
VNT	variable nozzle turbine	ω_{tc}	turbocharger speed	ω_e	engine speed
WG	waste-gate (alternative to VNT)	\dot{m}_e	total engine-in mass flow	\dot{m}_{egr}	exhaust gas recirculation

Fig. 1.4 – A typical configuration of a diesel engine (reprinted from [1])



2. Main Engine Parts

The whole engine can be divided into several parts. This chapter provides description of the main parts.

2.1. Compressor, Turbine (Turbocharger)

The maximum power of an engine is limited by the maximum burned fuel. In order to burn more fuel, it is necessary to deliver more air into the cylinders. The more air is compressed, the more air can be injected into the cylinder. Mechanical/electrical turbochargers or mechanical superchargers are used to compress the air. A supercharger compresses the air using a separate pump or a compressor driven by the engine power. A turbocharger consists of a compressor and a turbine held together by a single shaft. Energy of the exhaust gas drives the turbine, which is through one shaft connected to a compressor. That raises an inlet air density. Nowadays, some other methods are used to get extra air into the cylinder, e.g. a second turbine in the exhaust pipe directly connected to the engine drive shaft, a heat exchanger (called intercooler/aftercooler), a two-stage turbocharging or combination of these methods.

Applying the first and the second thermodynamic law to the control volume around the turbine gives us the work necessary to drive the compressor (1), where $\dot{Q} [\text{J} \cdot \text{s}^{-1}]$ is the heat transfer rate into the control volume, $\dot{W} [\text{J} \cdot \text{s}^{-1}]$ is the shaft work transfer rate out of the control volume, $\dot{m} [\text{kg} \cdot \text{s}^{-1}]$ is the mass flow rate, $h [\text{J} \cdot \text{kg}^{-1}]$ is the specific enthalpy, $\frac{C^2}{2} [\text{J} \cdot \text{kg}^{-1}]$ is the specific kinetic energy and $gz [\text{J} \cdot \text{kg}^{-1}]$ is the specific potential energy (can be omitted).

$$\dot{Q} - \dot{W} = \dot{m} \left[\left(h + \frac{C^2}{2} + gz \right)_{\text{out}} - \left(h + \frac{C^2}{2} + gz \right)_{\text{in}} \right] \quad (1)$$

Enthalpy-entropy diagrams for a compressor and for a turbine are expressed in Fig. 2.2, where 1, 3, 01, 03 are inlet states and 2, 4, 02, 04 are exit states. 01, 02, 03, 04 are stagnation (total) states. The pressure of the stagnation state is the

pressure at which the fluid comes to rest. 1, 2, 3, 4 are the static states. The pressure of the static state is the pressure at the nominated point of the fluid.

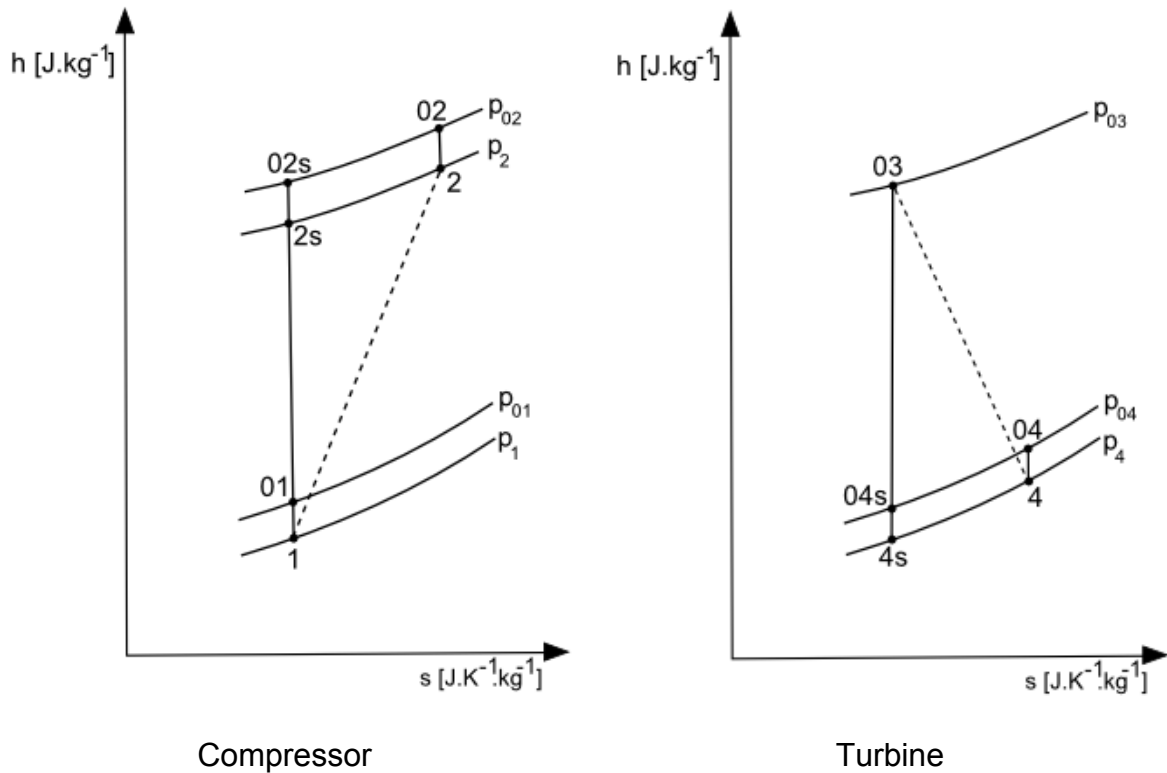


Fig. 2.1 – An enthalpy-entropy diagram (reprinted from [5])

The total or the stagnation temperature of the ideal gas T_0 [K] is described in (2), where c_p [$\text{J} \cdot \text{kg}^{-1}$] denotes the specific heat at constant pressure.

$$T_0 = T + \frac{C^2}{2c_p} \quad (2)$$

The total or the stagnation pressure p_0 [Pa] is defined in (3), where γ is the specific heat ratio ($\frac{c_v}{c_p}$, c_v [$\text{J} \cdot \text{kg}^{-1}$] is the specific heat at constant volume). The pressure is attained if the gas isentropically comes to rest.



$$p_0 = p \left(\frac{T_0}{T} \right)^{\frac{\gamma}{\gamma-1}}. \quad (3)$$

The stagnation or the total specific enthalpy h_0 [J.kg⁻¹] is expressed by (4)

$$h_0 = h + \frac{C^2}{2}. \quad (4)$$

By using expression (4) and neglecting the transfer heat rate \dot{Q} , we obtain the work transfer rate in the following form

$$-\dot{W} = \dot{m}(h_{0,\text{out}} - h_{0,\text{in}}). \quad (5)$$

The actual work transfer and the required (produced) work transfer ratio (an equivalent reversible adiabatic device operating under the same pressures) is called the compressor isentropic efficiency η_c [-]

$$\eta_c = \frac{\text{reversible_power_requirement}}{\text{actual_power_requirement}}. \quad (6)$$

The total-to-total compressor isentropic efficiency of gas processes $\eta_{c,\text{TT}}$ [-] in Fig. 2.1 is described by equation (7). The specific enthalpy should be replaced by the temperature because the specific heat at constant pressure c_p is essentially constant for an air or air-fuel mixture.

$$\eta_{c,\text{TT}} = \frac{h_{02s} - h_{01}}{h_{02} - h_{01}} = \frac{T_{02s} - T_{01}}{T_{02} - T_{01}}. \quad (7)$$

The subscript 1 stands for the inlet state, the subscript 2 for the exit state and the subscript s for the equivalent isentropic compressor state.



2.1.1. Compressor

By using (3) and (7), the work transfer rate \dot{W}_C [$\text{J} \cdot \text{s}^{-1}$] (power) required to drive the compressor is (the subscript i means inlet, the subscript C means compressor):

$$-\dot{W}_C = \dot{m}_C c_{p,i} (T_{02} - T_{01}) = \frac{\dot{m}_C c_{p,i} T_{01}}{\eta_{C,TT}} \left[\left(\frac{p_{02}}{p_{01}} \right)^{\frac{\gamma-1}{\gamma}} - 1 \right]. \quad (8)$$

Because of problems with recovering the gas kinetic energy, the pressure p_2 [Pa] is used instead of the pressure p_{02} [Pa]. When considering the mechanical losses in the compressor (η_m [-] compressor mechanical efficiency) and when using $\eta_{C,TS}$ [-] total-to-static compressor efficiency (better approximation for the real data), the work transfer rate to drive compressor $\dot{W}_{C,D}$ [$\text{J} \cdot \text{s}^{-1}$] is:

$$-\dot{W}_{C,D} = \frac{\dot{m}_C c_{p,i} T_{01}}{\eta_{C,TS} \eta_m} \left[\left(\frac{p_2}{p_{01}} \right)^{\frac{\gamma}{\gamma-1}} - 1 \right], \quad \eta_{C,TS} = \frac{\left(\frac{p_2}{p_{01}} \right)^{\frac{\gamma-1}{\gamma}} - 1}{\frac{T_{02}}{T_{01}} - 1}, \quad (9)$$

$$T_{02} = \left(1 + \frac{\left(\frac{p_2}{p_{01}} \right)^{\frac{\gamma}{\gamma-1}} - 1}{\eta_{C,TS}} \right) T_{01} \quad (10)$$

For simulation and for a practical usage, it is important to know the corrected compressor speed $N_{C,cor}$ [rpm] and the corrected mass flow rate $\dot{m}_{C,cor}$ [kg^{-1}] (the subscript *ref* stands for the standard atmospheric). A relation between the mass flow rate and the pressure ratio is given by the compressor operating map (Fig. 2.2.). The corrected values of the speed, the mass flow rate at certain pressure and the temperature ratios are used.

$$N_{C,cor} = N_C \sqrt{\left(\frac{T_{ref}}{T_{0,i}}\right)}, \dot{m}_{C,cor} = \dot{m}_C \left(\frac{p_{ref}}{p_{0,i}}\right) \sqrt{\left(\frac{T_{0,i}}{T_{ref}}\right)}. \quad (11)$$

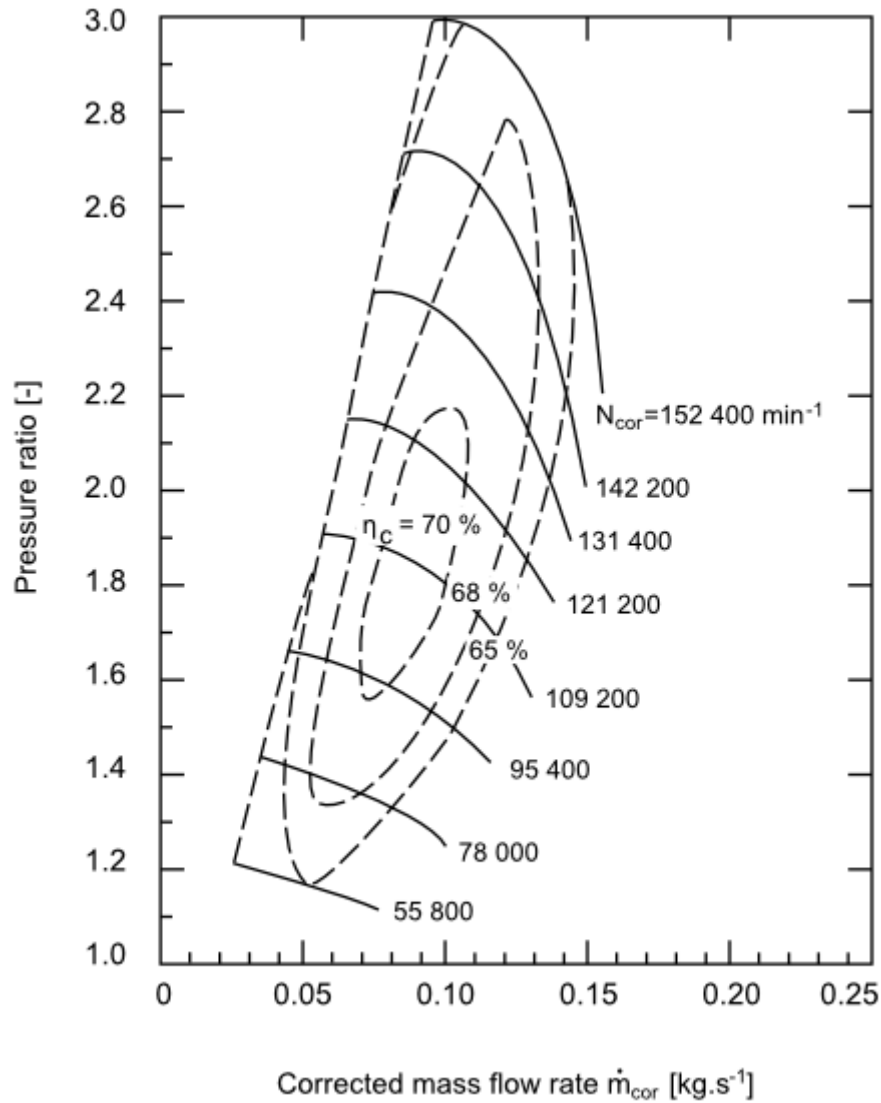


Fig. 2.2 – Centrifugal compressor operating map (reprinted from [5])

The reference mass flow rate depends on two dimensionless parameters – the head parameter Ψ [-] (12) and the normalized compressor flow rate Φ [-] (13), where the subscript i corresponds to the inlet, the subscript e to the exit, d_c [m] stands for the compressor wheel diameter, and ρ_a [kg · m⁻³] for the ambient air specific mass.



The normalized compressor flow rate is approximated by (13) – the k_i [-] parameters can be determined from the acquired data.

$$\Psi = \frac{c_p T_{\text{ref}} \left[\left(\frac{p_e}{p_{0,i}} \right)^{\frac{\gamma-1}{\gamma}} - 1 \right]}{\frac{1}{2} U_c^2}, U_c = \frac{\pi}{60} d_c N_{C,\text{cor}}, \quad (12)$$

$$\Phi = \frac{\dot{m}_{C,\text{cor}}}{\rho_a \frac{\pi}{4} d_c^2 U_c}, \Phi = \frac{k_3 \Psi - k_1}{\Psi + k_2}. \quad (13)$$

2.1.2. Turbine

The formula for the power delivered by a turbine is analogical to the formula for the power consumed by a compressor. It only differs in the “opposite direction” of the air flow (the subscript e means the exit). The quantity $\eta_{T,\text{TT}}$ [-] is the turbine total-to-total isentropic efficiency, $\eta_{T,\text{TS}}$ [-] is the turbine total-to-static efficiency. The quantity \dot{W}_T [$\text{J} \cdot \text{s}^{-1}$] represents the turbine work transfer rate. The quantity BSR [-] stands for the blade speed ratio and it is used to determine the turbine efficiency. It is a ratio that matches the blade speed U [$\text{m} \cdot \text{s}^{-1}$] and the velocity equivalent of the gas isentropic drop C_s [$\text{m} \cdot \text{s}^{-1}$] across the turbine stage:

$$\eta_{T,\text{TT}} = \frac{h_{03} - h_{04}}{h_{03} - h_{04s}} = \frac{T_{03} - T_{04}}{T_{03} - T_{04s}} = \frac{1 - \frac{T_{04}}{T_{03}}}{1 - \left(\frac{p_{04}}{p_{03}} \right)^{\frac{\gamma-1}{\gamma}}}, \quad (14)$$



$$\dot{W}_T = \dot{m}_T c_{p,e} T_{03} \eta_{T,TS} \left[1 - \left(\frac{p_{04}}{p_{03}} \right)^{\frac{\gamma_e - 1}{\gamma_e}} \right], \quad \eta_{T,TS} = \frac{1 - \frac{T_{04}}{T_{03}}}{1 - \left(\frac{p_4}{p_{03}} \right)^{\frac{\gamma - 1}{\gamma}}}, \quad (15)$$

$$N_{T,cor} = N_T \sqrt{\left(\frac{T_{ref}}{T_{0,i}} \right)}, \quad \dot{m}_{T,cor} = \dot{m}_T \left(\frac{p_{ref}}{p_{0,i}} \right) \sqrt{\left(\frac{T_{0,i}}{T_{ref}} \right)}, \quad (16)$$

$$BSR = \frac{U}{C_s} = \frac{\frac{\pi}{60} d_T N_{T,cor}}{\sqrt{2 c_p T_{ref} \left[1 - \left(\frac{p_e}{p_i} \right)^{\frac{\gamma - 1}{\gamma}} \right]}}. \quad (17)$$

There is a mechanical linkage between the turbine and the compressor in the engine (a turbocharger, to be precise). The work transfer rate $-\dot{W}_C$ [J · s⁻¹] (18) under the condition of the constant turbocharger speed, where η_m [-] denotes the turbocharger mechanical efficiency, is

$$-\dot{W}_C = \eta_m \dot{W}_T. \quad (18)$$

2.2. Intercooler

An intercooler is simply a heat exchanger between a turbocharger and an engine inlet. It cools down the compressed air and increases the air density to allow to inject more air into the intake manifold. A physical relation between the inlet gas temperature T_i [K] and the outlet gas temperature T_o [K] is linearized (for the mass flow approaching 0) in (19), where $\eta_{1,2}$ [-] are the heat transfer coefficients (represent the heat exchanger effectiveness), the quantity T_c [K] stands for the cooling medium temperature and \dot{m} [kg · s⁻¹] denotes the cooled medium mass flow.



$$T_o = T_i - (\eta_1 \dot{m} + \eta_2)(T_i - T_c) \quad (19)$$

2.3. Exhaust gas recirculation (EGR)

EGR is mainly used to reduce NO_x emissions. EGR puts the portion of the exhaust gases back into the intake manifold.

EGR used with the spark ignition engines increases the specific heat capacity which lowers an adiabatic flame temperature. There is 5 – 15 % exhaust gases routed back into cylinders. More exhaust gases can cause misfires or partial burns. EGR also slows down the combustion. The main procedure how to increase the engine efficiency via EGR is to reduce the throttling losses, the heat rejection, the chemical dissociation and the specific heat ratio.

EGR is also used in diesel engines in order to lower the NO_x emissions and to improve the combustion efficiency. Exhaust gases are cooled before they are routed into the intake manifold. On one hand it lowers the combustion temperature just like in the spark ignition engine and on the other it increases the quantity of particular matter in the exhaust gases. Particular matter has to be reduced by the particular matter filters.

2.4. Wastegate

A wastegate diverts exhaust gases out of the turbocharger (i.e. turbine) to control the speed of the turbine. Because of the linkage between a turbine and a compressor, the compressor speed is controlled simultaneously. The wastegate is primarily designed to control the boost pressure in the turbocharger. There are several types of the wastegate configuration (external/internal) and different types of control (pneumatic/electronic).

2.5. Cylinders and Combustion

Engine power is generated by the fuel combustion in cylinders. The description of these processes is determined by the first and the second thermodynamic law, the stoichiometric relation during the fuel-air combustion, the energy conservation law and a few other physical laws. For the model based control,



it is not necessary to describe the whole process in detail (see [5], [6]). It is essential to know the induced engine mass flow and the exhaust gas temperature. The induced mass flow \dot{m} [$\text{kg} \cdot \text{s}^{-1}$] is described in (20), where the quantity η_v [–] stands for volumetric efficiency, N [rpm] for engine speed, V [m^3] for engine displacement, p_i [Pa] for inlet gas pressure, T_i [K] for inlet gas temperature and R [$\text{J} \cdot \text{K}^{-1} \cdot \text{mol}^{-1}$] for gas constant,

$$\dot{m} = \eta_v \frac{N}{60} \frac{1}{2} \frac{p_i V}{T_i R}. \quad (20)$$

The exhaust gas temperature T_e [K] is described by equation (21) which is derived from thermodynamic laws. The quantity \dot{m}_{fuel} [$\text{kg} \cdot \text{s}^{-1}$] means the fuel mass flow, $H_{\text{fuel},l}$ [$\text{J} \cdot \text{kg}^{-1}$] is the fuel lower heating value, T_{air} [K] is the air temperature, $c_{p,e}$ [$\text{J} \cdot \text{kg}^{-1}$] – the exhaust gas specific heat at constant pressure, $c_{p,\text{air}}$ [$\text{J} \cdot \text{kg}^{-1}$] – the air specific heat at constant pressure, and K [–] is the coefficient that depends on the mass flow, on the engine speed, on the input and the output temperature and on the O_2 concentration. This coefficient is determined by empirical data.

$$T_e = \frac{\frac{\dot{m}_{\text{fuel}}}{\dot{m}}}{\frac{\dot{m}_{\text{fuel}}}{\dot{m}} + 1} \frac{H_{\text{fuel},l}}{c_{p,e}} K + \frac{c_{p,\text{air}}}{c_{p,e} \left(\frac{\dot{m}_{\text{f}}}{\dot{m}} + 1 \right)} T_{\text{air}}. \quad (21)$$



3. Engine Model Library

Engine modelling has one significant problem to be solved. It is a combination of very fast processes (milliseconds) on one side and slow processes (seconds) on the other. A very fast process is the combustion itself (Otto, Diesel). There are quick temperature and pressure changes during this process. On the other hand, there are slow actions and slowly reacting systems such as the gas intake, the gas exhaust system, turbocharger shaft etc. This thesis deals with the “slow” processes; however, the fast actions cannot be completely removed from the modelling. They are modelled as quasi-steady state actions. Systems with high level of differences between time constants are called stiff.

The library has been developed by Honeywell company. I am going to test and modify this library in order to deal with the problems such as stiffness, etc. The whole library is created in Matlab Simulink. Each block is written in ANSI C as a Simulink S-Function and represents a specific component of the combustion engine. These blocks and the whole library are designed to be used for completely different types of engines – small spark ignition or heavy duty diesel engines. An engineer has to feed each component with proper signals. Fig 3.1 presents an illustration of such an input/output engine model. Signals connecting the blocks represent pipes in a real engine. Each signal consists of different vector of values such as pressure, concentrations, temperatures, etc. A specific structure of the vector depends on the block requirements (inputs and outputs of the block).

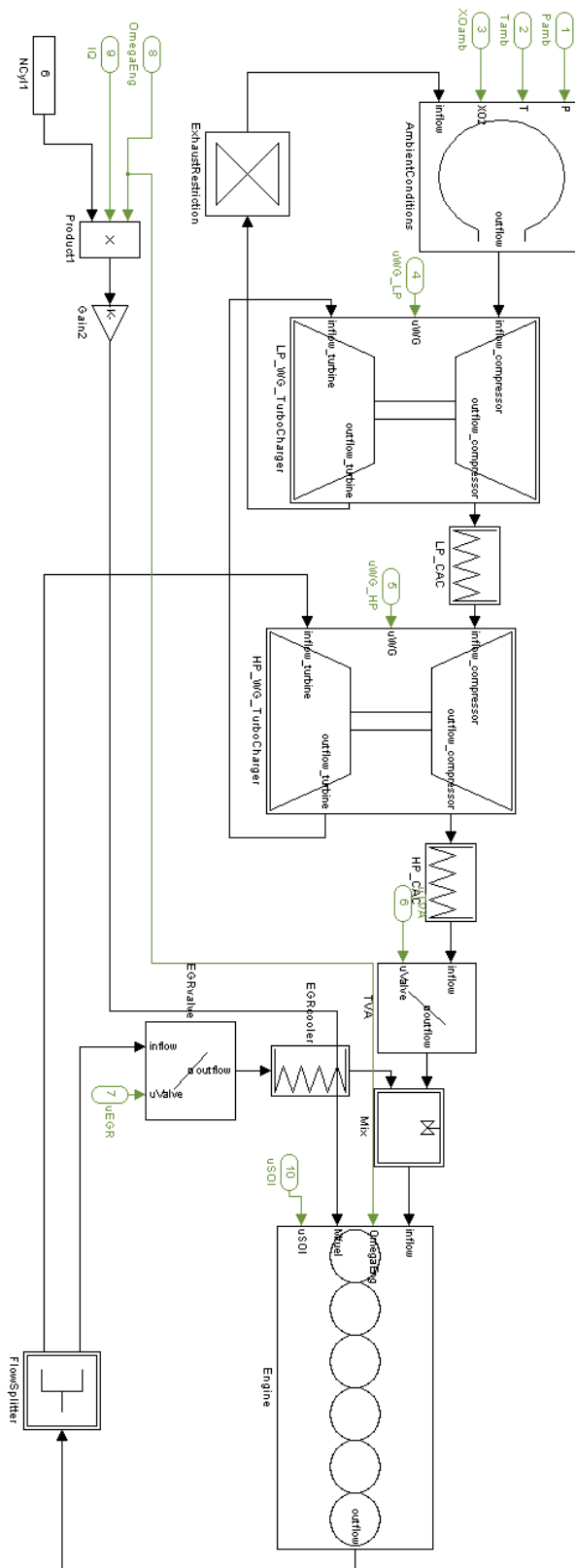


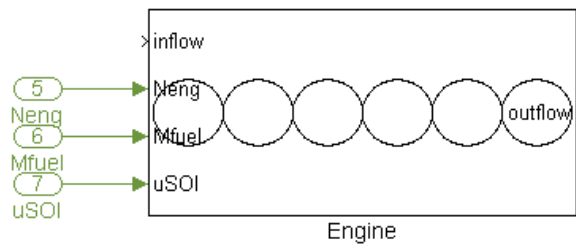
Fig. 3.1 – A diesel engine model overview



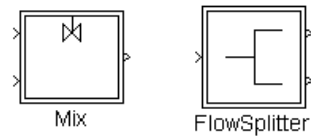
Mean value or discrete event models can be used for modelling and simulation. A mean value model assumes that all actions and effects are distributed throughout the engine cycle. The time is an independent variable in the mean value model. On the other hand discrete event models explicitly take into account the engine behaviour. Crankshaft angle (mostly used at the constant engine speed) is the independent variable in discrete event models.

The library uses SI units for all inputs, outputs and parameters (only the NO_x concentration is in ppm). It makes the application of the library easier and it also eliminates problems with imperial and metric system conversions. A library overview is in the Fig. 3.2.

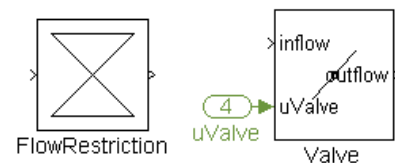
Engine (includes intake and exhaust manifold)



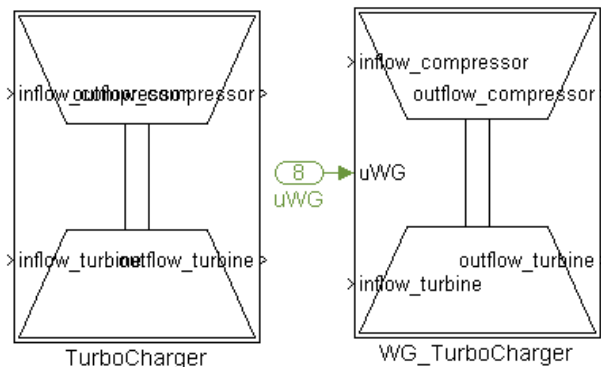
Flow Junction



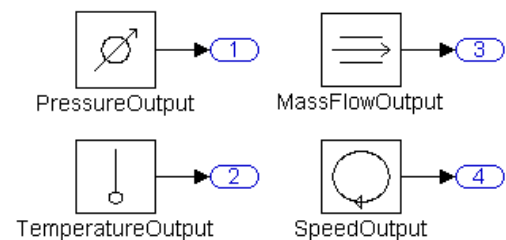
Flow Orifice



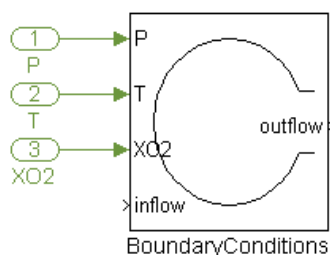
Turbocharger



Signal Output



External Boundary Conditions (e.g. Ambient Conditions)



Heat Exchanger



Fig. 3.2 – A Simulink library overview



3.1. Auxiliary blocks

3.1.1. Auxiliary manifold

This block represents an auxiliary gas reservoir used in the compressor, in the turbine and in the valve block. A gas accumulation in this manifold is modelled as an isothermal process. The isothermal process is chosen in order to eliminate algebraic loops in the model and to reduce system order. The gas pressure p_{aux} [Pa] in this manifold depends on the inlet and on the outlet mass flow \dot{m}_{in} [$\text{kg} \cdot \text{s}^{-1}$], \dot{m}_{out} [$\text{kg} \cdot \text{s}^{-1}$], on the inlet temperature T_{in} [K] and on the manifold's parameters, which is the reservoir volume V [m^3], the gas constant R [$\text{J} \cdot \text{K}^{-1} \cdot \text{mol}^{-1}$], the gas specific heat at constant pressure c_p [$\text{J} \cdot \text{kg}^{-1}$] and at constant volume c_v [$\text{J} \cdot \text{kg}^{-1}$] and the initial pressure p_0 [Pa].

$$\dot{p}_{\text{aux}} = \frac{c_p R T_{\text{in}}}{c_v V} (\dot{m}_{\text{in}} - \dot{m}_{\text{out}}), \text{ where } c_v = c_p - R \quad (22)$$

3.1.2. Valve

This block represents a valve controlled by an external signal. It is an application of the Bernoulli law on the laminar flow. The mass flow \dot{m}_{out} [$\text{kg} \cdot \text{s}^{-1}$] is determined by (23). The inlet temperature T_{in} [K], the inlet pressure p_{in} [Pa], the outlet pressure p_{out} [Pa] and the control signal C_{ctrl} [-] (0 – 1) are inputs of this block. The gas constant R [$\text{J} \cdot \text{K}^{-1} \cdot \text{mol}^{-1}$] and the maximal open valve cross-section A_{max} [m^2] are the parameters describing the valve.

$$\dot{m}_{\text{out}} = A_{\text{max}} C_{\text{ctrl}} \sqrt{2\rho \cdot \Delta p}, \text{ where } \Delta p = p_{\text{in}} - p_{\text{out}}, \rho = \frac{p_{\text{in}}}{RT_{\text{in}}} \quad (23)$$

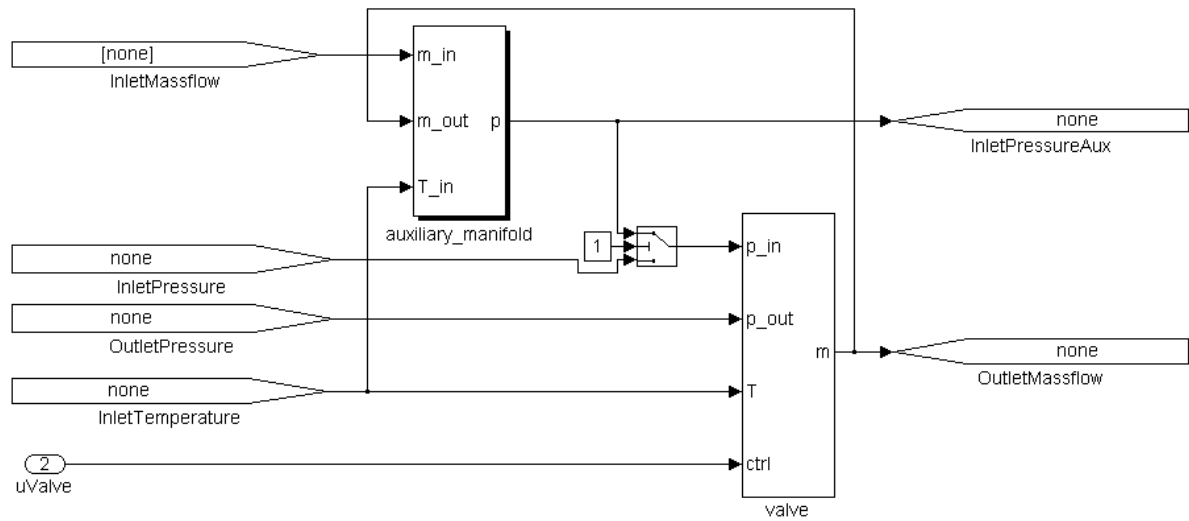


Fig. 3.3 – Valve Simulink block

3.1.3. Flow Restrictions

This block represents gas flow restrictions in an engine. The inlet pressure p_{in} [Pa] and the outlet pressure p_{out} [Pa] are inputs of this block. The output depends on the inlet and the outlet pressure difference, and on two dimensionless block parameters a and b . It is different from the valve block for more accurate modelling of a gas flow (turbulent streaming). The parameters a and b are fitted by using real engine data.

$$m_{out} = \left(\frac{\Delta p}{a} \right)^{\frac{1}{b}}, \text{ where } \Delta p = p_{in} - p_{out}. \quad (24)$$

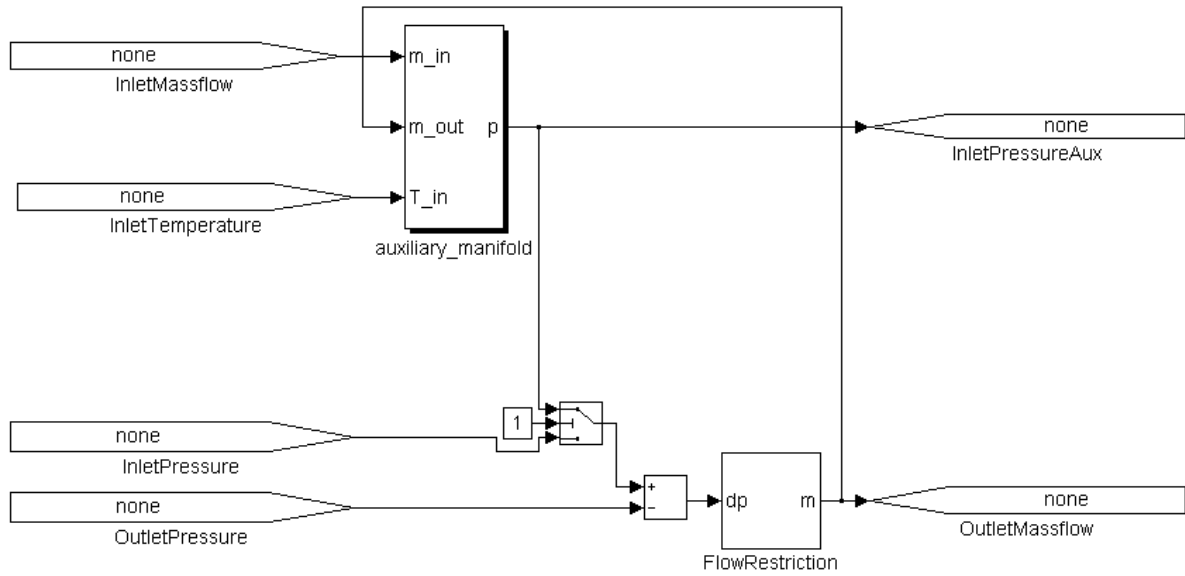


Fig. 3.4 – Flow restrictions Simulink block

3.1.4. Mix

Mixing of two streams is modelled by a mix block. Two inlet streams with their temperatures $T_{i,in}$ [K], pressures $p_{i,in}$ [Pa], mass flows $\dot{m}_{i,in}$ [kg · s⁻¹] and oxygen mass fractions $w_{i,O2,in}$ [-] are inputs. The inputs and the stream specific heat parameters determine the outlet mass flow \dot{m}_{out} [kg · s⁻¹], the outlet temperature T_{out} [K] and the oxygen outlet mass flow $\dot{m}_{O2,out}$ [kg · s⁻¹]. The quantity $c_{p,i,in}$ [J · kg⁻¹] stands for the gas specific heat at constant pressure.

$$\dot{m}_{out} = \dot{m}_{1,in} + \dot{m}_{2,in} , \quad (25)$$

$$T_{out} = \frac{c_{p,1,in} \dot{m}_{1,in} T_{1,in} + c_{p,2,in} \dot{m}_{2,in} T_{2,in}}{c_{p,1,in} \dot{m}_{1,in} + c_{p,2,in} \dot{m}_{2,in}} , \quad (26)$$

$$\dot{m}_{O2,out} = \dot{m}_{1,in} w_{1,O2,in} + \dot{m}_{2,in} w_{2,O2,in} . \quad (27)$$

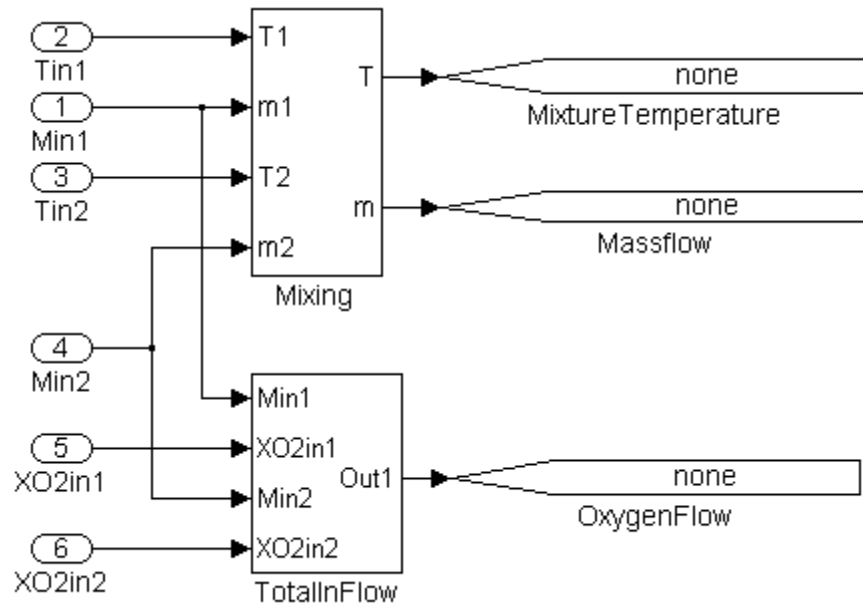


Fig. 3.5 – Mix Simulink block

3.1.5. Flow Splitter

This block separates a stream into two streams (the stream mass flow - $\dot{m}_{i,out}$ [kg · s⁻¹]). Mass flow ratio of the separated streams is determined by pressure differences and mass flows in the blocks to which these streams flow. While respecting boundary condition, we obtain equation (28).

$$\dot{m}_{in} = \dot{m}_{1,out} + \dot{m}_{2,out} \quad (28)$$

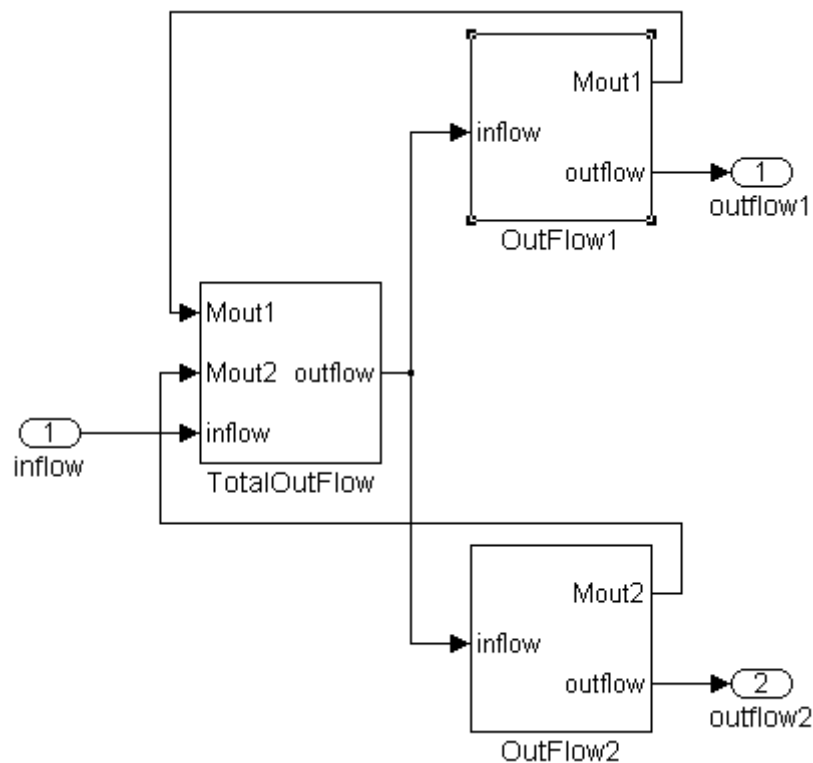


Fig. 3.6 – Flow splitter Simulink block

3.2. Engine

A block for modelling an engine consists of a few smaller blocks connected through several signals. A whole block with sub blocks is in Fig. 3.7. Smaller blocks are the intake and the exhaust manifold (modelling of the air reservoir before and after the engine), the volumetric pump (the movement of the cylinders) and the combustion (the fuel combustion).

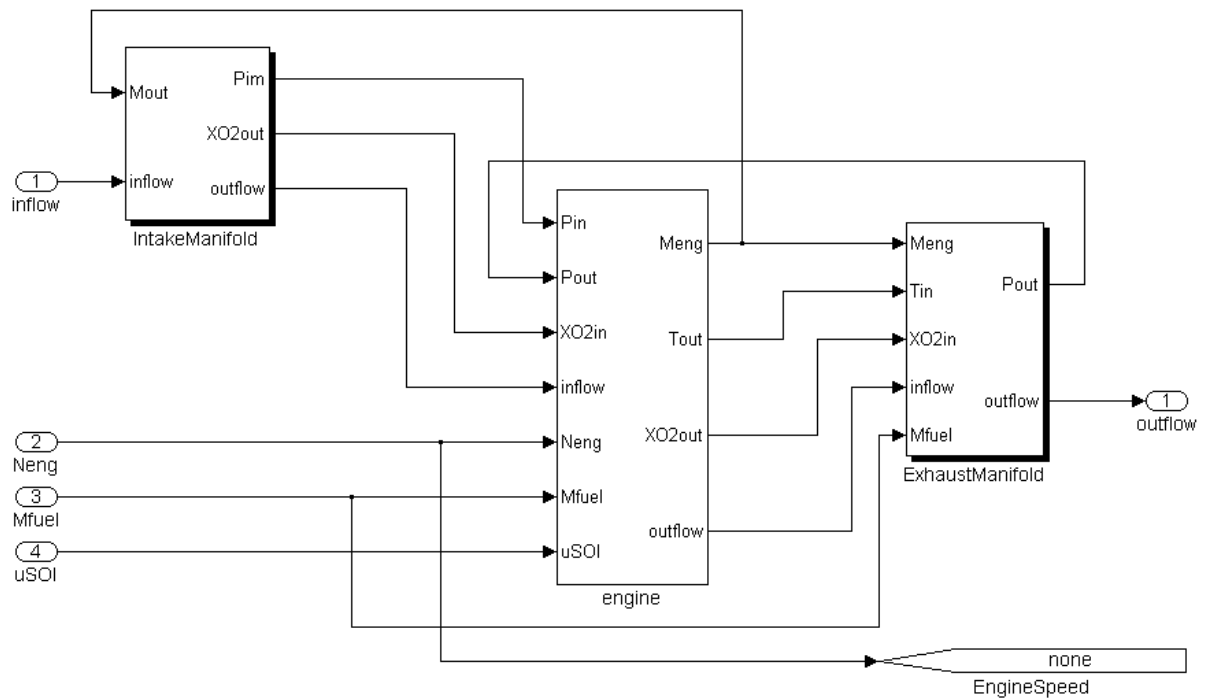


Fig. 3.7 – Engine Simulink block

3.2.1. Intake Manifold

This block represents an air isothermal reservoir before an engine. The isothermal reservoir is chosen in order to eliminate algebraic loops in the model and to reduce system order. The inlet gas mass flow \dot{m}_{in} [$\text{kg} \cdot \text{s}^{-1}$], the temperature T_{in} [K], the oxygen mass flow $\dot{m}_{O_2,in}$ [$\text{kg} \cdot \text{s}^{-1}$] and the outlet gas mass flow \dot{m}_{out} [$\text{kg} \cdot \text{s}^{-1}$] are inputs of this block. The outlet oxygen mass fraction $w_{O_2,out}$ [-] and the intake manifold gas pressure p_{im} [Pa] are outputs of the block. The manifold itself has several describing parameters – the reservoir volume V [m^3], the gas constant R [$\text{J} \cdot \text{K}^{-1} \cdot \text{mol}^{-1}$], the inlet gas specific heat at constant pressure c_p [$\text{J} \cdot \text{kg}^{-1}$] and at constant volume c_v [$\text{J} \cdot \text{kg}^{-1}$], the inlet gas initial pressure p_0 [Pa], and the initial oxygen mass fraction $w_{O_2,0}$ [-]. The outlet gas pressure is denoted by equation (29) and the oxygen mass fraction by (30)

$$\dot{p}_{out} = \frac{c_p R T_{in}}{c_v V} (\dot{m}_{in} - \dot{m}_{out}), \text{ where } c_v = c_p - R, \quad (29)$$

$$\dot{w}_{O2,out} = \frac{R T_{in}}{p_{in} V} (\dot{m}_{O2,in} - w_{O2,out} \dot{m}_{in}). \quad (30)$$

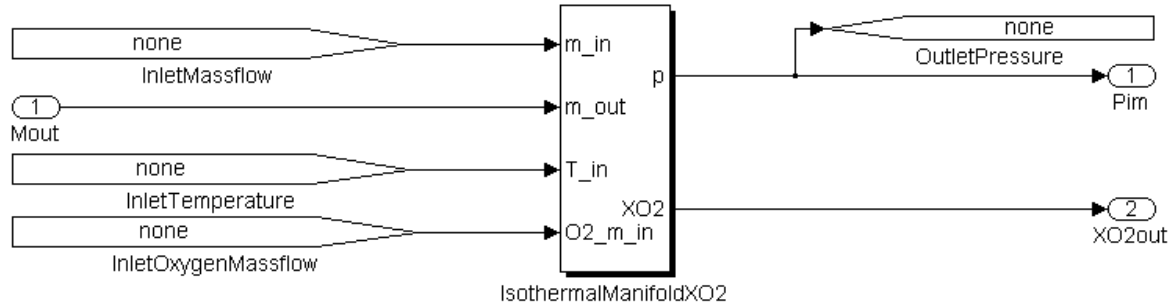


Fig. 3.8 – Intake manifold Simulink block

3.2.2. Exhaust Manifold

A gas flow in the exhaust gas reservoir is modelled like an adiabatic process. The fuel mass flow \dot{m}_{fuel} [kg · s⁻¹] and the engine gas mass flow \dot{m}_{eng} [kg · s⁻¹], the inlet temperature T_{in} [K] and the inlet oxygen mass fraction $w_{O2,in}$ [-] are the input quantities. Engineers are interested in the following output parameters – the outlet gas pressure p_{out} [Pa], the temperature T_{out} [K] and the oxygen mass fraction $w_{O2,out}$ [-]. These parameters depend on the input and the internal block parameters i.e. the reservoir volume V , the gas constant R [J · K⁻¹ · mol⁻¹], the gas specific heat at constant pressure c_p [J · kg⁻¹] and at constant volume c_v [J · kg⁻¹], the initial pressure p_0 [Pa], the initial oxygen mass fraction $w_{O2,0}$ [-] and the initial temperature T_0 [K]. The outlet gas pressure is denoted by equation (31), the temperature by (32) and the oxygen mass fraction by (34)

$$\dot{p}_{out} = \frac{c_p R}{c_v V} (\dot{m}_{in} T_{in} - \dot{m}_{out} T_{out}), \text{ where } c_v = c_p - R, \dot{m}_{in} = (\dot{m}_{eng} + \dot{m}_{fuel}) \quad (31)$$

$$\dot{T}_{out} = \frac{T_{out} R}{p_{out} V c_v} \left(c_p \dot{m}_{in} T_{in} - c_p \dot{m}_{out} T_{out} - c_v (\dot{m}_{in} - \dot{m}_{out}) T_{out} \right) \quad (32)$$

$$\dot{w}_{O2,out} = \frac{RT_{out}}{p_{out} V} (\dot{m}_{O2,in} - w_{O2,out} \dot{m}_{in}), \text{ where } m_{O2,in} = m_{in} w_{O2,in}. \quad (33)$$

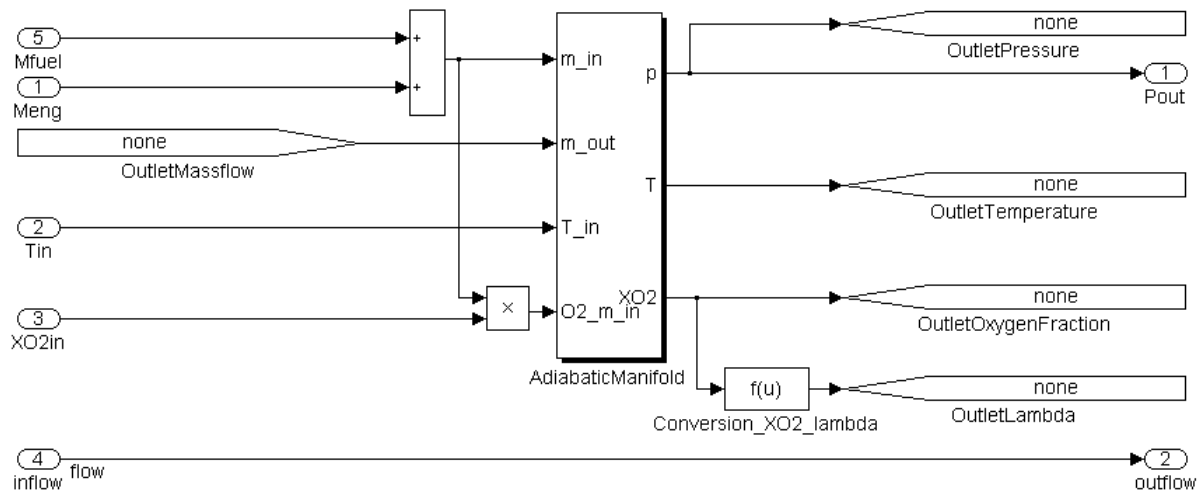


Fig. 3.9 – Exhaust manifold Simulink block

3.2.3. Volumetric Pump

Cylinder movement is modelled like a volumetric pump. The inlet gas pressure p_{in} [Pa], the outlet gas pressure p_{out} [Pa], the inlet gas temperature T_{in} [K] and the engine angular velocity ω_{eng} [$\text{rad} \cdot \text{s}^{-1}$] are inputs of this block. Necessary parameters are the engine displacement V [m^3], the gas constant R [$\text{J} \cdot \text{K}^{-1} \cdot \text{mol}^{-1}$] and the empirically found volumetric efficiency η_{eng} [-]. The output of this block is the engine mass flow \dot{m}_{eng} [$\text{kg} \cdot \text{s}^{-1}$] determined by equation (34)

$$\dot{m}_{eng} = \frac{\eta_{eng} p_{in} V \omega_{eng}}{4\pi R T_{in}}. \quad (34)$$

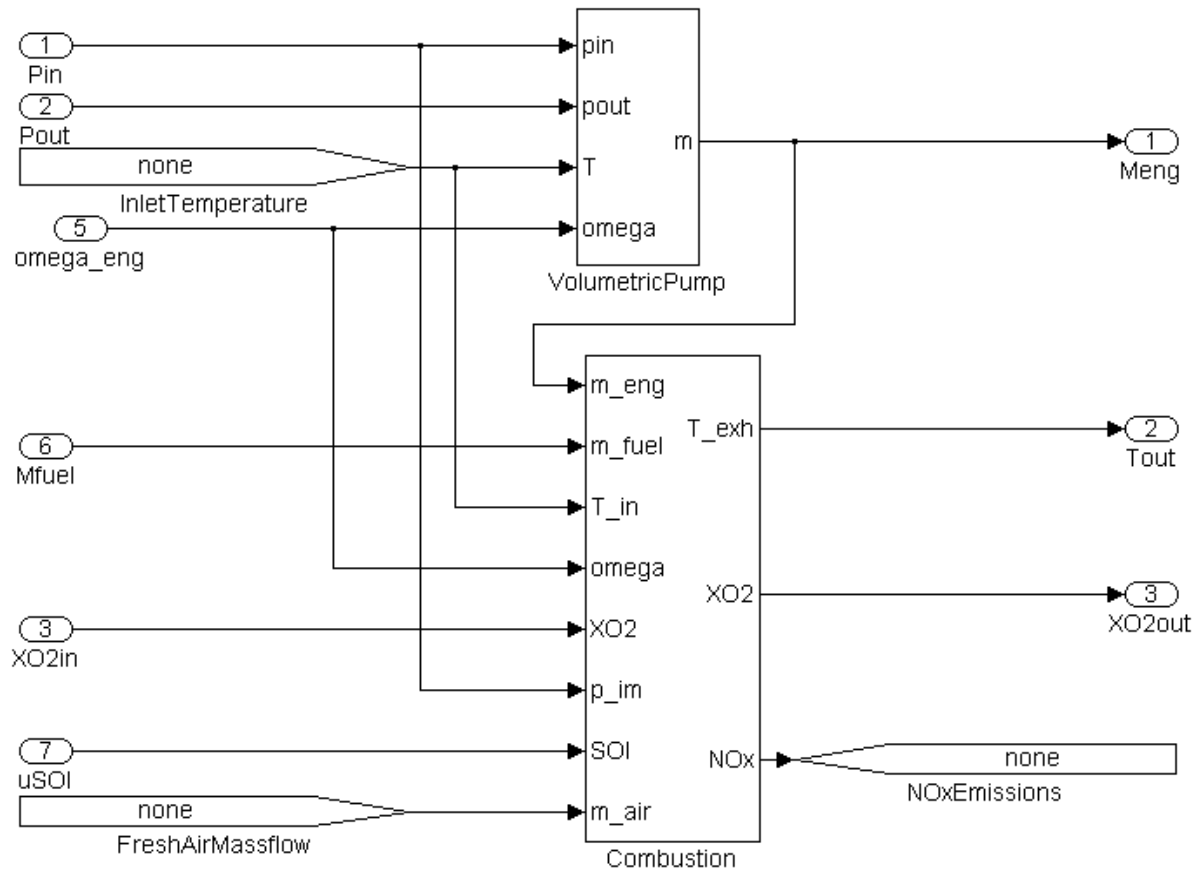


Fig. 3.10 – Engine Simulink block – detail of volumetric pump and combustion

3.2.4. Combustion

The NO_x [ppm] concentration, the exhaust gas temperature T_{out} [K] and the oxygen mass fraction $w_{\text{O}_2, \text{out}}$ [-] are outputs of the combustion block. It represents burning of the fuel and the gas (oxygen) injected into the cylinders. The outputs depend on the engine mass flow \dot{m}_{eng} [$\text{kg} \cdot \text{s}^{-1}$], the fuel mass flow \dot{m}_{fuel} [$\text{kg} \cdot \text{s}^{-1}$], the engine angular velocity ω_{eng} [$\text{rad} \cdot \text{s}^{-1}$], the inlet gas oxygen mass fraction $w_{\text{O}_2, \text{in}}$ [-], the inlet gas pressure p_{in} [Pa] and the temperature T_{in} [K], the fresh air mass flow \dot{m}_{air} [$\text{kg} \cdot \text{s}^{-1}$] and the start of injection SOI [$^\circ$]. They also depend on several internal block parameters i. e. the fuel low heating value H_{fuel} [$\text{J} \cdot \text{kg}^{-1}$], the fresh air/fuel mixture specific heat at constant pressure $c_{p, \text{air}}$ [$\text{J} \cdot \text{kg}^{-1}$], the air/fuel stoichiometric ratio $A_{\text{air, fuel}}$ [-], the exhaust gas specific heat at constant pressure c_p [$\text{J} \cdot \text{kg}^{-1}$], the



number of cylinders N [-] and the coefficient K [-] acquired from real data depending on the engine mass flow, the engine speed, the inlet and the outlet temperature, the oxygen mass fraction and the number of cylinders. The NO_x [ppm] concentration is described by equation (38) where \bar{p} is the vector of the empirically found coefficients of data acquired during the model fitting. The elements of \bar{G} are the element products of vector \bar{F} defined in (37).

$$T_e = \frac{c_p \left(K \cdot H_{\text{fuel}} \frac{\dot{m}_{\text{fuel}}}{\dot{m}_{\text{eng}}} + T_{\text{in}} c_{p,\text{air}} \right)}{\frac{\dot{m}_{\text{fuel}}}{\dot{m}_{\text{eng}}} + 1}, \quad (35)$$

$$w_{\text{O2,out}} = \frac{\dot{m}_{\text{eng}} w_{\text{O2,in}} - \dot{m}_{\text{fuel}} A_{\text{air,fuel}} w_{\text{O2,air}}}{\dot{m}_{\text{eng}} + \dot{m}_{\text{fuel}}}, \quad (36)$$

$$\bar{F} = \left[\frac{\dot{m}_{\text{fuel}}}{\dot{m}_{\text{air}}}, T_{\text{in}}, p_{\text{in}}, w_{\text{O2,in}}, \text{SOI}, N, 1 \right], \bar{G} = [F_1 F_1, F_1 F_2, \dots, F_1 F_7, F_2 F_2, \dots, F_2 F_7, \dots, F_7 F_7] \quad (37)$$

$$\text{NO}_x = e^S, \text{ where } S = \sum_{i=1}^{28} p_i G_i \quad (38)$$

3.3. Turbocharger

There are two types of a block for modelling a turbocharger – with or without a wastegate valve. A turbocharger consists of some sub blocks such as compressor, turbine, etc.

3.3.1. Rotating shaft

This block represents a solid shaft connecting a turbine and a compressor. It transforms the input power balance W_{in} [$\text{J} \cdot \text{s}^{-1}$] of the compressor power W_c [$\text{J} \cdot \text{s}^{-1}$] and the turbine power W_t [$\text{J} \cdot \text{s}^{-1}$] to the shaft. The shaft rotates at the angular



velocity ω_{tc} [$\text{rad} \cdot \text{s}^{-1}$]. It is described by equation (39). The moment of inertia I [$\text{kg} \cdot \text{m}^2$] is an internal parameter of this block.

$$\dot{\omega}_{tc} = \frac{W_{in}}{I\omega_{tc}}, \text{ where } W_{in} = W_t - W_c \quad (39)$$

3.3.2. Compressor

The inlet gas pressure p_{in} [Pa], the outlet gas pressure p_{out} [Pa], the shaft angular velocity ω_{tc} [$\text{rad} \cdot \text{s}^{-1}$] and the inlet gas temperature T_{in} [K] are inputs of the compressor block. Compressor efficiency η_c [-] is an exponential function of the inputs and the empirically found vector \bar{p} (vector elements found during the model fitting by using real data). The inputs and the compressor wheel diameter d_c [m], the reference temperature T_{ref} [K], the reference pressure p_{ref} [Pa], the specific heat capacity ratio γ [-], the gas constant R [$\text{J} \cdot \text{K}^{-1} \cdot \text{mol}^{-1}$], the head parameter Ψ [-] and the compressor efficiency parameter η_c [-] are the necessary quantities to determine the compressor output mass flow \dot{m}_c [$\text{kg} \cdot \text{s}^{-1}$], the power consumed by the compressor W_c [$\text{J} \cdot \text{s}^{-1}$] and the outlet temperature T_{out} [K].

$$\Psi = \frac{c_p T_{ref} \left(\left(\frac{p_{out}}{p_{in}} \right)^{\frac{\gamma-1}{\gamma}} - 1 \right)}{\frac{1}{2} U_c^2}, U_c = \frac{d_c}{2} \frac{\omega_{tc}}{\sqrt{\frac{T_{in}}{T_{ref}}}}, \Phi = \frac{k_3 \Psi - k_1}{\Psi + k_2} \quad (40)$$

$$\dot{m}_c = \dot{m}_{ref} \frac{p_{in}}{p_{ref}} \sqrt{\frac{T_{ref}}{T_{in}}}, \text{ where } \dot{m}_{ref} = \frac{p_{ref}}{RT_{ref}} \frac{\pi}{4} d_c^2 \Phi U_c \quad (41)$$

$$W_c = \frac{\dot{m}_c c_p T_{in} \left(\left(\frac{p_{out}}{p_{in}} \right)^{\frac{\gamma-1}{\gamma}} - 1 \right)}{\eta_c}, \quad (42)$$

$$T_{out} = T_{in} \left(1 + \frac{\left(\frac{p_{out}}{p_{in}} \right)^{\frac{\gamma-1}{\gamma}} - 1}{\eta_c} \right). \quad (43)$$

$$\eta_c = e^{-\left(N_{tc,ref}^2 p_1 + N_{tc,ref} \dot{m}_{ref} p_2 + N_{tc,ref} p_3 + \dot{m}_{ref}^2 p_4 + \dot{m}_{ref} p_5 + p_6 \right)}, \text{ where } N_{tc,ref} = \frac{30 \omega_{tc}}{\pi \sqrt{\frac{T_{in}}{T_{ref}}}} \quad (44)$$

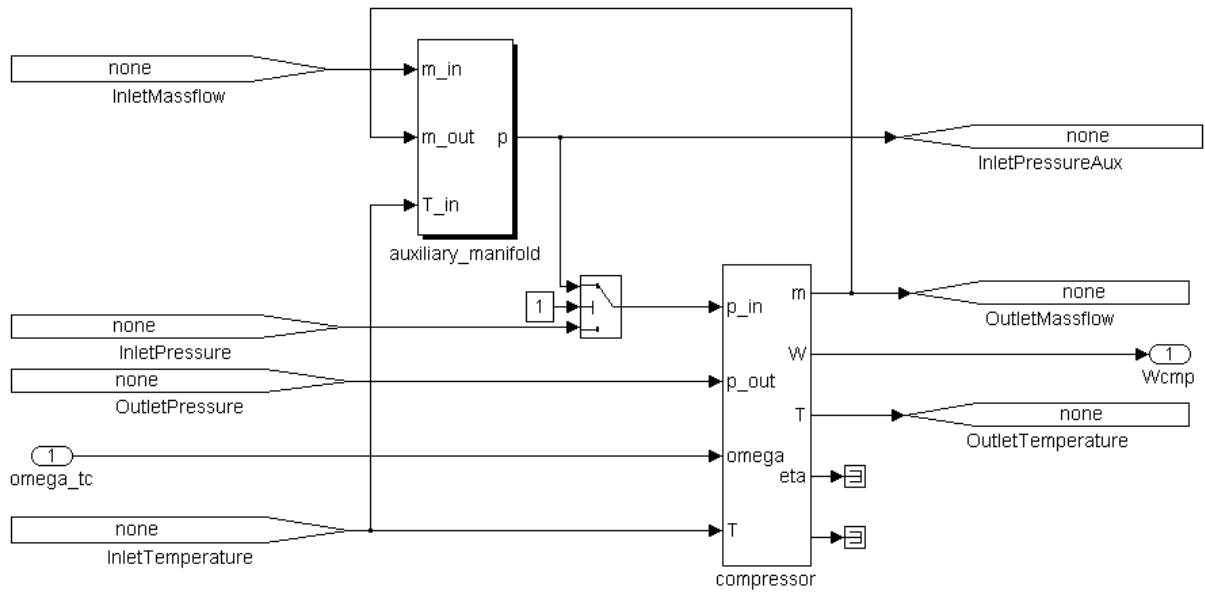


Fig. 3.11 – Compressor Simulink block

3.3.3. Turbine

The turbine model block processes the following inputs – the inlet gas mass flow \dot{m}_{in} [$\text{kg} \cdot \text{s}^{-1}$], the inlet gas pressure p_{in} [Pa], the outlet gas pressure p_{out} [Pa], the shaft angular velocity ω_{tc} [$\text{rad} \cdot \text{s}^{-1}$] and the inlet gas temperature T_{in} [K]. The



necessary parameters are the reference temperature T_{ref} [K], the reference pressure p_{ref} [Pa], the specific heat capacity ratio γ [-], the gas specific heat at constant pressure c_p [$\text{J} \cdot \text{kg}^{-1}$], the area S_t [m^2], the turbine wheel diameter d_t [m], the empirically found turbine parameter k [-] and the vector of the efficiency coefficients \bar{p} . The turbine mass flow \dot{m}_t [$\text{kg} \cdot \text{s}^{-1}$] is described by equation (45), the turbine power W_t [$\text{J} \cdot \text{s}^{-1}$] by (46), the outlet gas temperature T_{out} [K] by (47) and the turbine efficiency η_t [-] by (49). A turbine without a wastegate does not use the mixing and the valve blocks. The other parts are same.

$$\dot{m}_t = \dot{m}_{\text{ref}} \frac{p_{\text{in}}}{p_{\text{ref}}} \sqrt{\frac{T_{\text{ref}}}{T_{\text{in}}}}, \text{ where } \dot{m}_{\text{ref}} = S_t \left(\frac{p_{\text{in}}}{p_{\text{ref}}} \right)^k \sqrt{\left(\frac{p_{\text{in}}}{p_{\text{ref}}} \right)^{\frac{\gamma+1}{\gamma}}} \quad (45)$$

$$W_t = \dot{m}_t c_p T_{\text{in}} \eta_t \left(1 - \left(\frac{p_{\text{out}}}{p_{\text{in}}} \right)^{\frac{\gamma-1}{\gamma}} \right), \quad (46)$$

$$T_{\text{out}} = T_{\text{in}} \left(1 - \eta_t \left(1 - \left(\frac{p_{\text{out}}}{p_{\text{in}}} \right)^{\frac{\gamma-1}{\gamma}} \right) \right). \quad (47)$$

$$BSR = \frac{d_t \omega_{\text{tc,ref}}}{\sqrt{2c_p T_{\text{ref}} \left[1 - \left(\frac{p_{\text{out}}}{p_{\text{in}}} \right)^{\frac{\gamma-1}{\gamma}} \right]}}, \text{ where } \omega_{\text{tc,ref}} = \frac{\omega_{\text{tc}}}{\sqrt{\frac{T_{\text{in}}}{T_{\text{ref}}}}} \quad (48)$$

$$\eta_t = e^{-\left(BSR^2 \cdot p_1 + BSR \cdot N_{\text{tc,ref}} p_2 + BSR \cdot p_3 + N_{\text{tc,ref}}^2 p_4 + N_{\text{tc,ref}} p_5 + p_6 \right)}, \text{ where } N_{\text{tc,ref}} = \frac{30\omega_{\text{tc}}}{\pi} \quad (49)$$

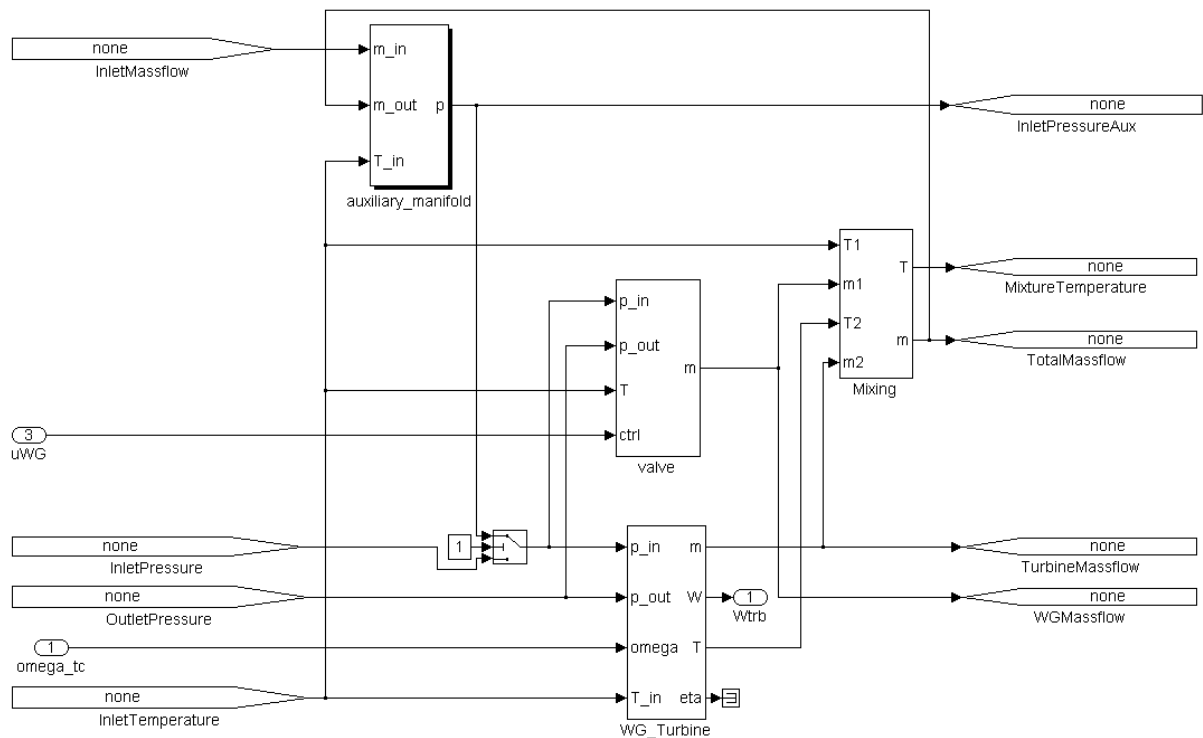


Fig. 3.12 – Turbine with wastegate valve Simulink block

3.4. Heat Exchanger

This block modelled the heat exchange between two streams (the gas flow and the cooling medium). The inlet gas temperature T_{in} [K] and the inlet gas mass flow \dot{m}_{in} [kg · s⁻¹] are inputs. The temperature T_{cm} [K] of a cooling medium and the heat exchange efficiency coefficients η_1 [-], η_2 [-] are the internal block parameters. The output temperature T_{out} [K] of this block is described by (50).

$$T_{out} = T_{in} - (\eta_1 \dot{m}_{in} + \eta_2)(T_{in} - T_{cm}). \quad (50)$$

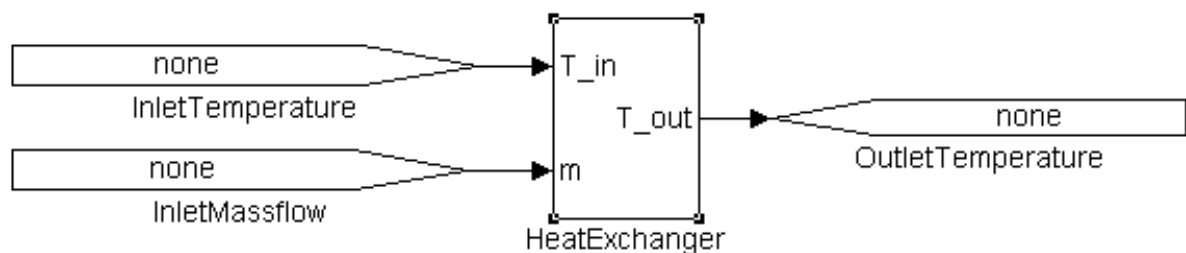


Fig. 3.13 – Heat exchanger Simulink block



4. Model Verification

The Simulink library is verified by using real data from the four-cylinder, 2.2 l, turbocharged diesel engine and the six-cylinder, 12 l, bi-turbocharged heavy duty diesel engine. The Simulink blocks are connected according to the technological scheme of the engine and the whole model is fitted using measured steady state data. Different physical equations (mentioned above) are used for each component. Polynomial regressions or lookup table are utilized to fit the model parameters.

The biggest issue to deal with is a turbocharger map fitting. This part has to be the most precise among all components. Lookup tables for performance data are not suitable for control-oriented turbocharger models because of non-continuously differentiable standard linear interpolation. This could lead to discontinuities or crashes of the simulation. It acts quite well for operating points inside the mapped data range but not for the outside area (mainly at low turbocharger speeds). That happens because the turbocharger manufacturers normally provide the measured compressor and turbine maps for higher speeds and for higher pressure ratios. Problems at low speeds are caused mainly by heat conduction from the hot lubricating oil to the cool compressor (at higher speeds this conduction is reversed) and by the accuracy of flow sensors. Several numerical methods exist for turbocharger maps fitting. Jensen's & Kristensen's polynomials [7] based on the Winkler simplification [9] are the most suitable for this library. These polynomials use the head parameter Ψ [-] mentioned above in the compressor description. Results of the compressor fitting are in Fig. 4.1 and Fig. 4.2.

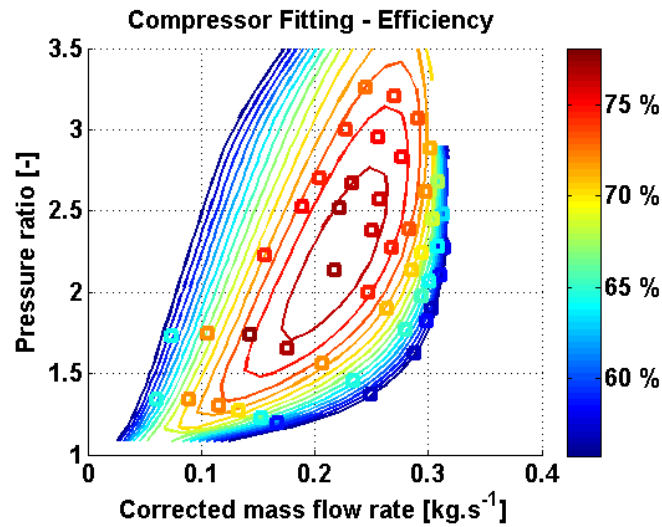


Fig. 4.1 – Compressor fitting - efficiency

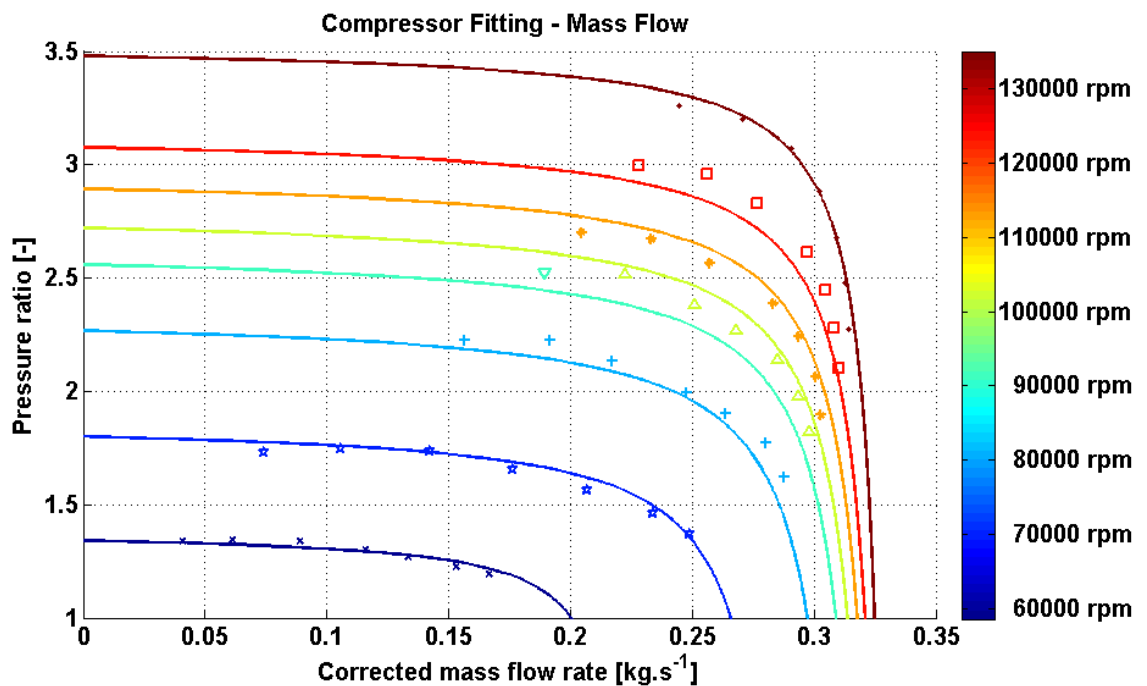


Fig. 4.2 – Compressor fitting – mass flow

A steady state fitted model can be used for simulation and further usage in the robust model based control of the engine. The relation between the model and the engine steady states of the most important quantities (pressure in the intake manifold P_{im} , turbine speed n_{trb} , temperature of the turbine outlet gas $T_{trb,out}$, air mass flow m_{air}) for the four-cylinder turbocharged engine are shown in scatter plots in Fig. 4.3.

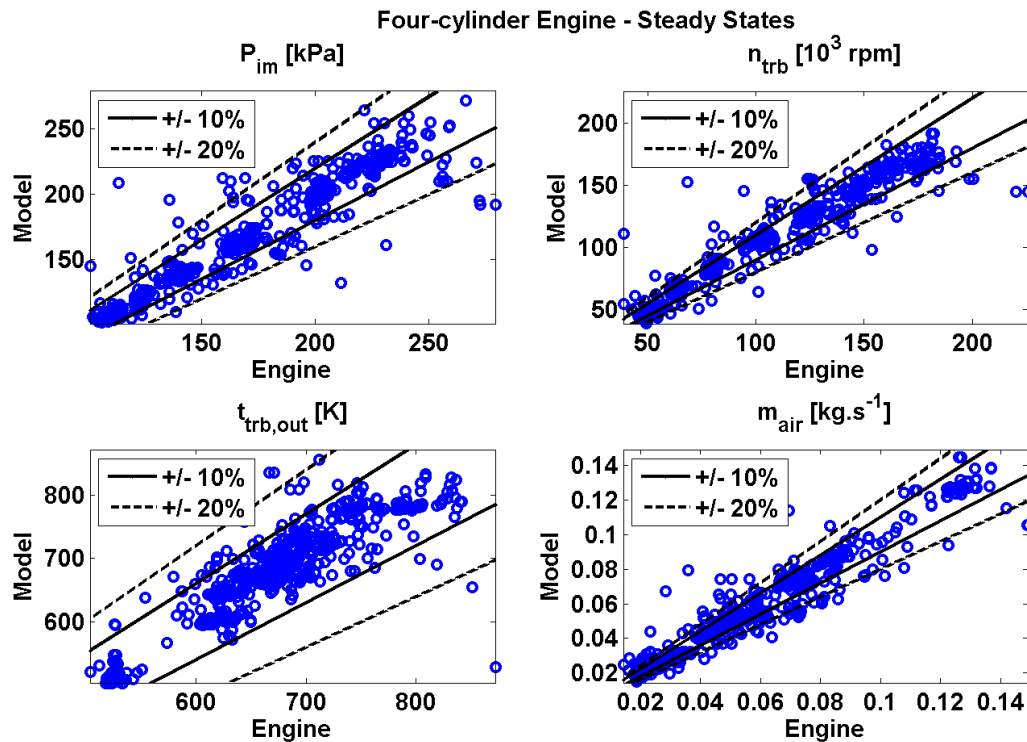


Fig. 4.3 – A four-cylinder turbocharged engine – steady state comparison

The main aim is to design a robust model predictive control for a real engine. A robust controller can deal with a large difference between the real and the simulated value. A serious problem for this type of controller is the sign difference between the real and the simulated gain. Step responses of the model and engine most important quantities are shown in Fig 4.4 and in Fig 4.5. Step quantities are EGR valve position and high pressure turbocharger wastegate valve (WG_{HP}) position.

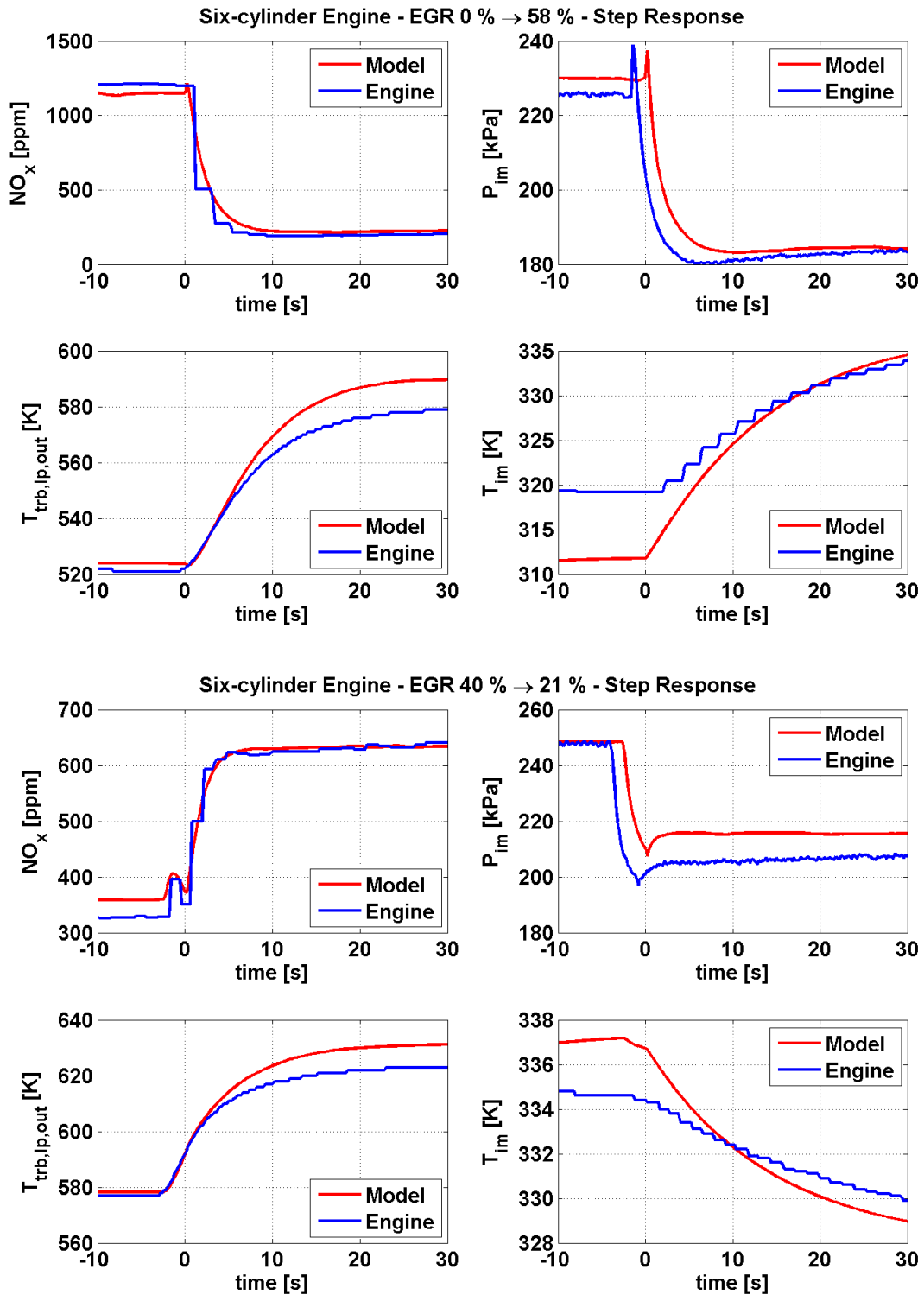


Fig. 4.4 – A six-cylinder bi-turbocharged engine – transient comparison EGR steps

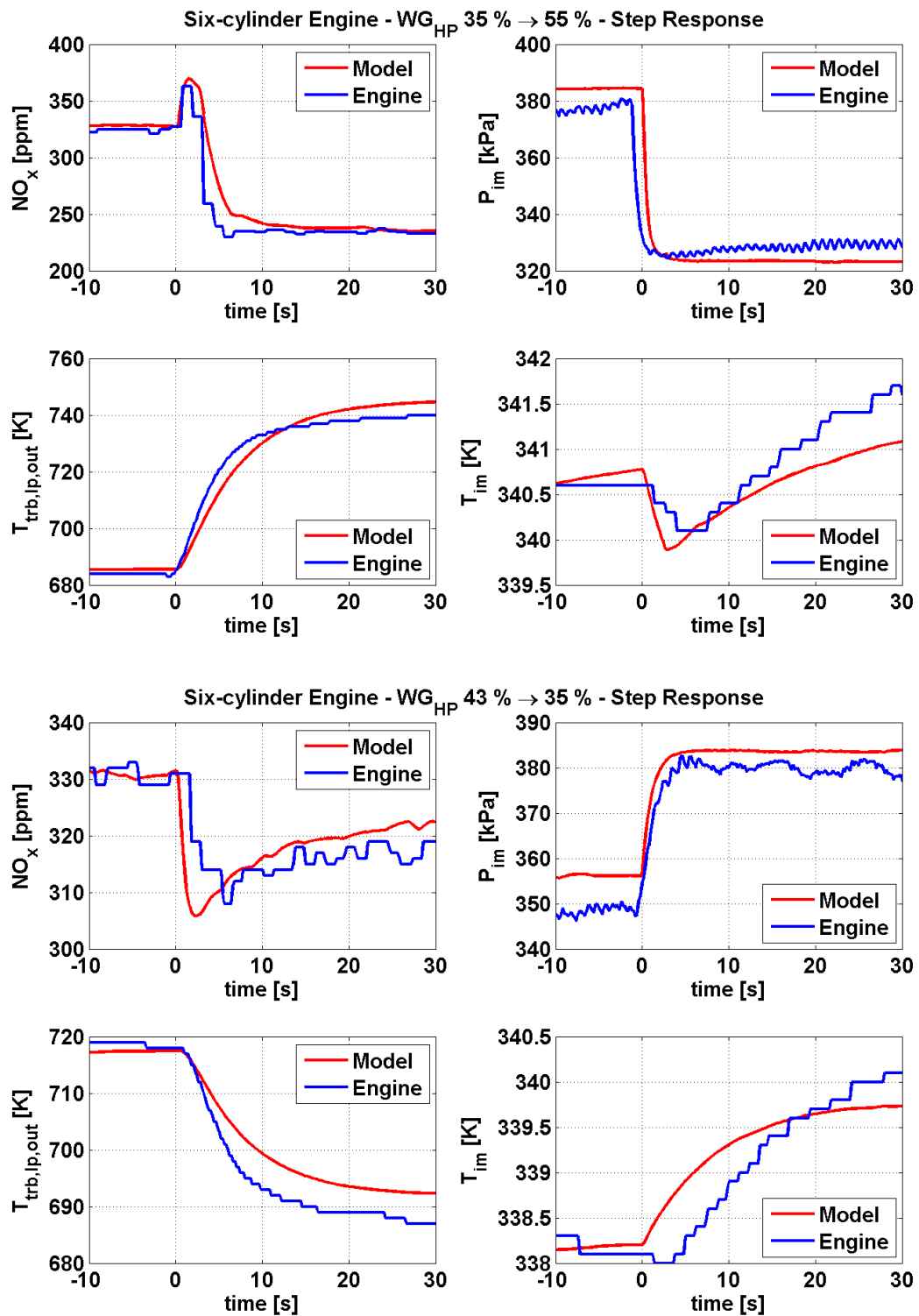


Fig. 4.5 – A six-cylinder bi-turbocharged engine – transient comparison WG_{HP} steps

A real NO_x measuring has a longer sampling period than the other quantities. The course of output quantities corresponds with the first order system that could be



characterized by a time constant and a gain. Example of the gain and the time constant scatter plot for high pressure turbine input pressure $P_{trb,hb,in}$ is shown in Fig. 4.6. Scatter plots of the other important quantities can be found in Appendix 8.1.

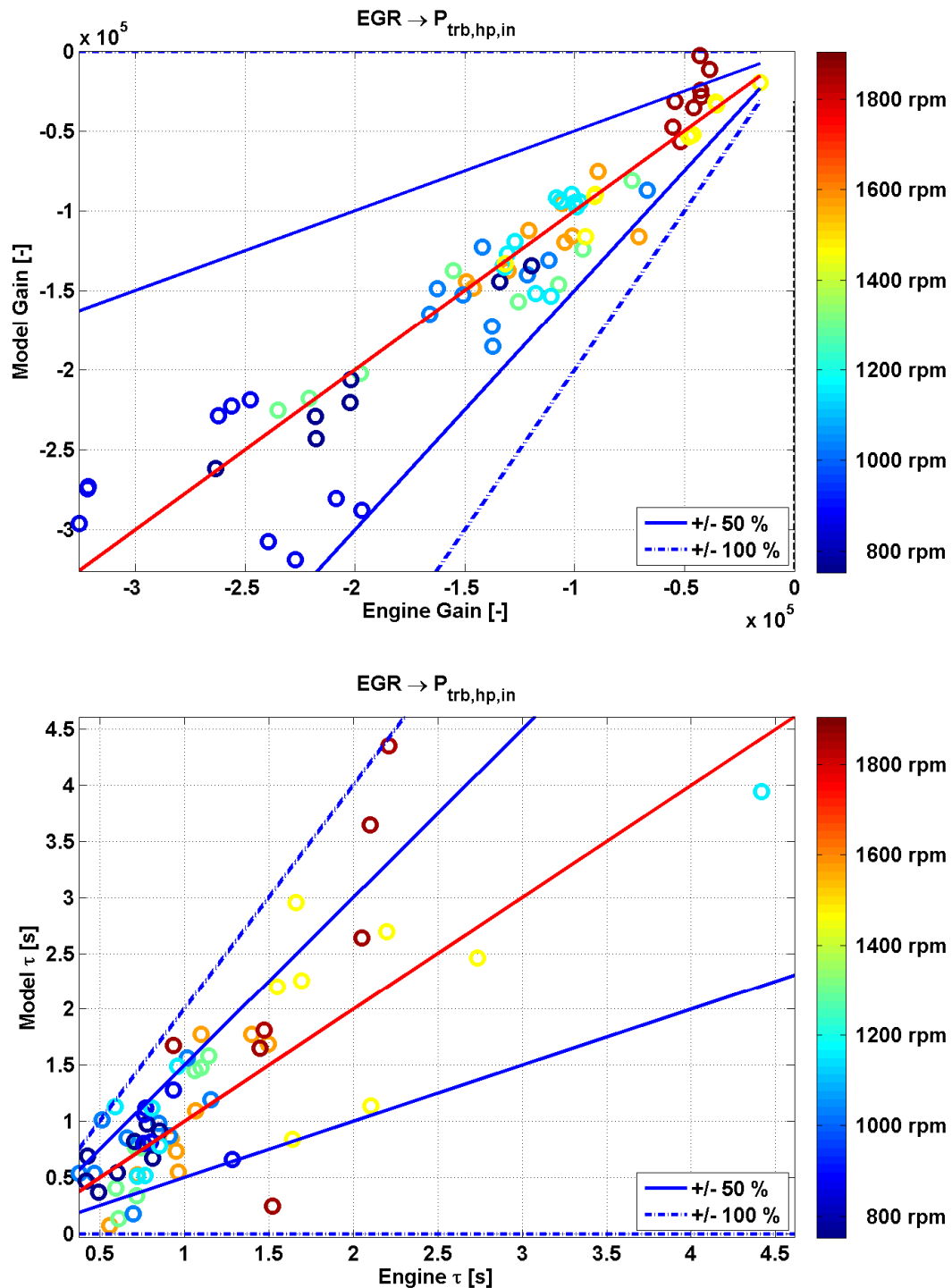


Fig. 4.6 –A six-cylinder bi-turbocharged engine – gain, time constant – EGR steps



5. Stiffness and nonlinearity

Engine models have serious problems with the stiff and the nonlinear equations describing the processes. Problem with stiffness is described using a simple first-order differential equation (51). The right side represents a general function of x and of y . General function has a root $y = G(x)$ for each value of x .

$$\frac{dy}{dx} = \frac{y - G(x)}{a(x, y)}. \quad (51)$$

If Δx is the desired resolution of x , then this equation is stiff if

$$\left| \frac{a(x, y)}{\Delta x} \right| \ll 1 \quad (52)$$

and $G(x)$ is well behaved (it varies in x considerably more slowly than does $e^{\frac{x}{a(x, G(x))}}$).

This geometrical significance of stiffness is shown in Fig. 5.1.

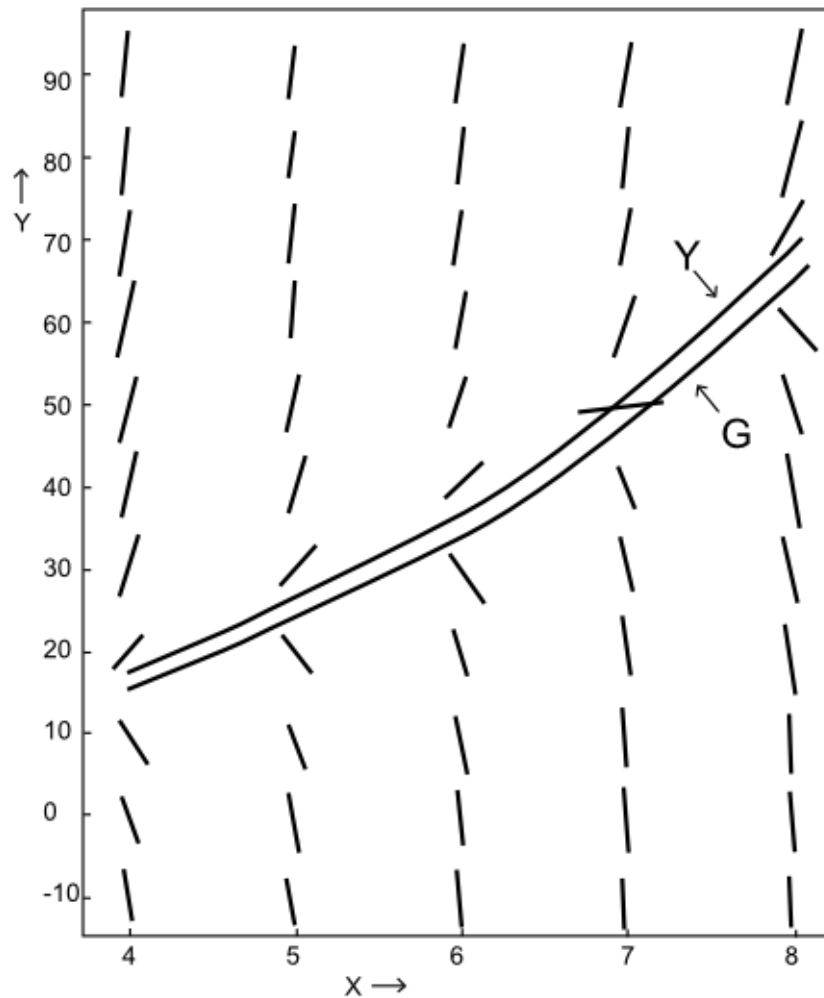


Fig. 5.1 – Slopes, $\frac{dy}{dx}$, for stiff equation $\frac{dy}{dx} = 5(y - x^2)$, reprinted from [11]

Fig 5.1 shows that for a particular x and a large y the slope $\frac{dy}{dx}$ is very steep and positive, and for a small y is very steep and negative. In vicinity of $y = G(x)$ the slope changes rapidly.

Stiff system described by the system of differential equations has significantly different time constants (the large ratio $S = \frac{\max|\operatorname{Re}\{\lambda_i\}}{\min|\operatorname{Re}\{\lambda_i\}}$, where λ_i are the eigenvalues of the differential equations). One of the claims from Curtiss & Hirschfelder says [11]: *stiff equations are equations where certain implicit methods, in particular BDF, perform better, usually tremendously better, than explicit ones.*



The difference between the explicit and the implicit methods is explained using the Euler method and a differential equation (53).

$$\dot{y} = f(x, y) \quad (53)$$

The explicit methods use the actual value to determine the value in the next time step. The explicit Euler method (the forward Euler method) is described by (54).

$$\frac{y_{k+1} - y_k}{h} = f(x_k, y_k), \text{ where } h \text{ is a time step} \quad (54)$$

The implicit methods use the value in the next time step instead of the actual one. The implicit Euler method (the backward Euler method) is described by (55).

$$\frac{y_{k+1} - y_k}{h} = f(x_{k+1}, y_{k+1}), \text{ where } h \text{ is a time step} \quad (55)$$

Problems with finding a solution through the implicit method are illustrated by the use of a simple ordinary differential equation (56).

$$\dot{y} = -y^2, y \in [0, a], y(0) = 1, \text{ the time step } h = \frac{a}{n}, \quad (56)$$

The explicit Euler method yields to a simple equation (57)

$$y_{k+1} = y_k - hy_k^2, \quad k = 0, 1, \dots, n. \quad (57)$$

The implicit Euler method yields to a quadratic equation (58)

$$y_{k+1} + hy_k^2 = y_k, \quad k = 0, 1, \dots, n. \quad (58)$$



It is much more difficult to find a solution for (58) than for (57). Solving (58) could lead us out from the possible region because of the two roots of the quadratic equation.

This example shows the difference between the explicit and the implicit methods. For complicated nonlinear equations it is possible that the implicit solver determines the solution out of the possible region during the iteration process (out of physical boundaries, etc.). That leads to simulation crashes. The term “Physical boundaries” means, for example, a compressor and a turbine inlet and outlet pressures ratio. If $\frac{p_{c,out}}{p_{c,in}} < 1$, $\frac{p_{t,out}}{p_{t,in}} < 1$ the simulation crashes on account of existence of singularities in a solution of the equation describing a compressor and a turbine. The other problem is the choice of the time step for the numerical solver. The time step can be so short that the trend of the slow states seems to be constant.

5.1. Singular Perturbation Theory

This theory focuses on the problems with a variable parameter for which the solutions of the problems are at limits of the parameter that differs in character. The idea is in time separations or length scales. It reduces the problem and makes it easier to solve and to find an approximation of the original problem.

In order to use the singular perturbation theory, it is necessary to divide systems into groups of slow (long time constants, the limits $\text{Re}\{\lambda_i\} < 0, |\lambda_i| \rightarrow 0$) and fast states (short time constants, the limits $\text{Re}\{\lambda_i\} < 0, |\lambda_i| \rightarrow \infty$). The principles of the singular perturbation theory are explained using a simple system described by equation (59) with separated fast and slow states.

$$\begin{bmatrix} \dot{x}_s \\ \dot{x}_f \end{bmatrix} = \begin{bmatrix} A_{11} & A_{12} \\ A_{21} & A_{22} \end{bmatrix} \begin{bmatrix} x_s \\ x_f \end{bmatrix} \quad (59)$$

If $\dot{x}_f \rightarrow 0$, then from (59) we obtain equation (60) depending only on the states and not on their derivations



$$A_{21}x_s + A_{22}x_f = 0. \quad (60)$$

If A_{22} is a regular matrix, then the steady states for the fast states should be expressed by (61)

$$\bar{x}_f = -A_{22}^{-1}A_{21}x_s. \quad (61)$$

Now substitute (61) and $\dot{x}_f \rightarrow 0$ to (60). That leads to the differential equation (62) depending only on slow states

$$T_s \dot{x}_s = A_{11}x_s - A_{12}A_{22}^{-1}A_{21}x_s. \quad (62)$$

Solution of (62) has no longer problems with highly different time constants (eigenvalues) and the numerical solution is simpler, faster and more stable.

5.2. Constrained State Reduction

An engine model is not only a stiff problem but also a combination of a stiff and a highly nonlinear system with a lot of physical and numerical boundaries. In order to deal with these problems, it is necessary to find a different model design.

The idea of the constrained state reduction method is the same as the idea of the singular perturbation theory i.e. a separation of the fast and the slow states. The method is explained via the states but it can be applied on any combinations of states. The system is described according to the following equations (the derivations are functions of the fast and slow states and of inputs)

$$\dot{x}_s = f_s(x_f, x_s, u), \quad \dot{x}_f = f_f(x_f, x_s, u). \quad (63)$$

The difference between this method and the singular perturbation method is in finding of the solution of fast states. This method uses an optimization of the $f_f(x_f, x_s, u)$, where $\dot{x}_f = 0$ is the necessary criterion. There should also exist other optional criteria such as physical boundaries, etc. for determination of the value of

the fast states. The state reduction and the optional criteria should make simulation more numerically stable and faster. That also solves the problems connected with nonlinearities because the values of the fast states have to be found in the possible region.

$$\hat{x}_f(x_s, u) = \min_G \|f_f(x_f, x_s, u)\|, G = \{\dot{x}_f = 0; \dots\}. \quad (64)$$

Using fast states values $\hat{x}_f(x_s, u)$ found in (64) and system description (63) we obtain system which is not dependent on the fast state derivation

$$\dot{x}_s = f_s(\hat{x}_f(x_s, u), x_s, u). \quad (65)$$

The advantage of the constrained state reduction lies in removing the stiff character from equations (same as with using singular perturbation theory) and in specifying the optional criteria. That should remove numerical instabilities and crashes of the simulation because of determining the states only in the possible region. In summary, solving the differential equation using this method is more stable, easier to find etc.

A scheme of iteration solving process using the constrained state reduction is in Fig. 5.2.

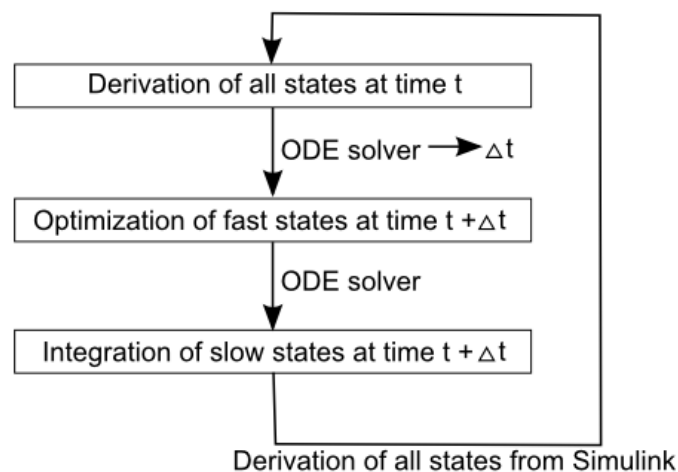


Fig. 5.2 – Iteration solving process of the simulation for the reduced state model

This method was tested on the model of a four-cylinder turbocharged diesel engine (its simple gas flow scheme is in Fig. 5.3) and a six-cylinder bi-turbocharged diesel engine.

The model of the four-cylinder turbocharged diesel engine is used as an example of how to use this method for simulation. Generally speaking, the mass conservation law says gas mass cannot disappear. The quantity of the gas mass in the input to the manifold has to be equal to the quantity of the gas mass in the output (if the gas is not accumulated). It is similar to the Kirchhoff's current law for the nodes. As soon as we change the actuator value (make step), all states tries to reach their equilibrium points and find out the balance for the gas flow. Pressures, temperatures and concentration changes are much faster than the shaft rotation.

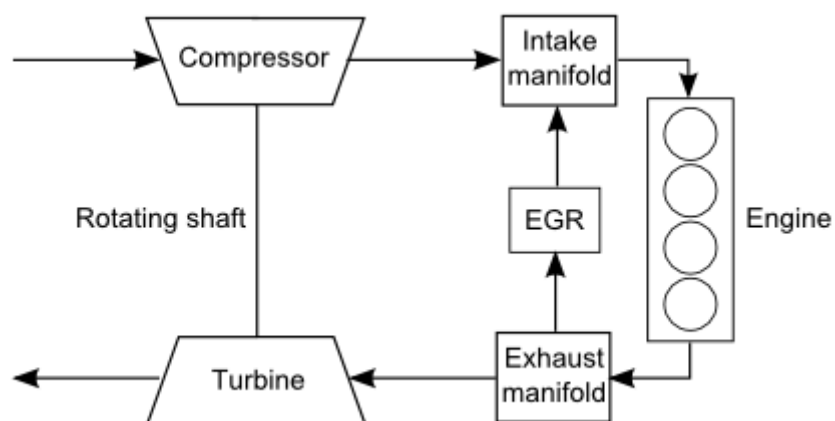


Fig. 5.3 – Engine scheme – gas flow

The four-cylinder turbocharged engine model uses 7 state quantities. They are the turbine speed (n_{trb} [rpm]), the pressure in the intake manifold (p_{im} [Pa]), the O_2 concentration in the intake manifold ($X_{\text{O}_2,\text{im}}$ [%]), the pressure before turbine ($p_{\text{trb},\text{in}}$ [Pa]), the temperature before turbine ($T_{\text{trb},\text{in}}$ [K]), the O_2 concentration in the exhaust manifold ($X_{\text{O}_2,\text{em}}$ [%]), and the pressure after compressor ($p_{\text{cmp},\text{out}}$ [Pa]). Simulation results are compared in the several most important quantities – the pressure in the intake manifold (p_{im}), the turbine speed (n_{trb}), the temperature after

turbine ($T_{\text{trb,out}}$ [K]) and the fresh air mass flow (m_{air} [$\text{kg} \cdot \text{s}^{-1}$]). They are compared with step responses of the following quantities – the exhaust gas recirculation valve position (EGR), the throttle valve actuator position (TVA), the engine speed, the injection quantity (IQ) and the vane position.

A comparison is made for the model with 1, 6 and 7 slow states (order 1, 6 and 7). The first order model has only one slow state: the turbine speed. The other states are fast states. Model with 6 slow states has also only one fast state: the pressure after compressor. Model with 7 slow states does not use constrained state reduction.

Fig. 5.4 shows a raising iterations count according to a raising number of slow states during determining the solution. Fig. 5.5 shows a course of the most important output quantities depending on the number of slow states in the model. A comparison for the other actuators can be found in Appendix 8.2.

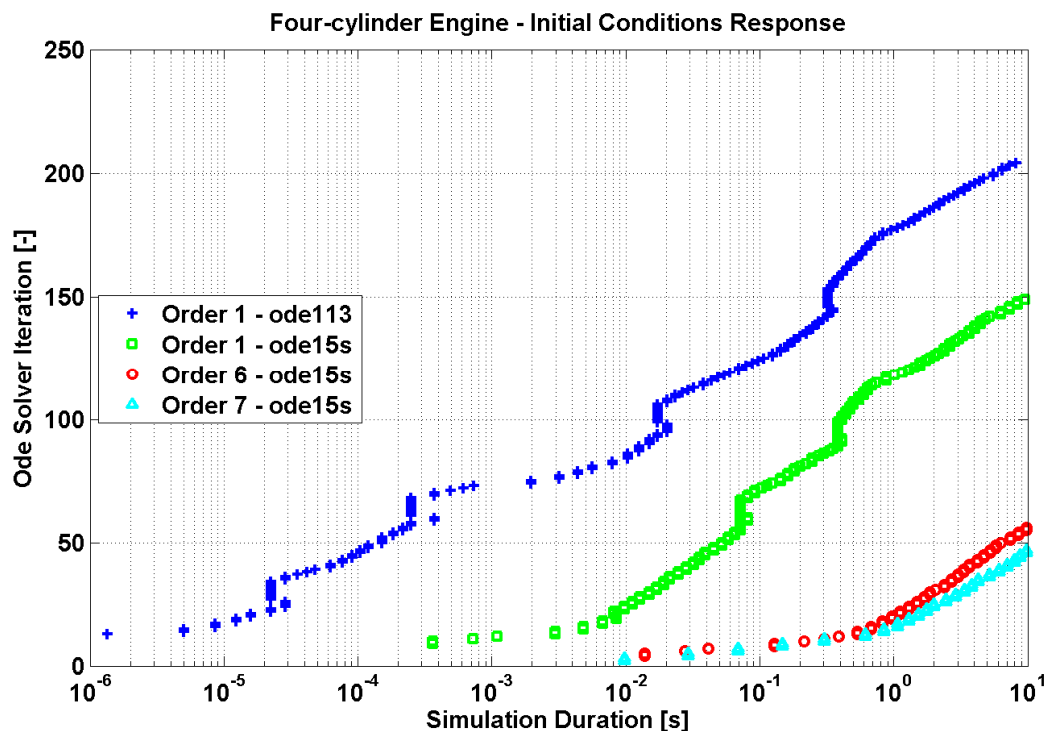


Fig. 5.4 – A four-cylinder turbocharged engine – simulation duration

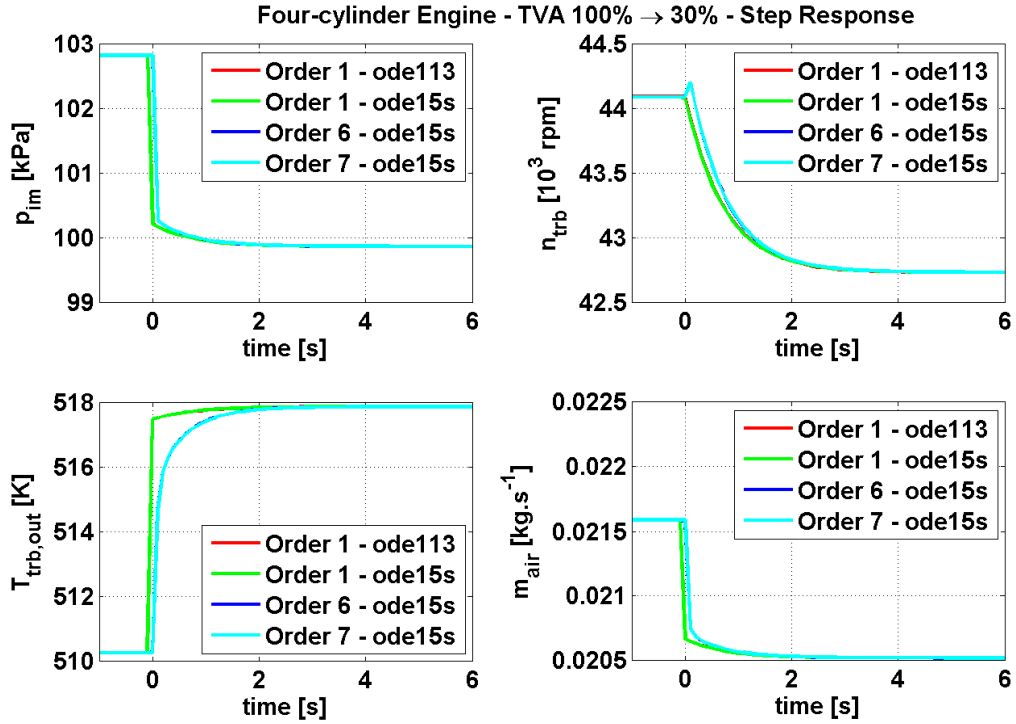


Fig. 5.5 – A four-cylinder turbocharged engine – state reduction (TVA valve)

The six-cylinder bi-turbocharged engine model uses 11 state quantities. These are the high and the low pressure turbine speeds ($n_{trb, hp}$ [rpm], $n_{trb, lp}$ [rpm]), the pressure in the intake manifold (p_{im} [Pa]), the O_2 concentration in the intake manifold ($X_{O_2, im}$ [%]), the pressure before high pressure turbine ($p_{trb, hp, in}$ [Pa]), the temperature before the high pressure turbine ($T_{trb, hp, in}$ [K]), the O_2 concentration in the exhaust manifold ($X_{O_2, em}$ [%]), the pressure after the high and the low pressure compressors ($p_{cmp, hp, out}$ [Pa], $p_{cmp, lp, out}$ [Pa]) and the pressure after the high and the low pressure turbines ($p_{trb, hp, out}$ [Pa], $p_{trb, lp, out}$ [Pa]). Simulation results are compared in several most important quantities – the NO_x concentration, the pressure in the intake manifold (p_{im}), the temperature after the low pressure turbine ($T_{trb, lp, out}$ [K]), and the temperature in the intake manifold (T_{im} [K]). They are compared to step responses of the following quantities – the exhaust gas recirculation valve position (EGR), the throttle valve actuator position (TVA), the engine speed, the injection quantity (IQ) and the high pressure turbocharger waste gate valve position (WG_{HP}).



A comparison is made for the model with 2, 3, 7 and 11 slow states (order 2, 3, 7 and 11). The second order model consists of two slow states – the high and the low pressure turbine speed. The other states are fast. The model with 3 slow states has the following slow states: the high and the low pressure turbine speed and the pressure in the intake manifold.. The seventh order model uses the following slow states: the high and the low pressure turbine speed, the pressure in the intake manifold, the O₂ concentrations in the intake and in the exhaust manifold, and the pressure and the temperature before the high pressure turbine. The other states are fast. Model with 11 slow states does not use the constrained state reduction.

Fig. 5.6 depicts a raising iterations count according to a raising number of slow states during determining the solution. Fig. 5.7 shows courses of the most important output quantities depending on the number of slow dynamical states of the model. A comparison for the other actuators can be found in Appendix 8.3.

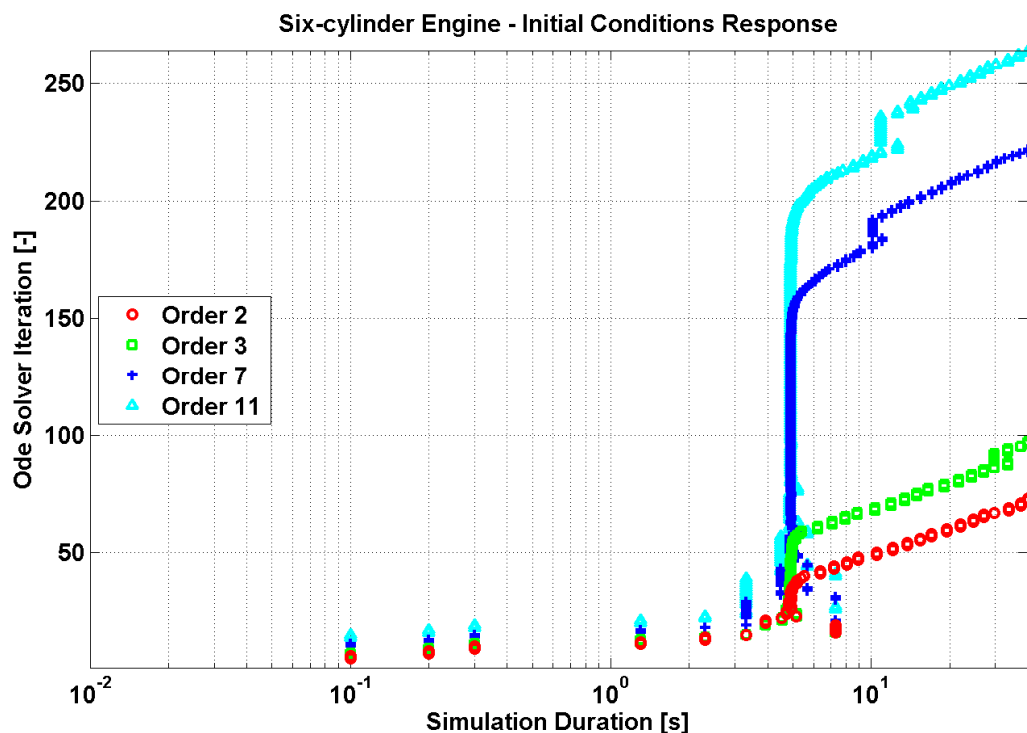


Fig. 5.6 – A six-cylinder bi-turbocharged engine – simulation duration

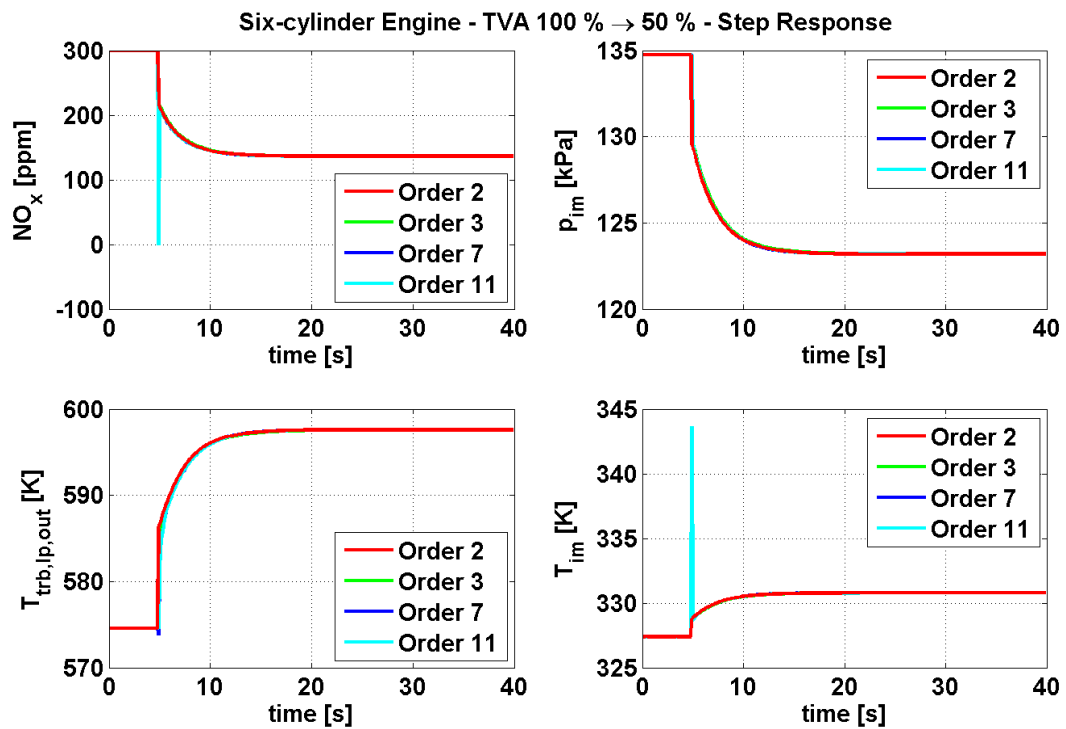


Fig. 5.7 – A six-cylinder bi-turbocharged engine – state reduction (TVA valve)



6. Conclusion

The main goal of this diploma thesis is to verify and modify a computer model (a block library for model creation) of the combustion engine for the modern controller design based on models such as MPC. This library has been developed by Honeywell company. In order to create a model, engineers have to connect the blocks according to the technological scheme and fit its parameters using data acquired from a real engine.

A combustion engine is a very complicated system. That is why its simulation scheme was simplified to fit our requirements. It is not necessary to obtain a complex engine model but it is important to obtain the model suitable for the advanced controller design. The developed library uses basic physical principles of thermodynamics and fluids dynamics and some empirically determined characteristics (a turbine and a compressor efficiency, etc.).

The library was verified using data acquired from two different engines – a four-cylinder, 2.2 l, turbocharged diesel engine and a six-cylinder, 12 l, bi-turbocharged heavy duty diesel engine. Comparison of the steady states and transient data shows that the simplification and the library design has been done correctly and it meets the requirements for tolerances between the model and the data. A robust controller can handle a big difference between the model quantity value and the real data. A serious problem for the robust controller could be a gain sign difference. Tests show that sign changes occur only in the area near zero where they are acceptable.

A well connected and fitted model has several issues to deal with. There are both fast and slow states. Systems with such characteristics are called stiff systems. Stiffness and nonlinear quantity dependencies acting together cause a lot of problems during a simulation – long duration of the simulation, numerical mistakes, crash of the simulation, etc.

These problems were reduced (solved) by changing the model design by using the constrained state reduction. This method modifies the model design by reducing the number of states and adds a possibility to specify criteria for quantity boundaries (physical barriers and limits, etc.).



The best results are achieved when the number of slow states was reduced to the number of turbochargers. It means that only the turbocharger rotating shafts act like slow states. It is assumed that the other states are fast. Their values are found through optimizing under the main criteria of their zero derivations.

The constrained state reduction improves numerical stability and shortens duration of the simulation because it finds values of the fast states in the appropriate region. This method also removes peaks at the step time. These peaks do not occur in a real engine.

The next step is to develop more effectively optimized algorithms and to set up other criteria for fast states according to physical boundaries and limits. Fast and slow parts of the model have to correspond not only with the states but also with the combinations of the states. Further progression in the division of the system into the fast and slow parts also enhances the numerical stability of the simulation. These improvements should be made by spectral decomposition of the state equation matrices. Refining the empirically found dependencies between quantities such as turbocharger efficiency leads to achieving a more accurate model as well.



7. References

- [1] GUZZELA L., ONDER CH., *Introduction to Modeling and Control of Internal Combustion Engine System*, Berlin, Heidelberg, Springer-Verlag, 2010.
- [2] ERICSON C., *Model Based Optimization of a Complete Diesel Engine/SCR System*, Lund, Lund University – Faculty of Engineering, Department of Energy Sciences, Doctoral Thesis, 2009.
- [3] Emmisions Standards: Europe: Heavy-Duty Diesel Truck and Bus Engines
<http://www.dieselnet.com/standards/eu/hd.php>, Ecopoint Inc., 09.2009.
- [4] *Energy efficiency of vehicles*
http://resources.edb.gov.hk/~senenergy/transport/print/vehicle_phy_print_e.html,
Ecopoint Inc., 02.2010.
- [5] HEYWOOD J. B., *Internal Combustion Engine Fundamentals*, New York, McGraw-Hill Science/Engineering/Math, 2010.
- [6] POINSOT T., VEYNANTE D., *Theoretical and numerical combustion*, Philadelphia, R.T. Edwards, Inc., 2001.
- [7] JENSEN J.-P., KRISTENSEN A. F., SORENSON S. C., HOUBEK N., HENDRICKS E., *Mean Value Modelling of a Small Turbocharged Diesel Engine*, Detroit, SAE 910070, 1991.
- [8] MORAAL P., KOLMANOVSKY I., *Turbocharger Modeling for Automotive Control Applications*, Detroit, SAE 1999-01-0908, 1999.
- [9] WINKLER G., *Steady State and Dynamic Modeling of Engine Turbomachinery Systems, PhD. Thesis*, University of Bath, 1977.
- [10] TAYLOR C. F., *Internal Combustion Engine in Theory and Practice*, The MIT Press (several re-editions).
- [11] CURTIS C. F., HIRSCHFELDER J. O., *Integration of Stiff Equations*, The Naval Research Laboratory, University of Wisconsin, Madison, 1951.
- [12] *Explicit and implicit methods*, Wikipedia,
http://en.wikipedia.org/wiki/Explicit_and_implicit_methods, 17 Dec 2009.



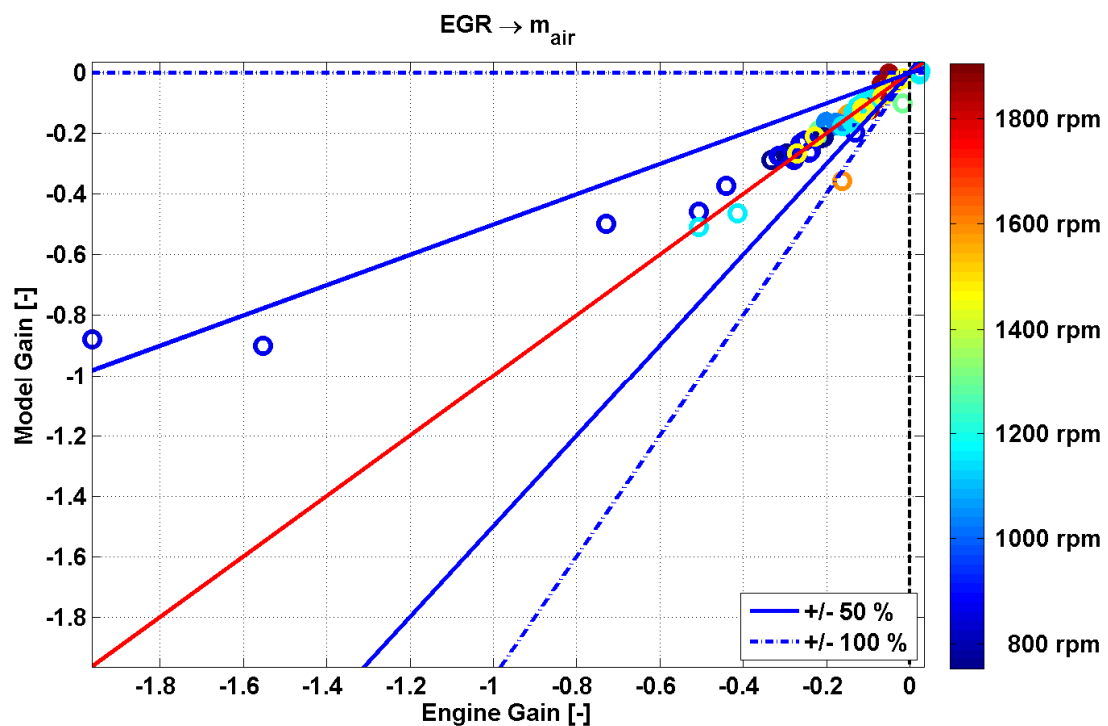
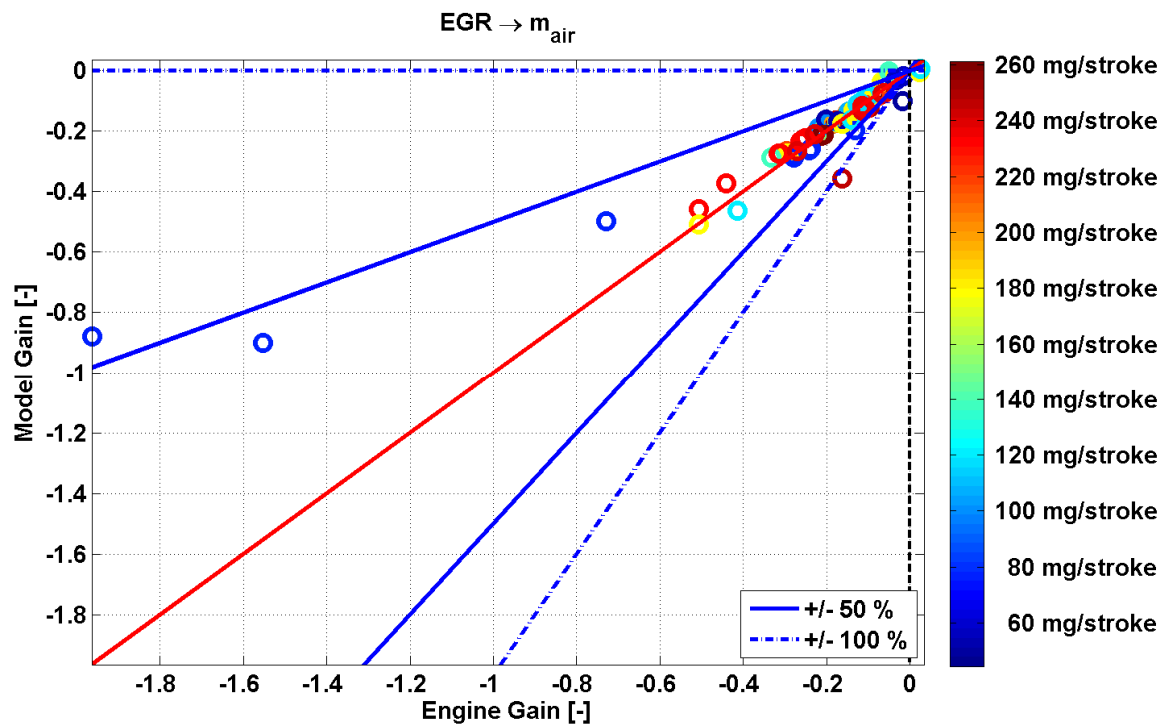
- [13] FROLOVSKY V. D., LANDOVSKY V. V., *Explicit and Implicit Integration in the Problem of Modeling of Fabric Based on Particles Method*, KORUS'2005, IEEE Informational Technologies, 2005.

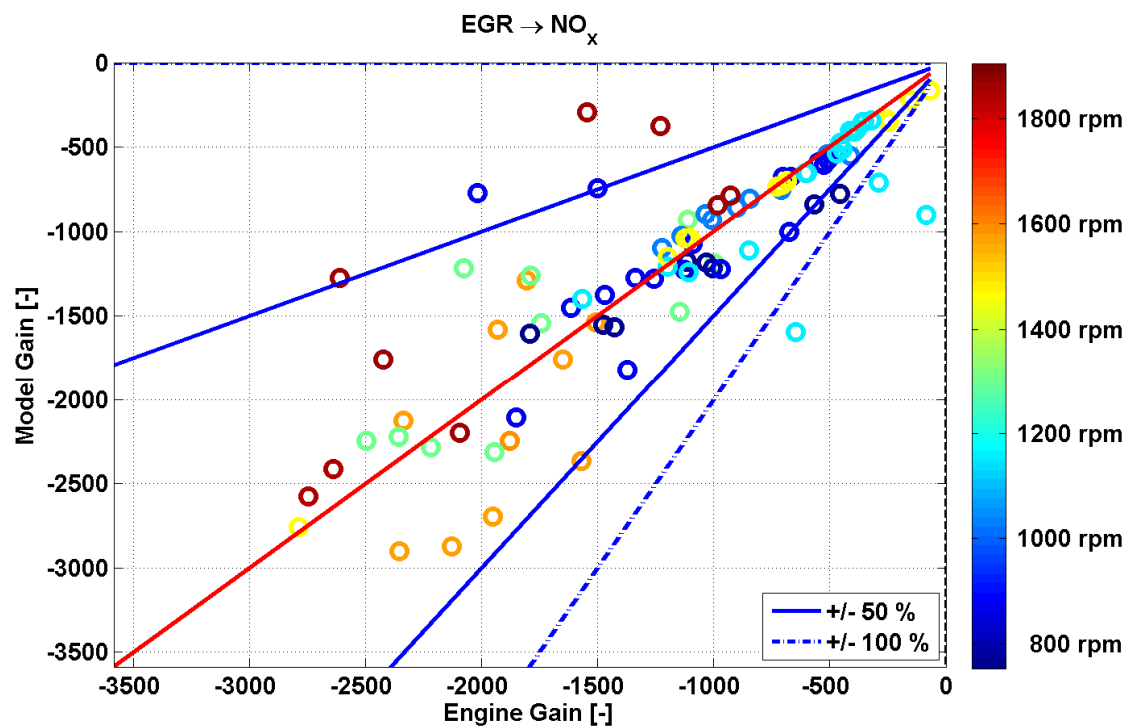
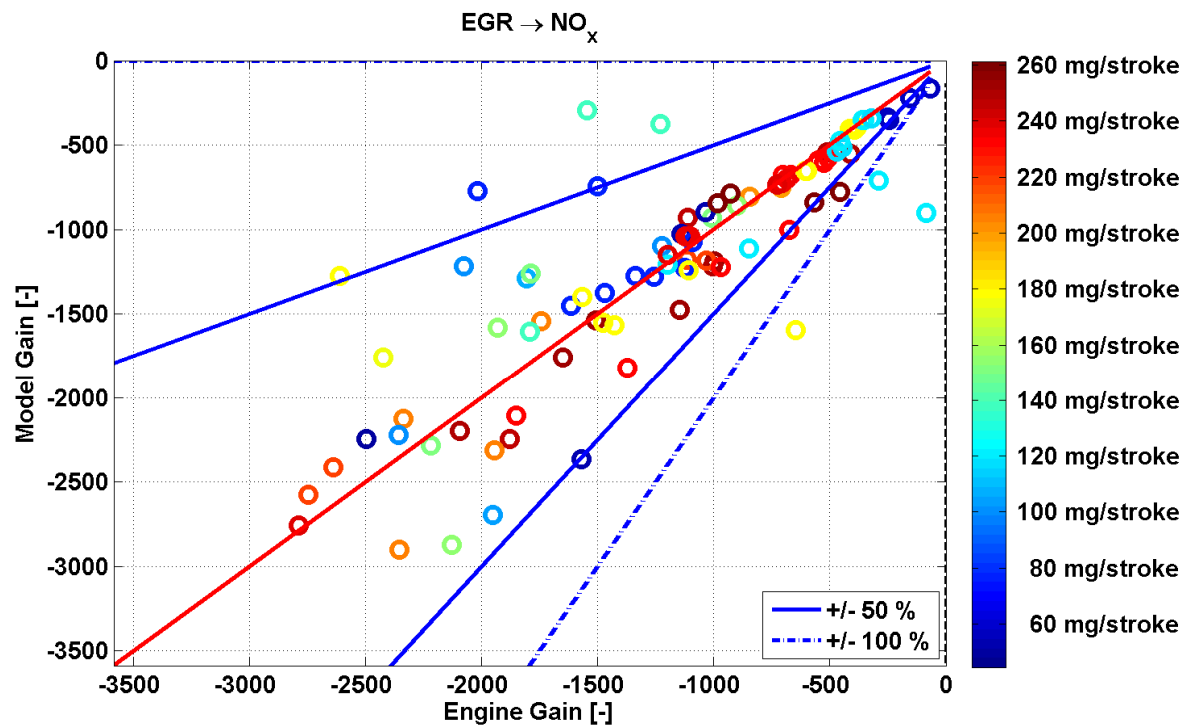
- [14] TRIPATHY S. C., RAO N. D., ELANGO VAN S., *Comparison of Stability Properties of Numerical Integration Methods for Switching Surges*, IEEE Transactions on Power Apparatus and System, Vol. PAS-97, No. 6, Nov/Dec 1978.

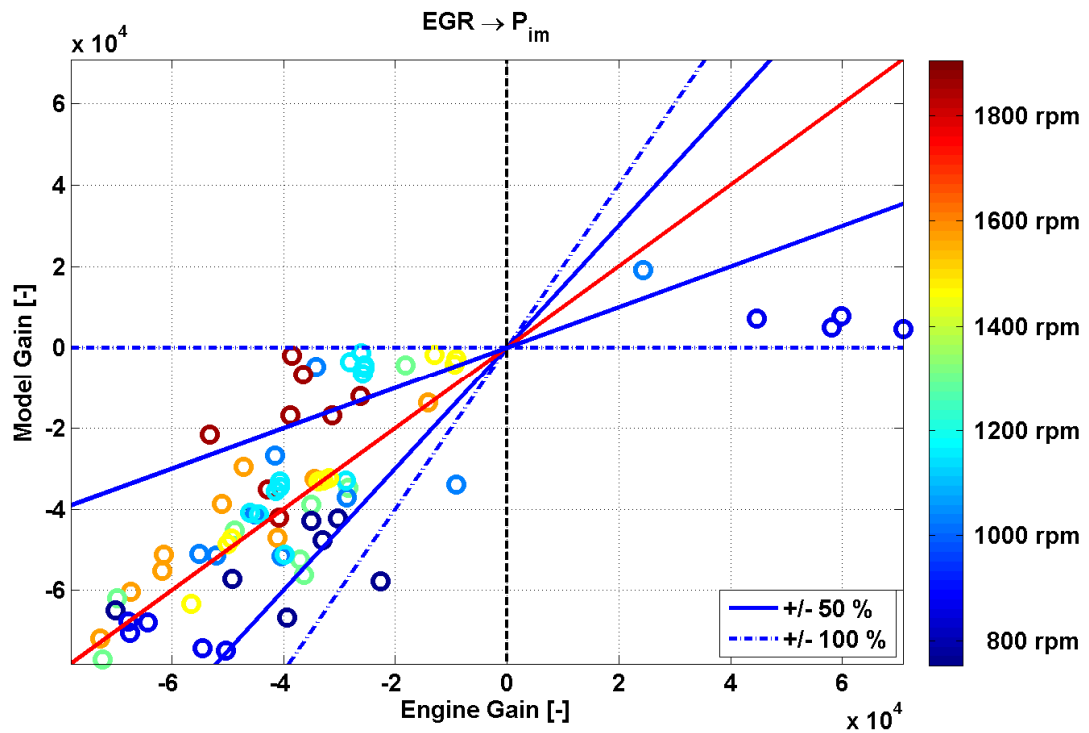
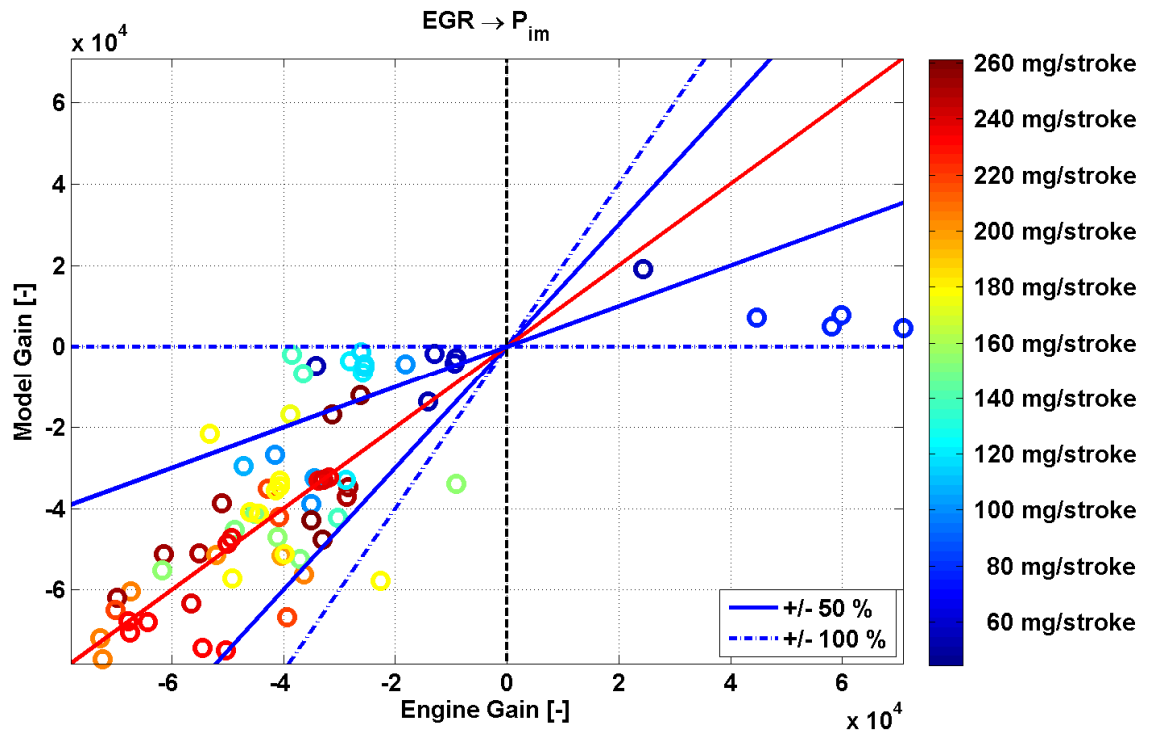


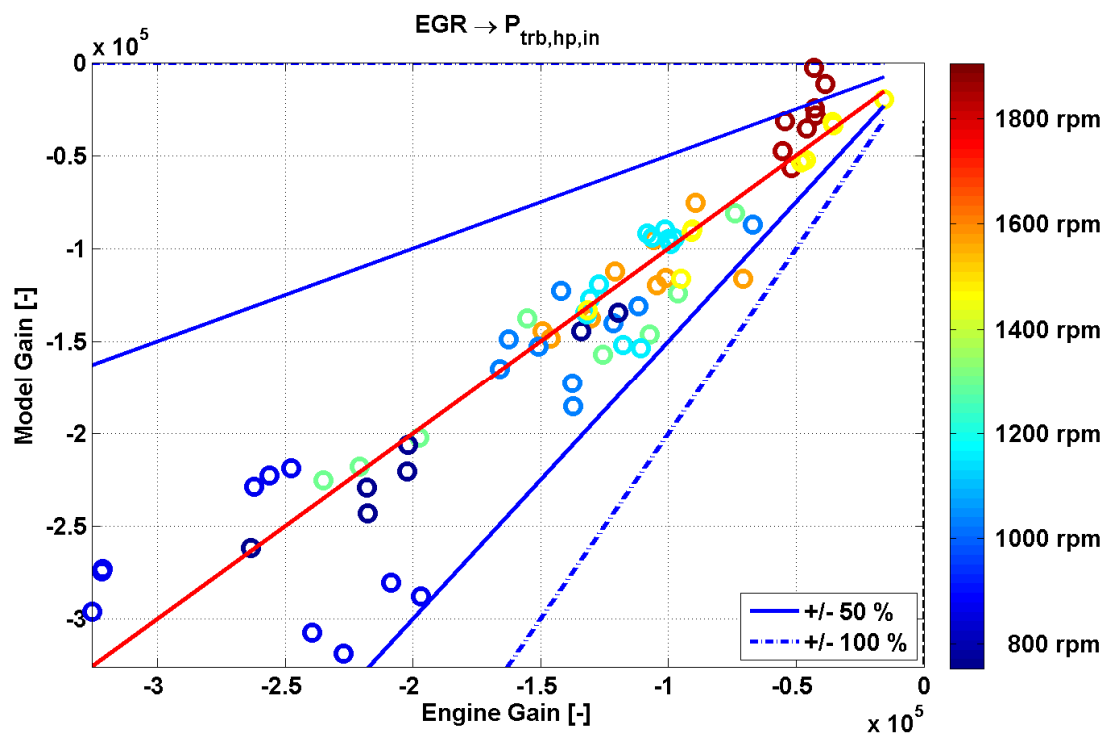
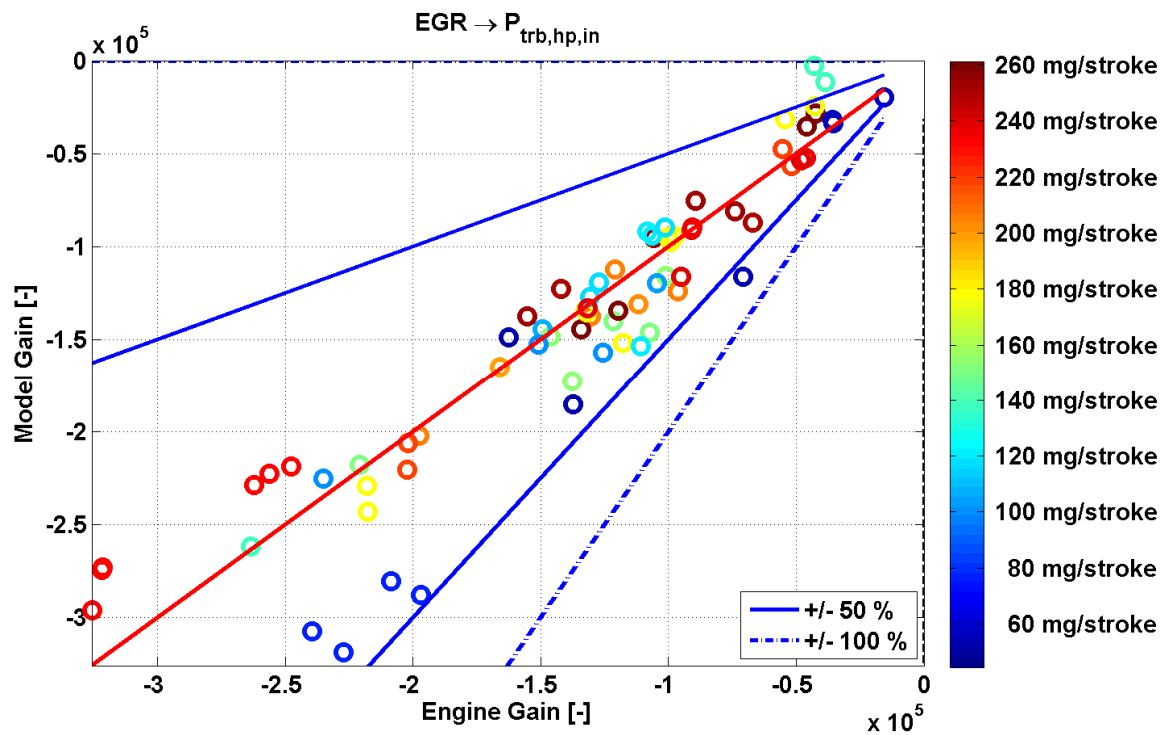
8. Appendix

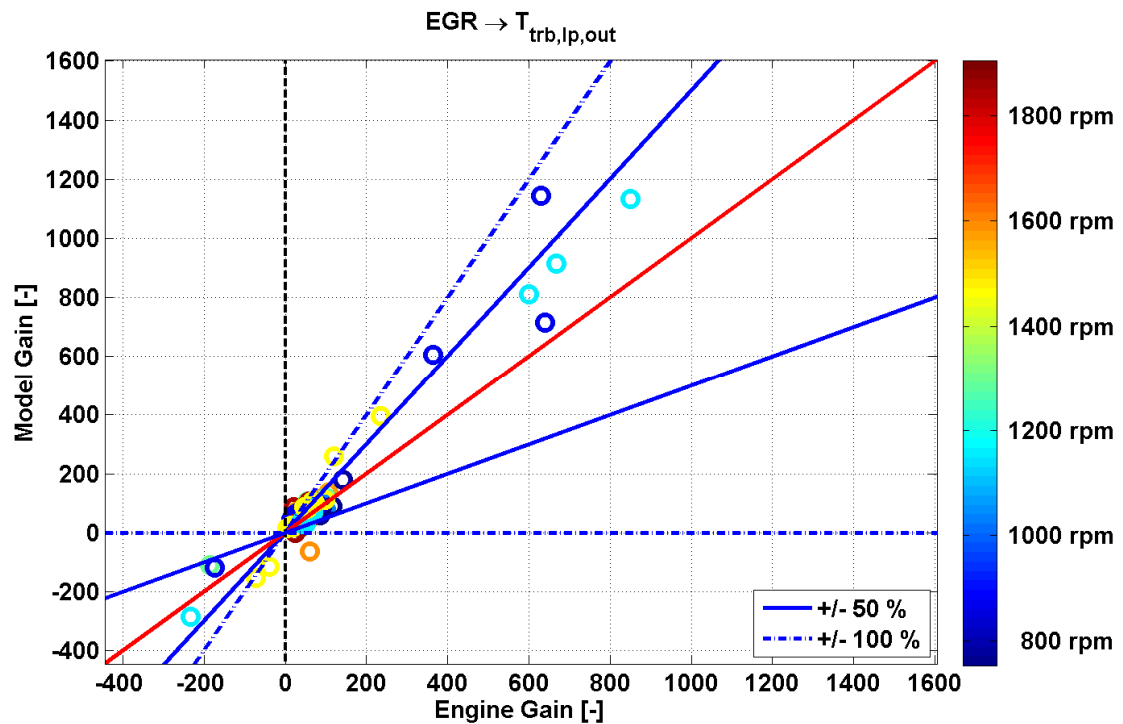
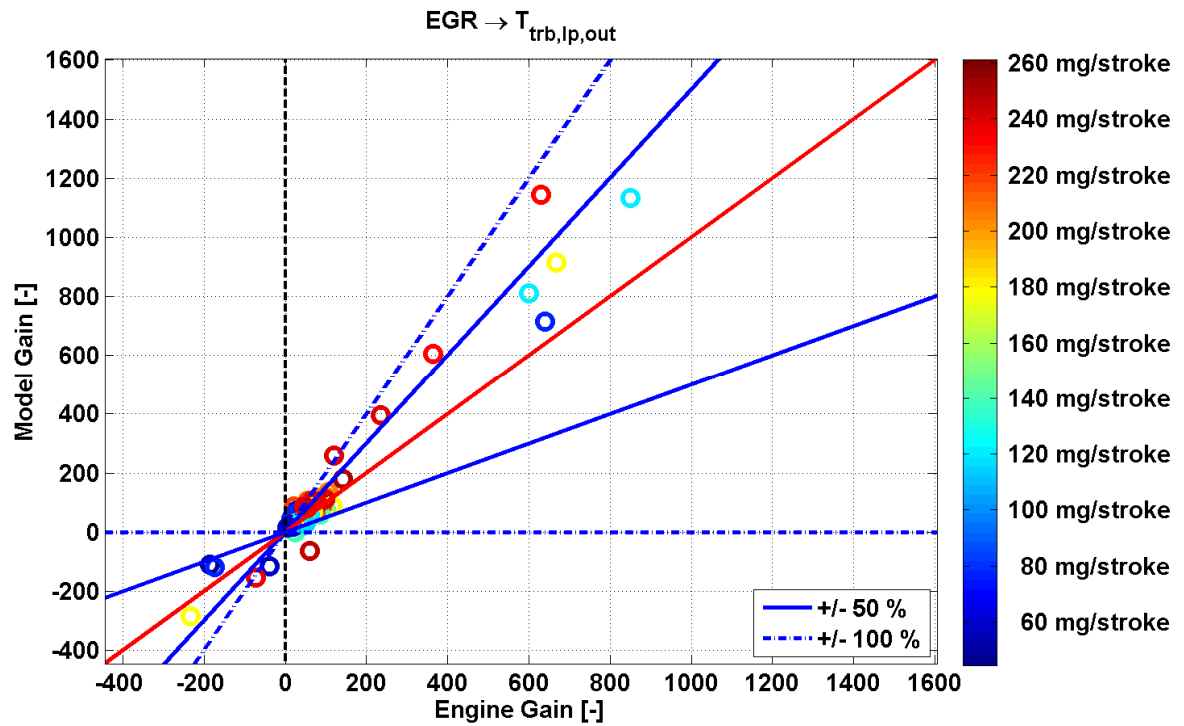
8.1. Six-cylinder Bi-turbocharged Engine – Gain and Time Constant

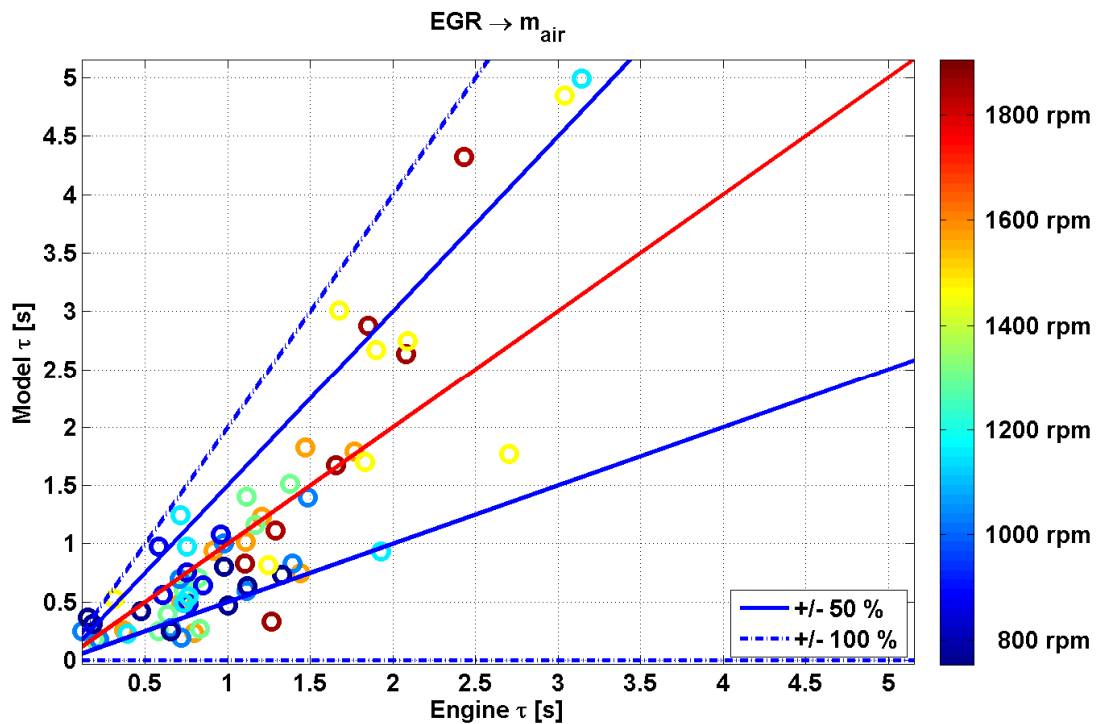
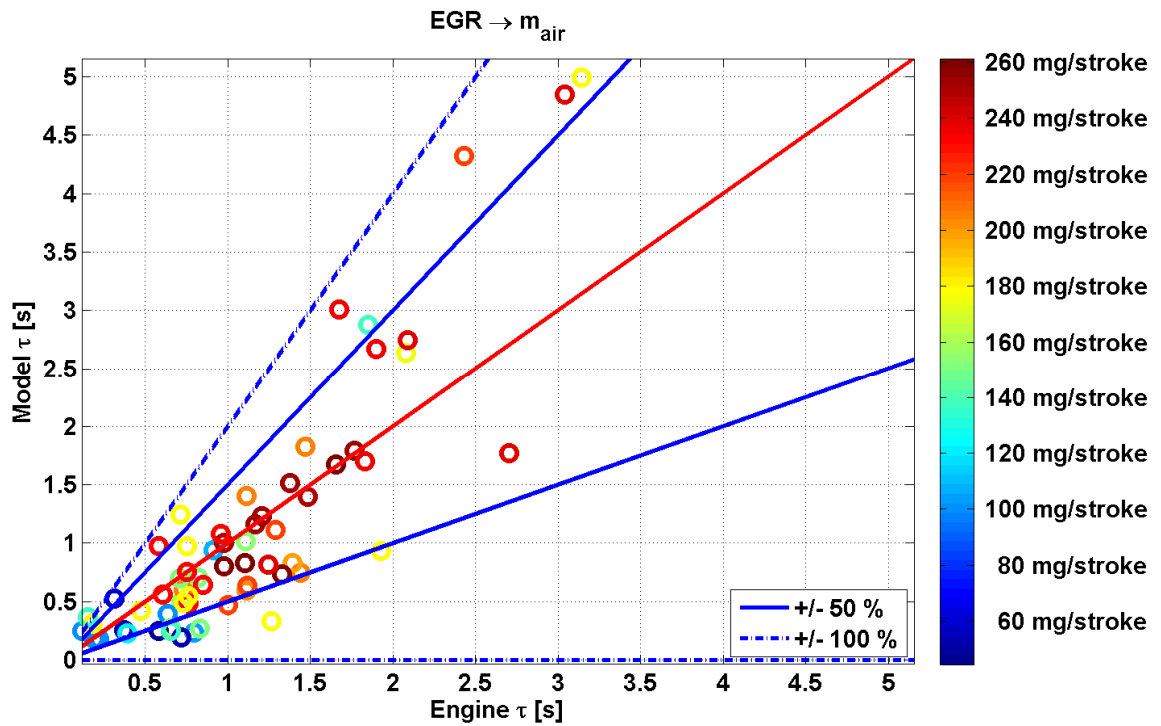


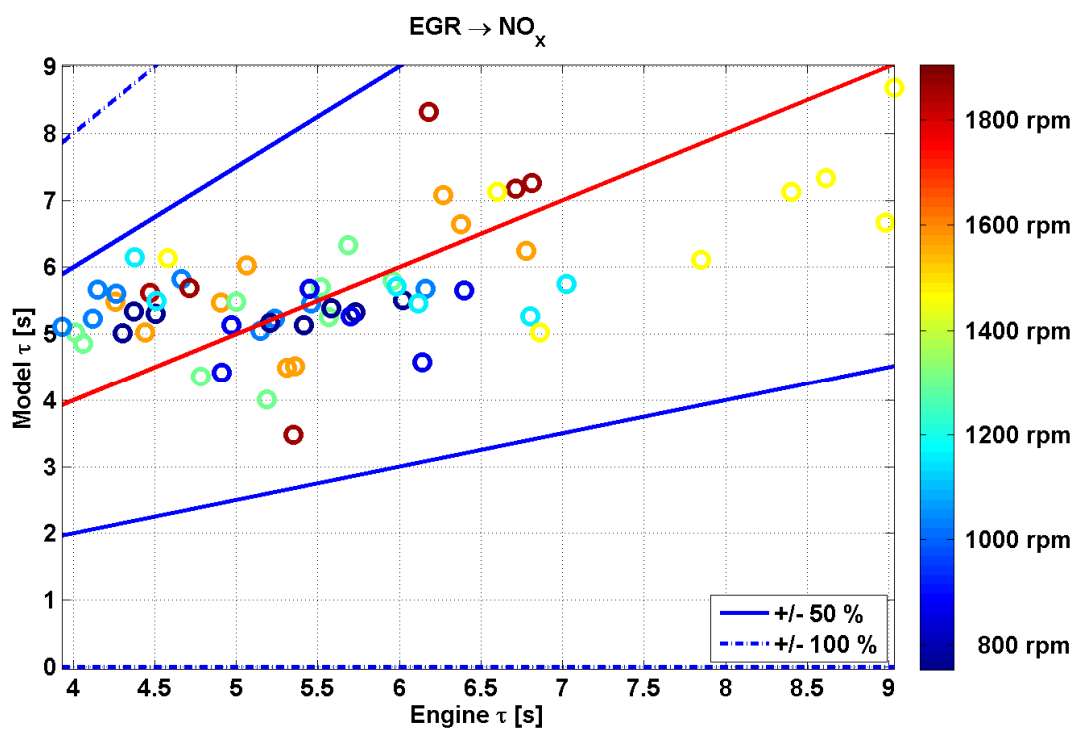
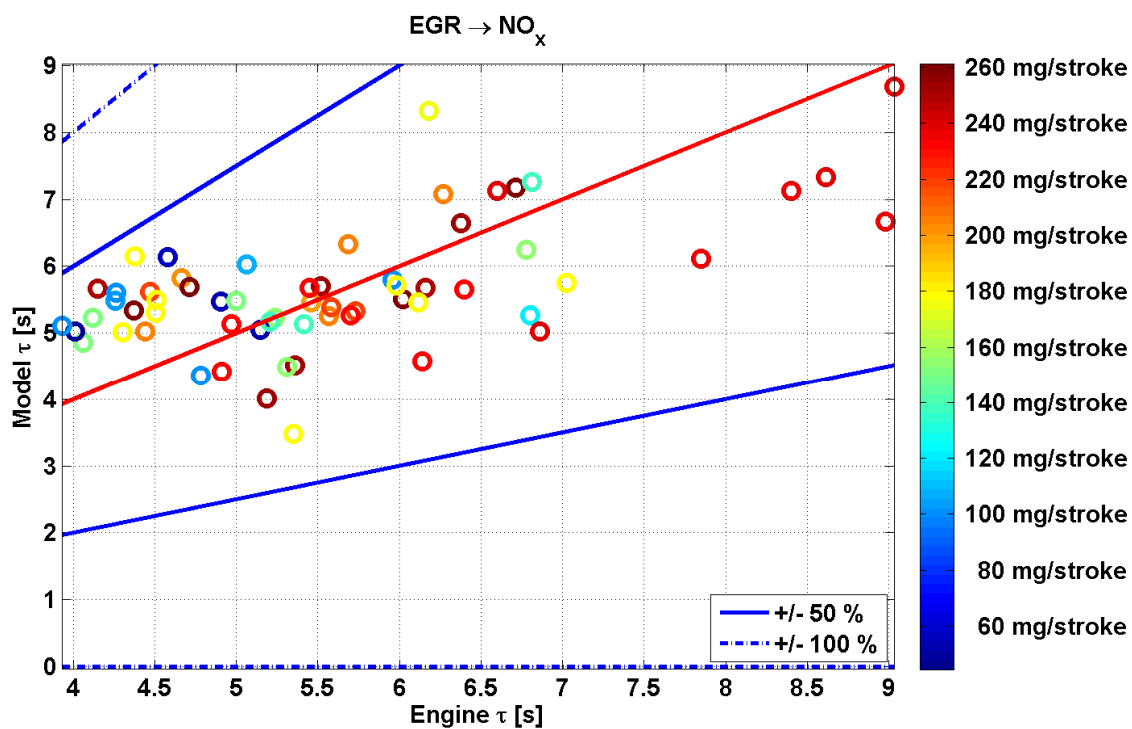


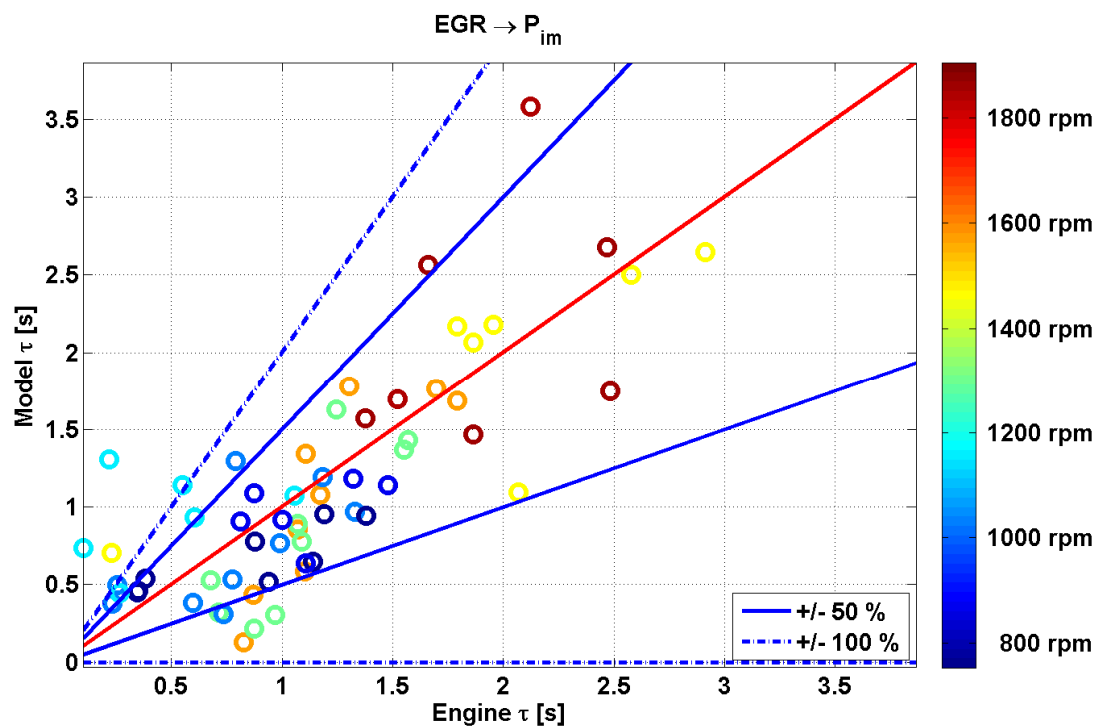
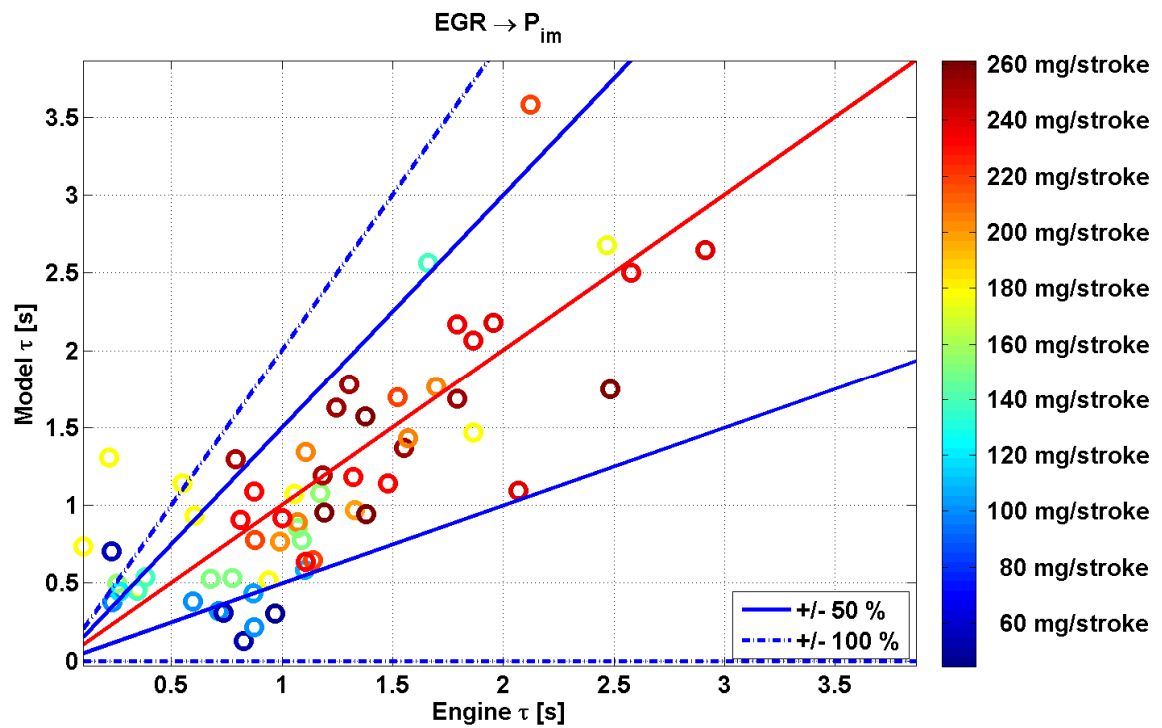


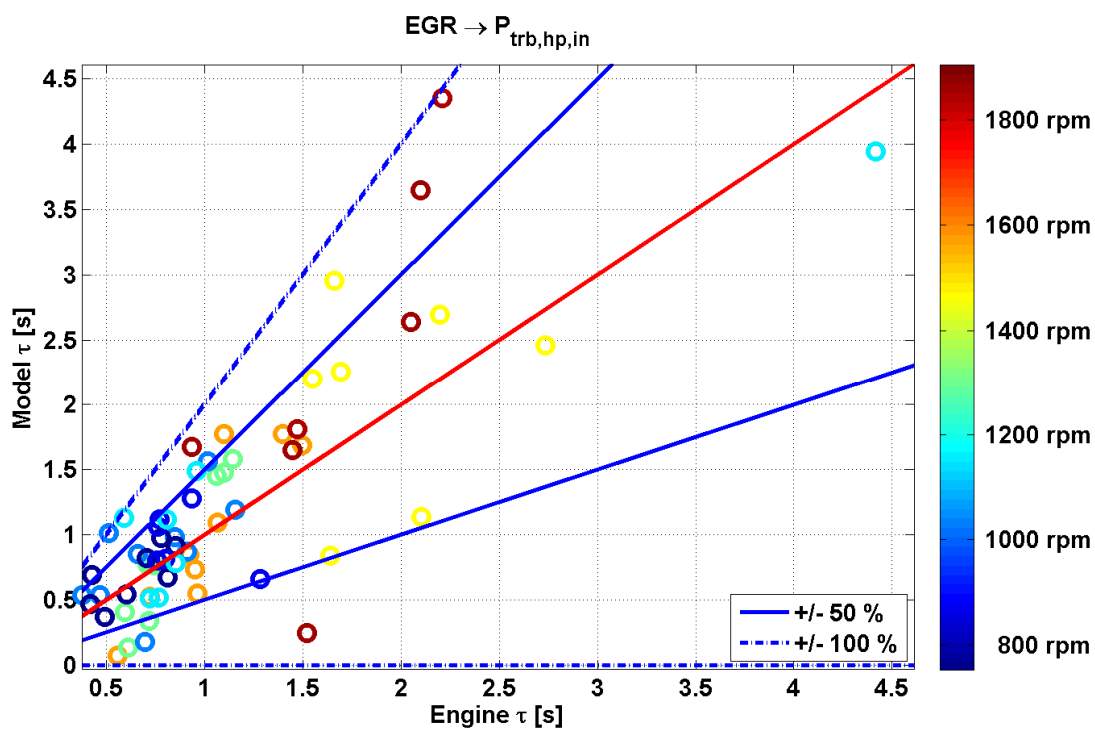
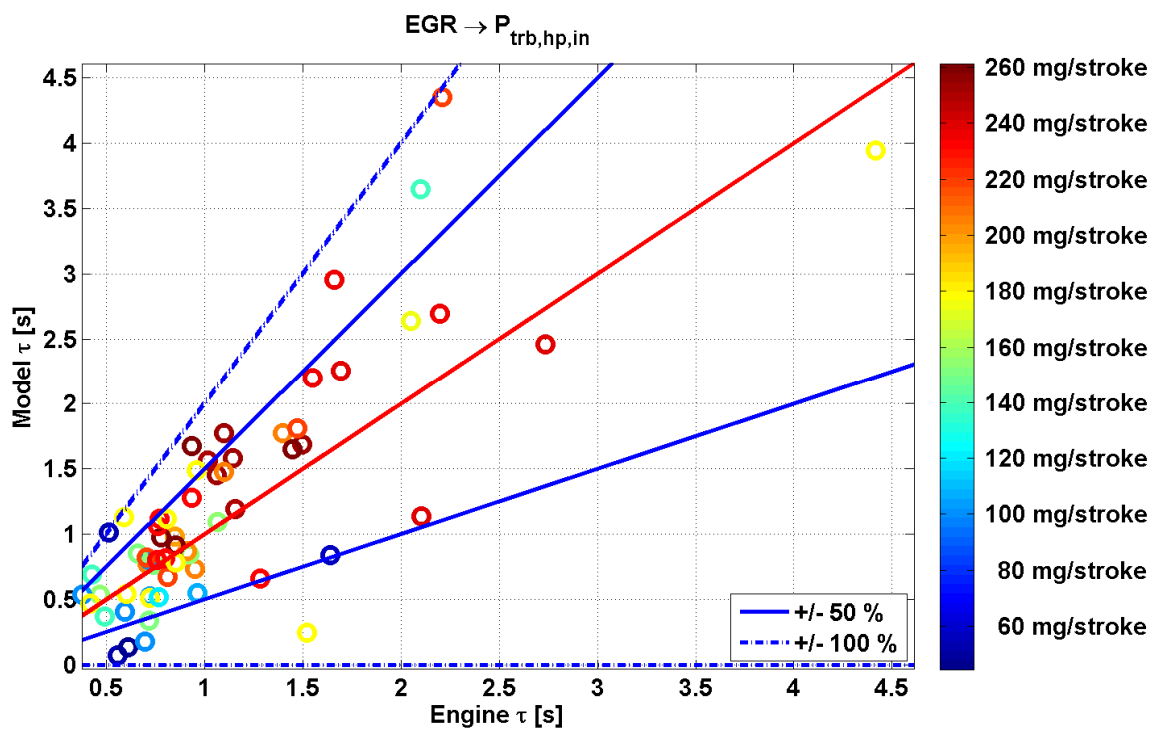


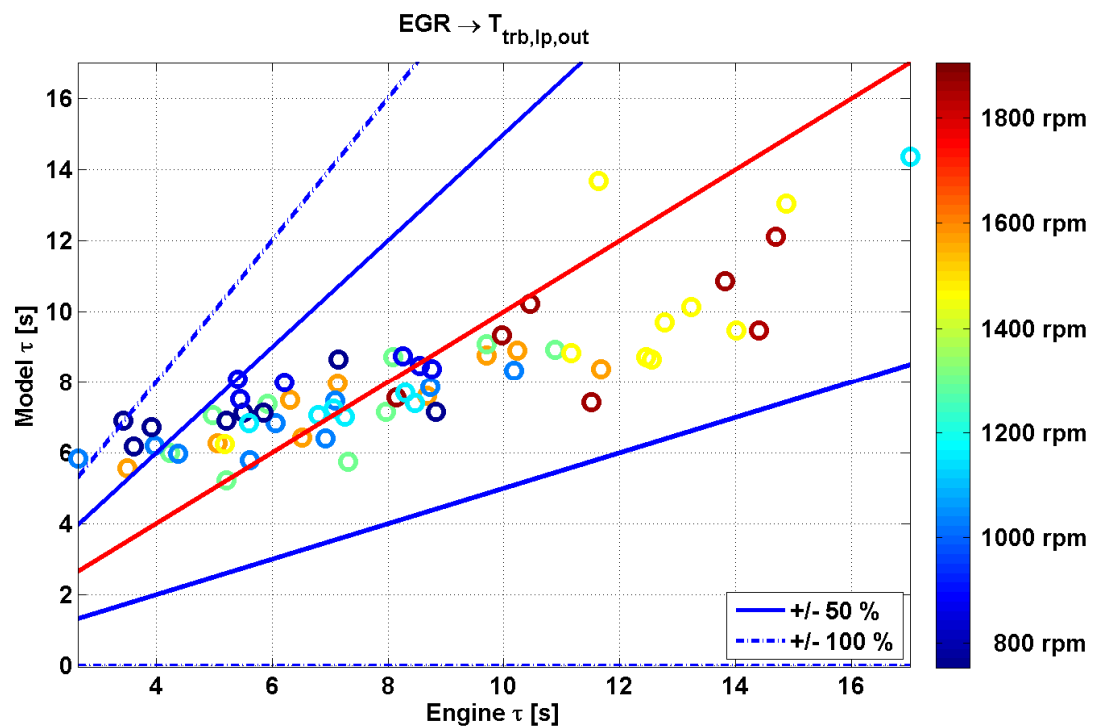
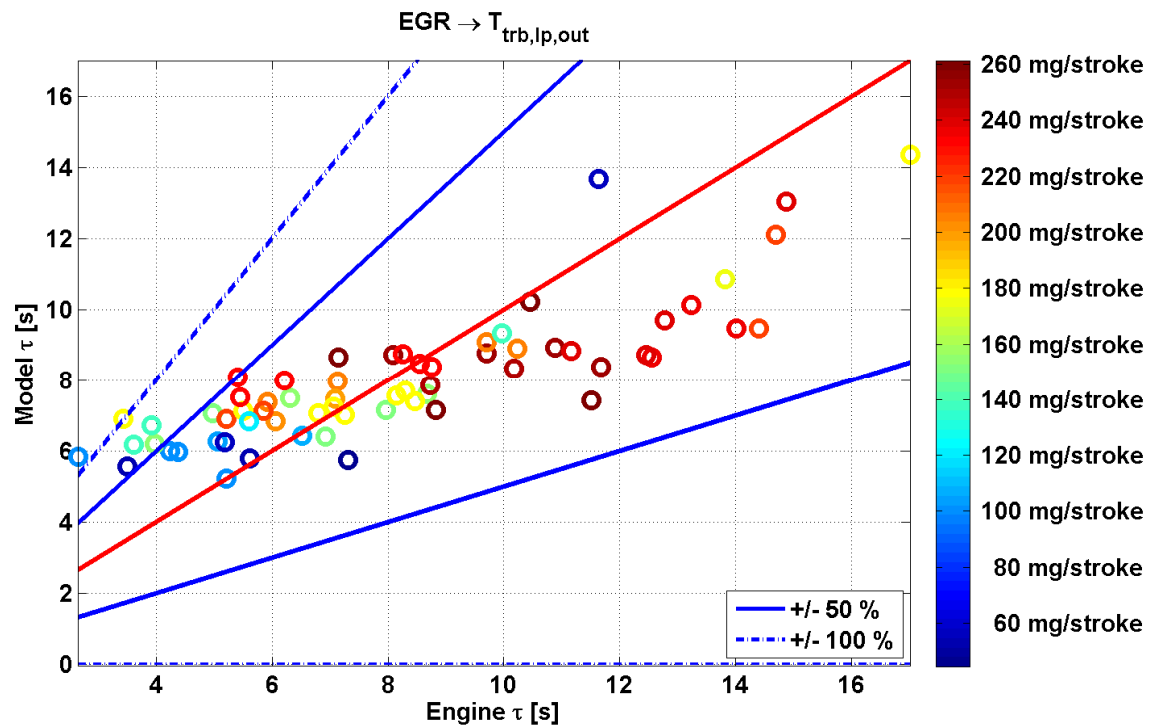


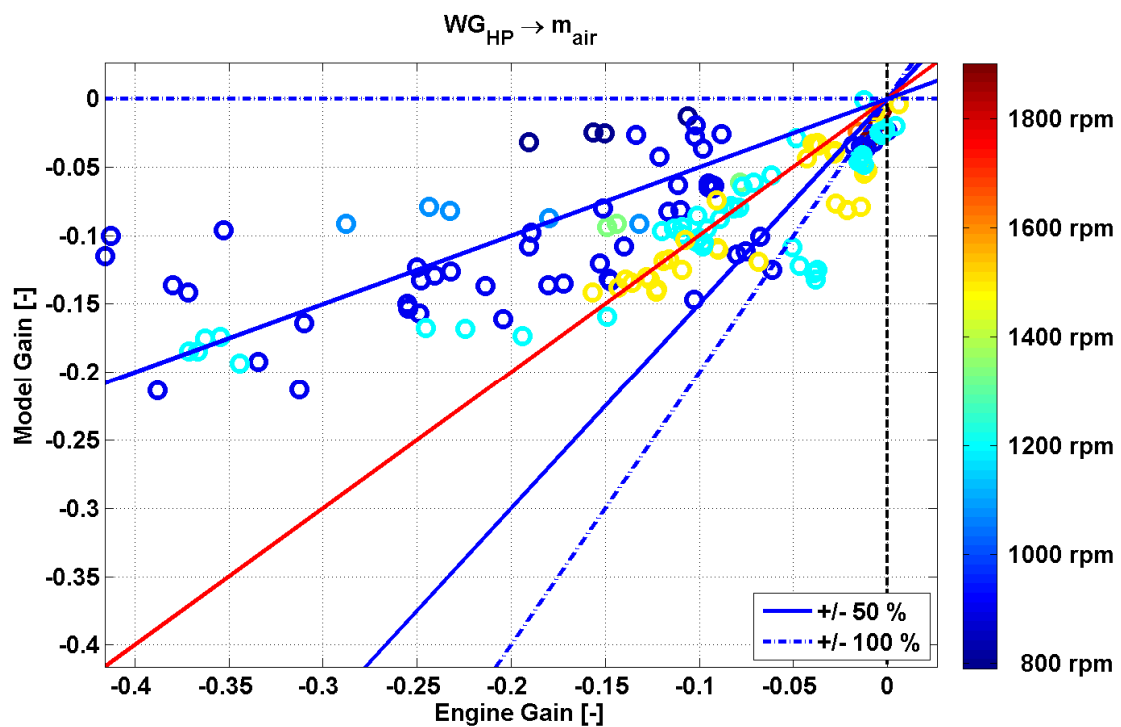
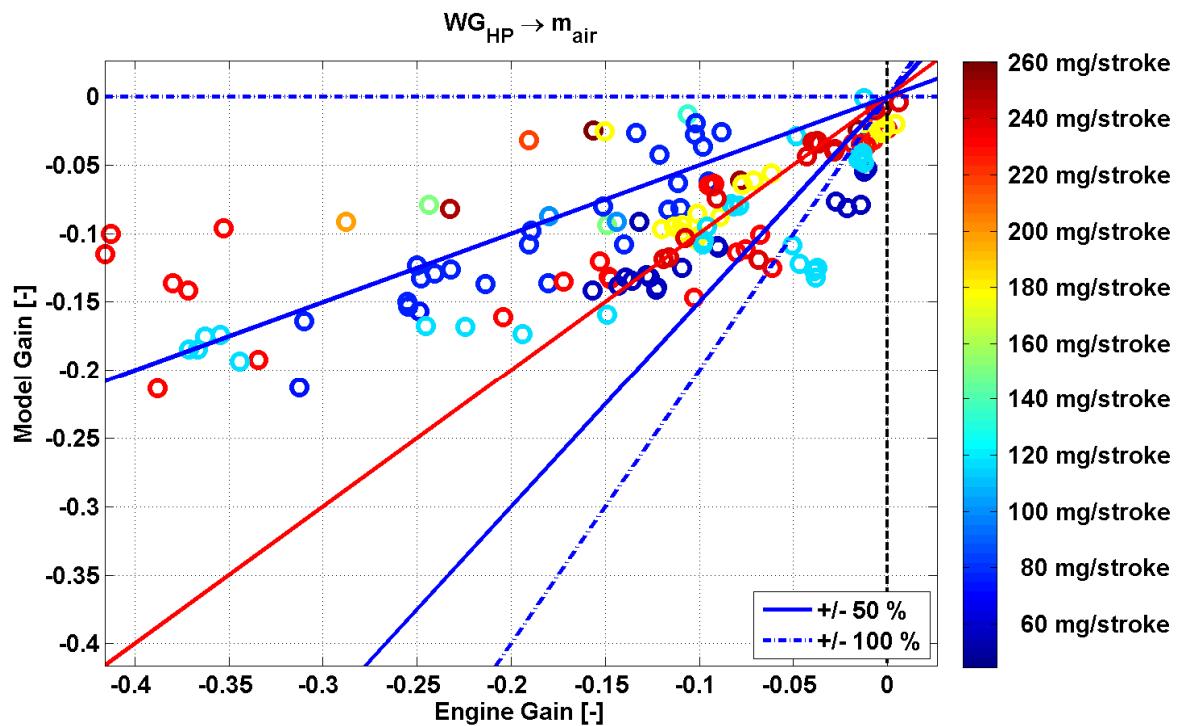


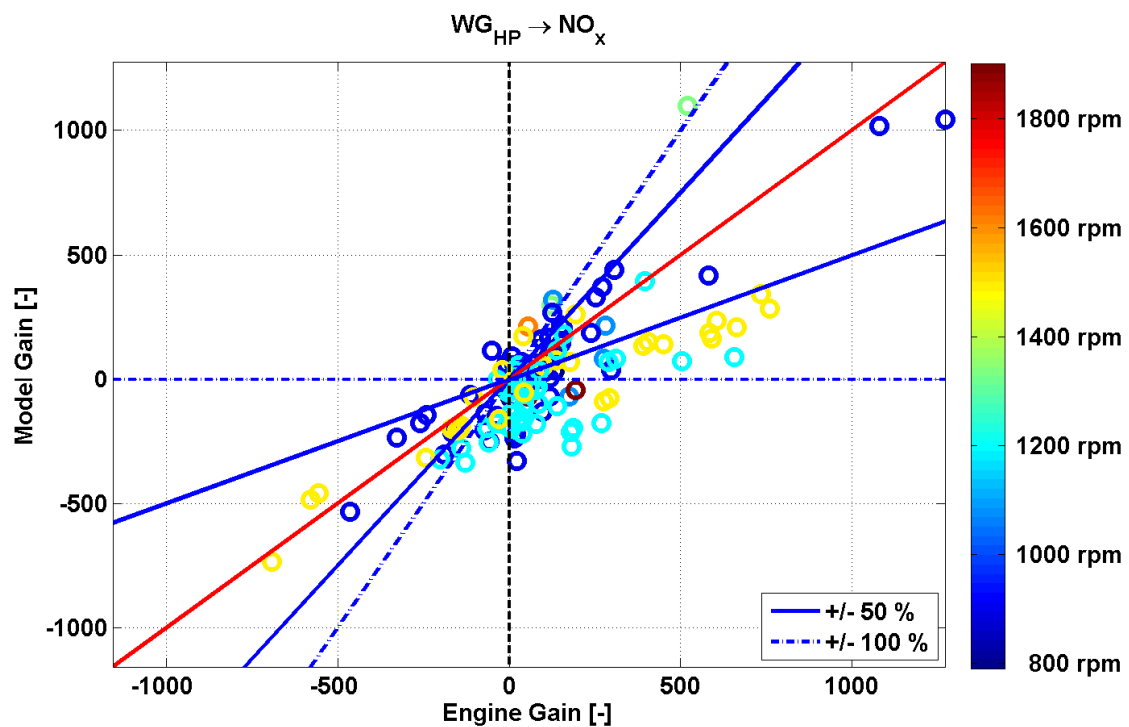
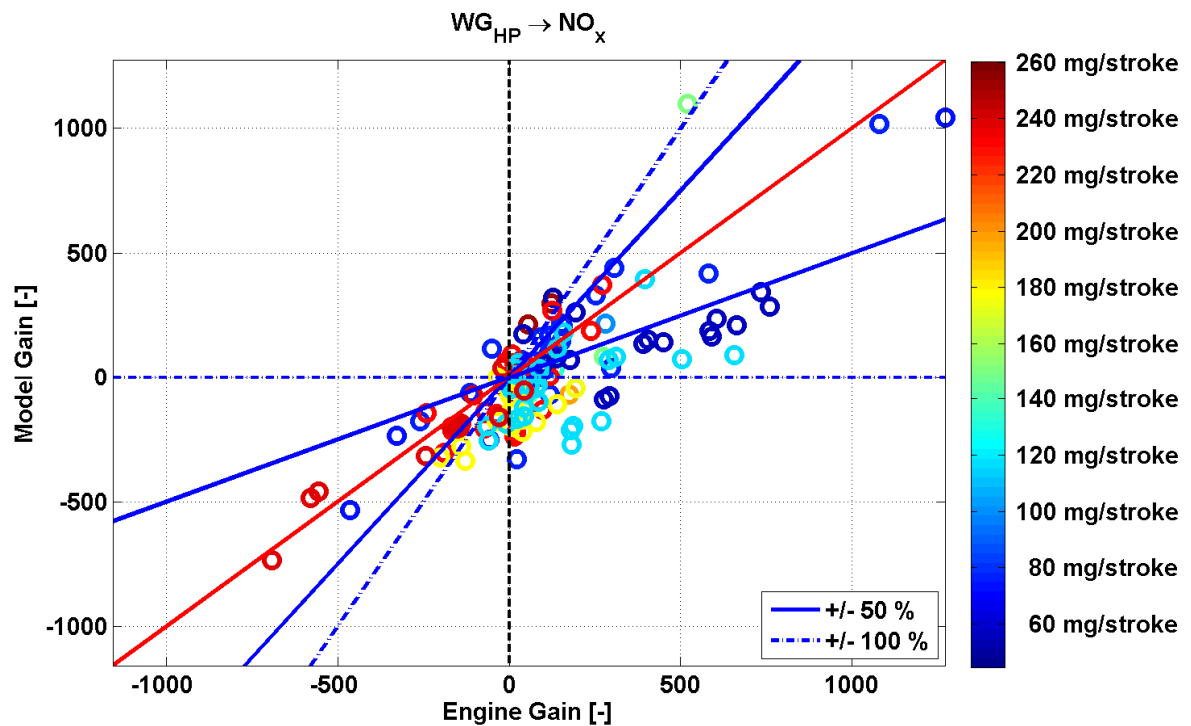


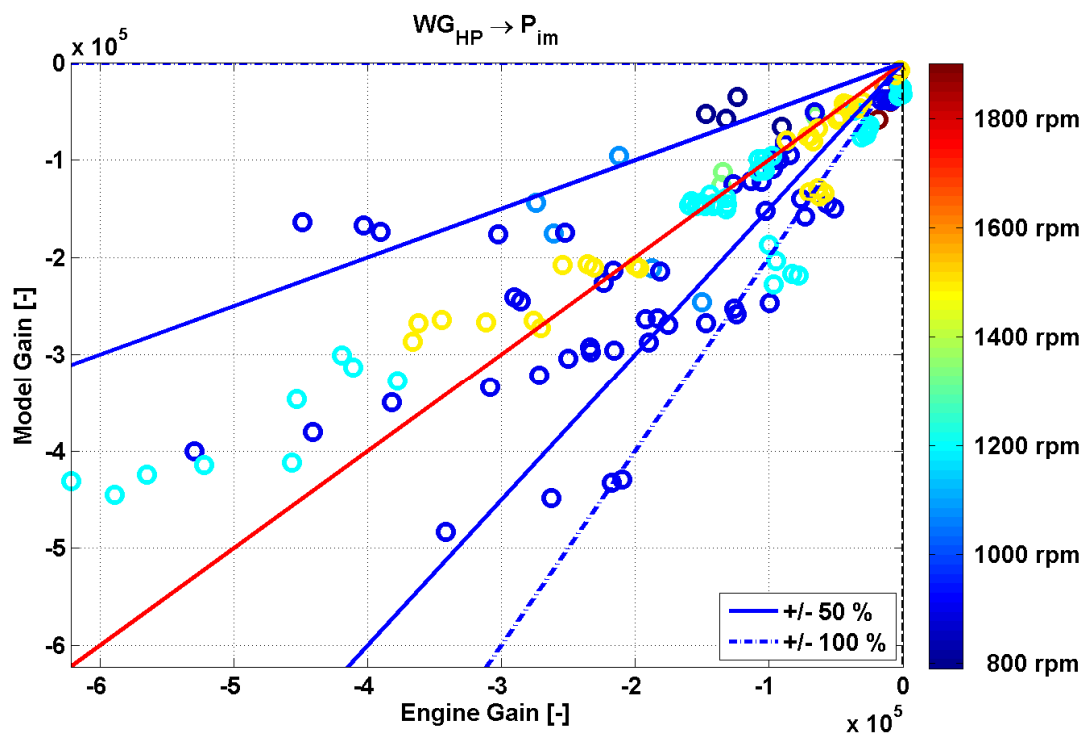
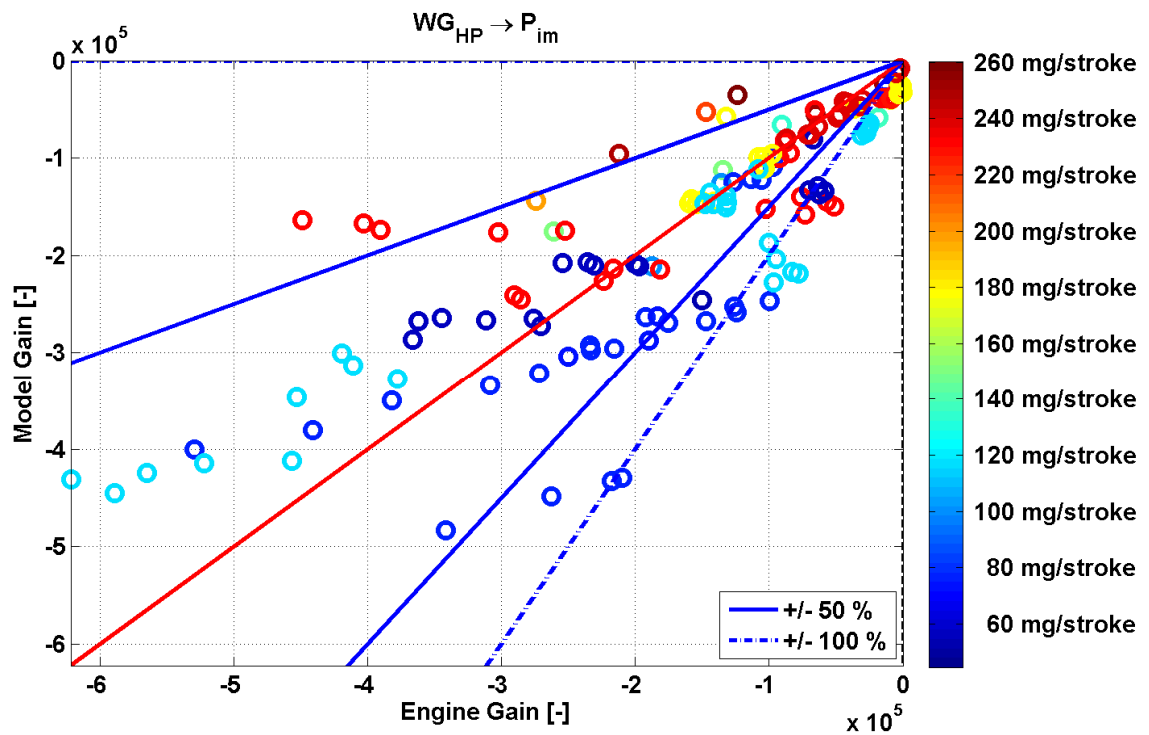


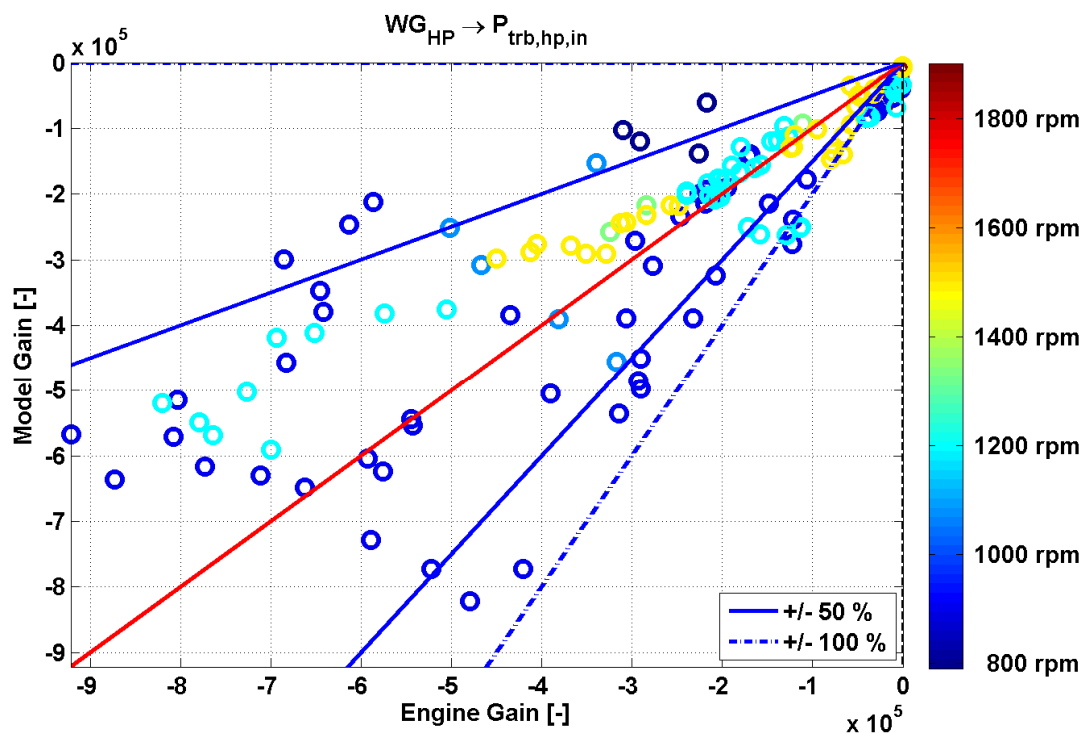
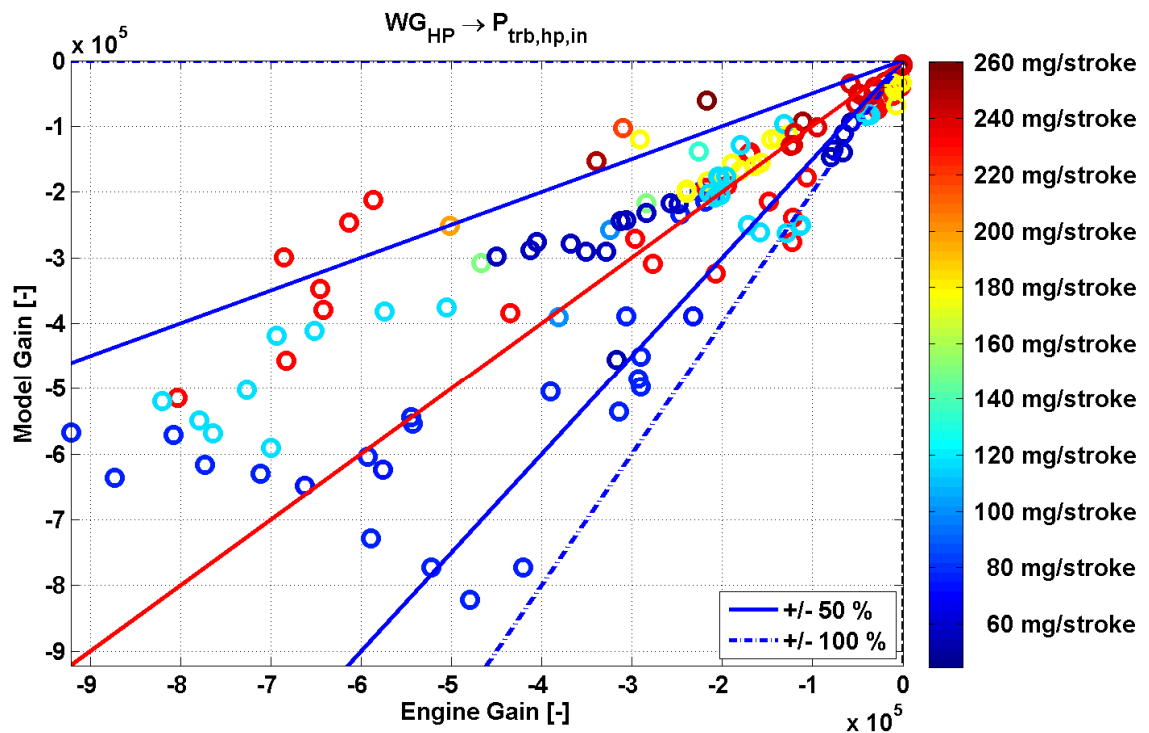


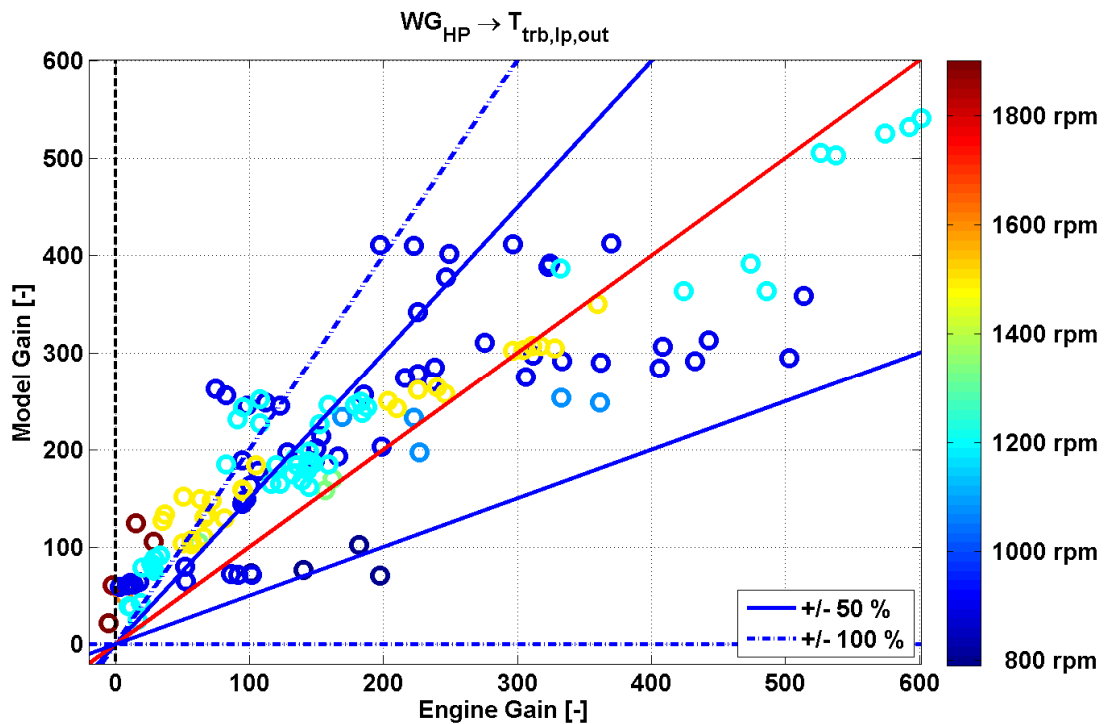
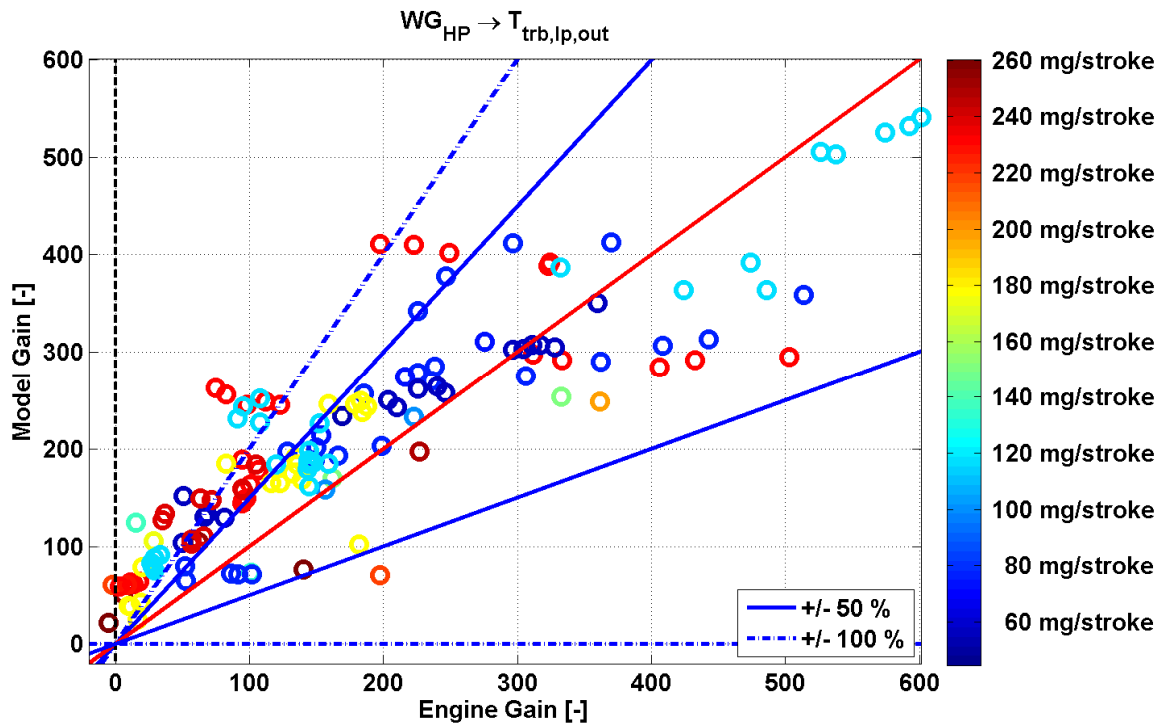


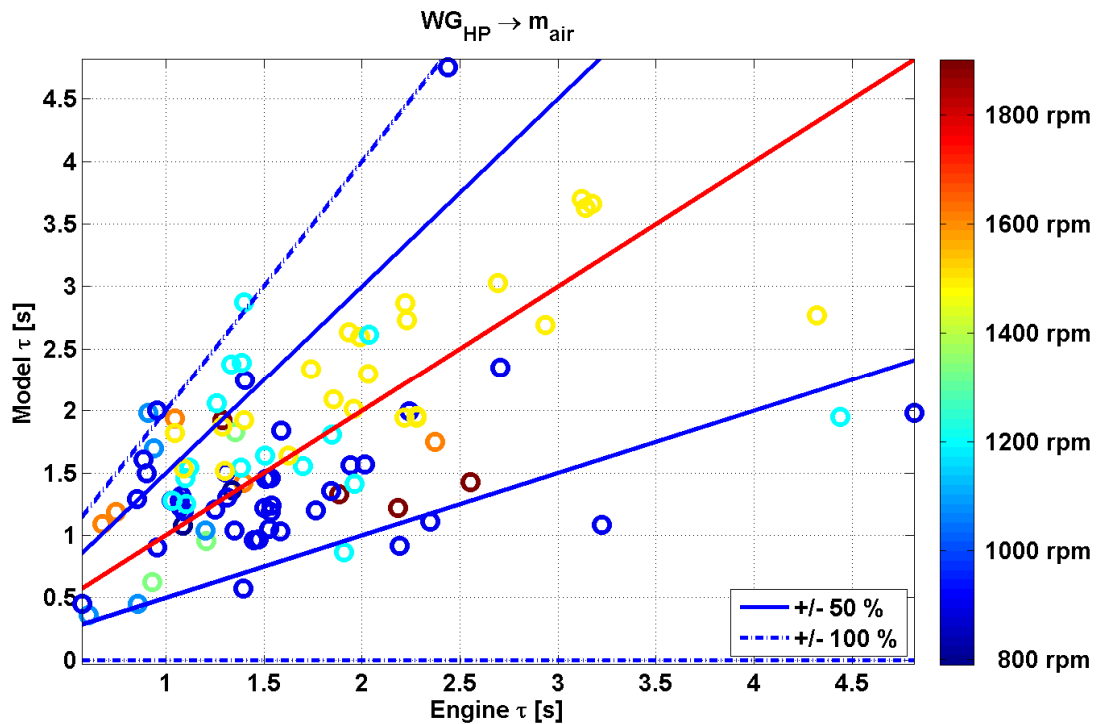
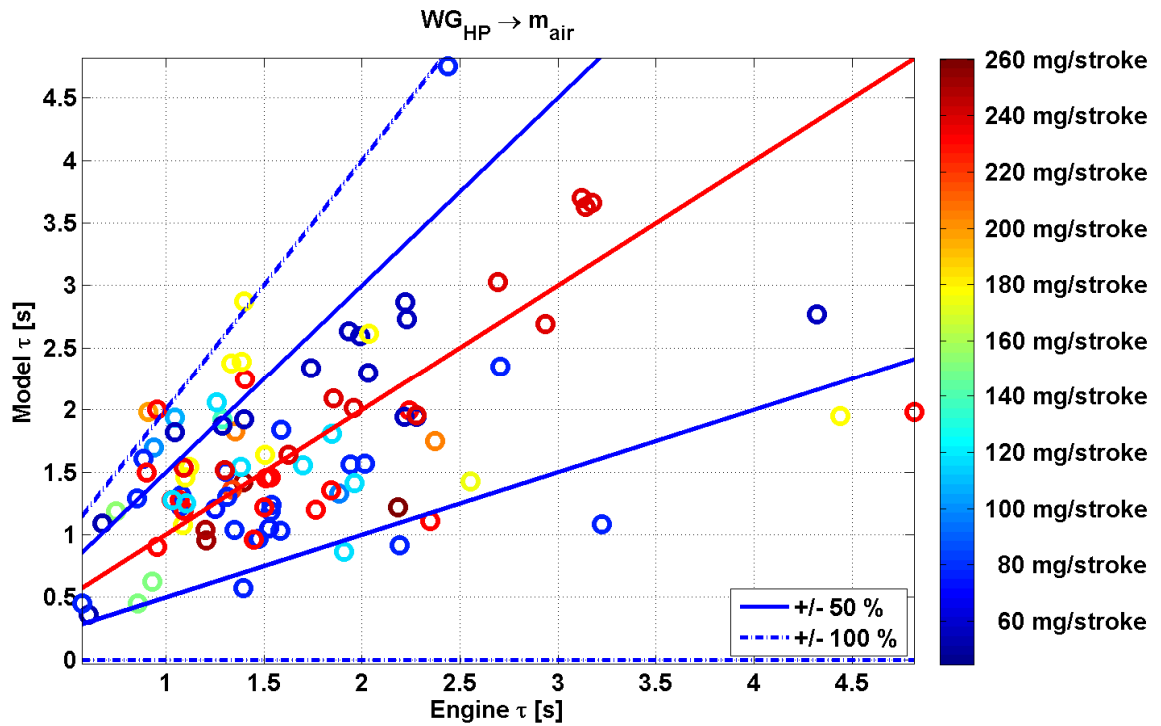


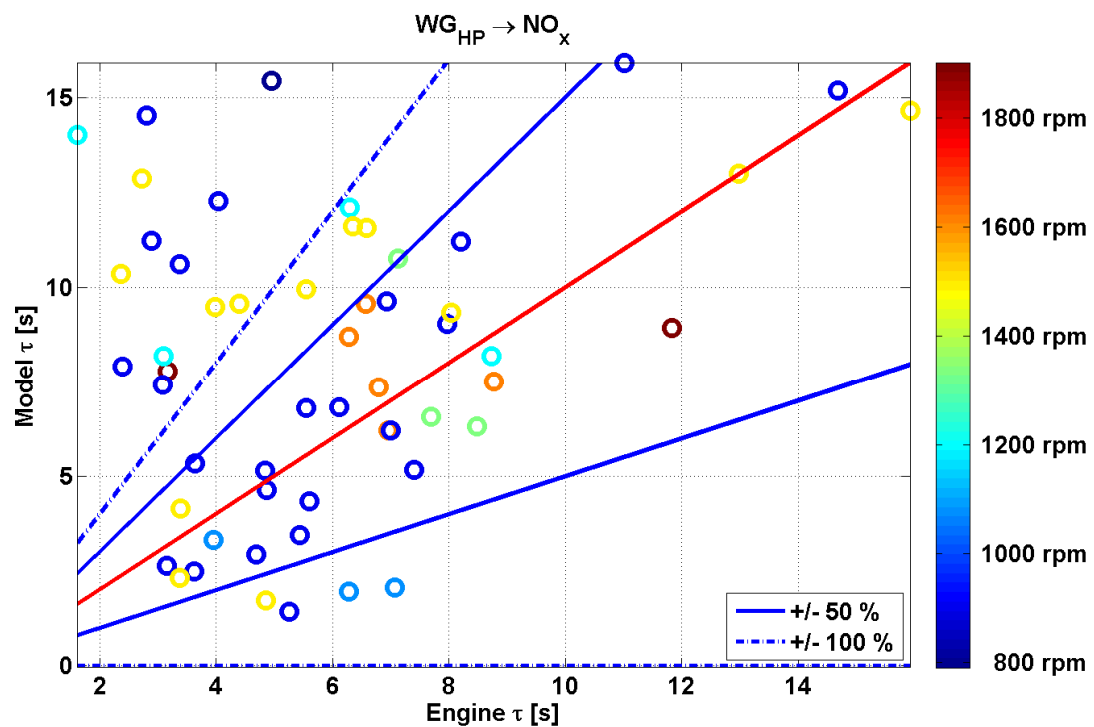
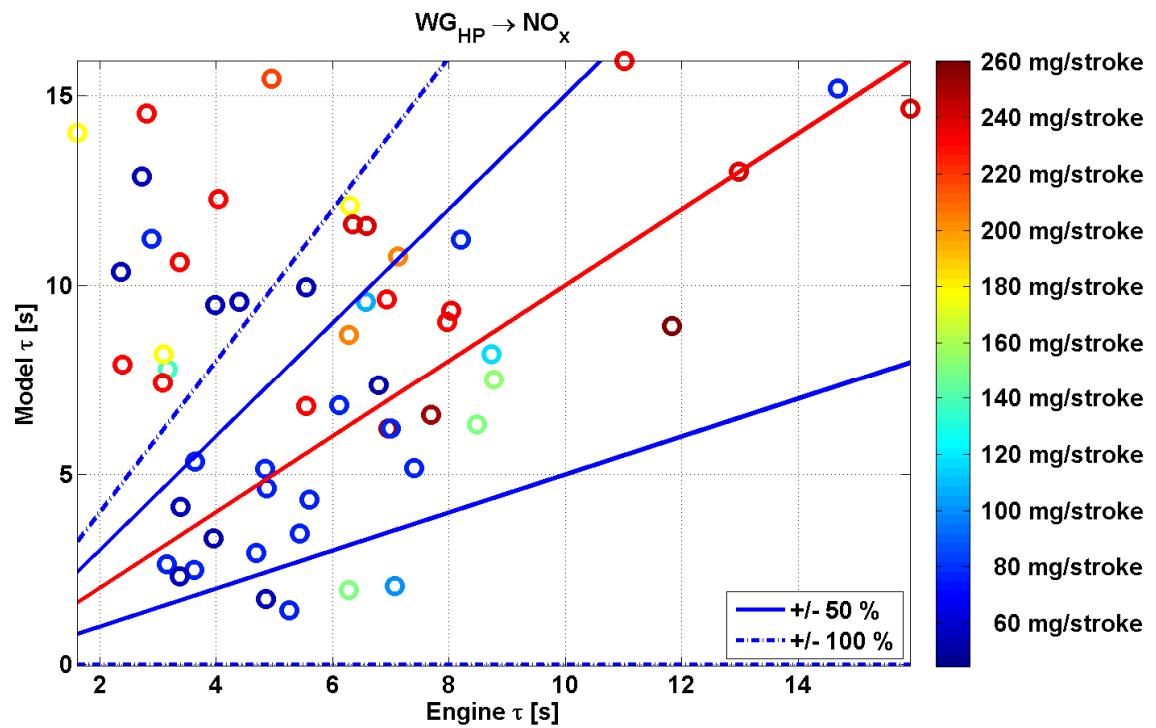


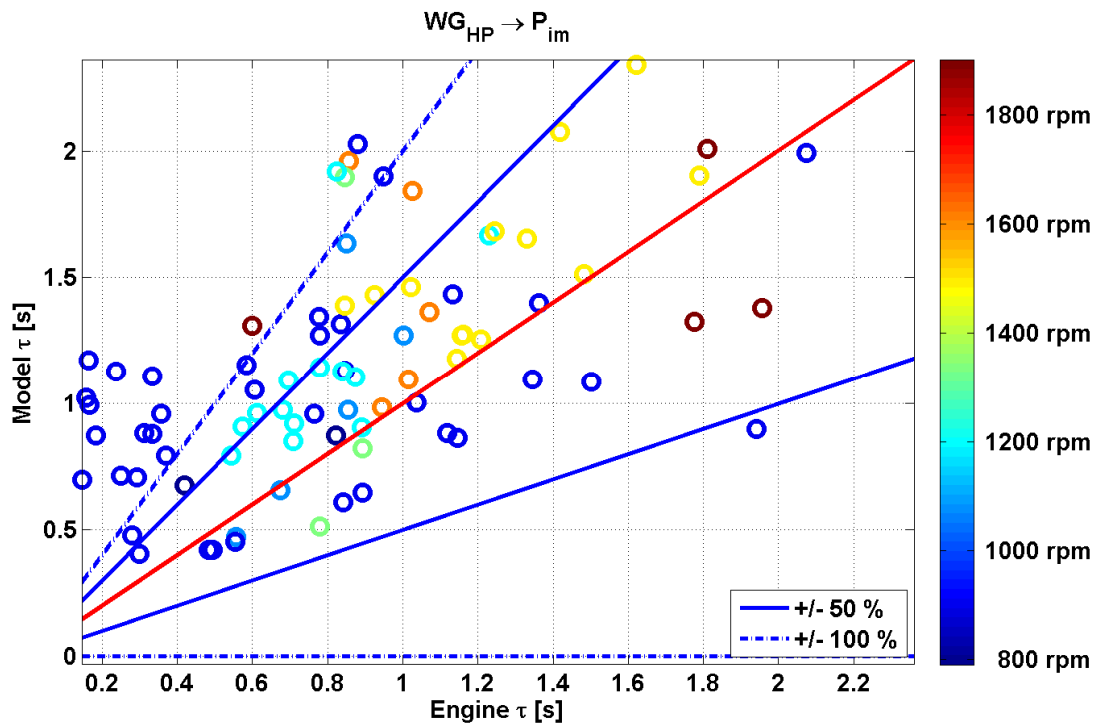
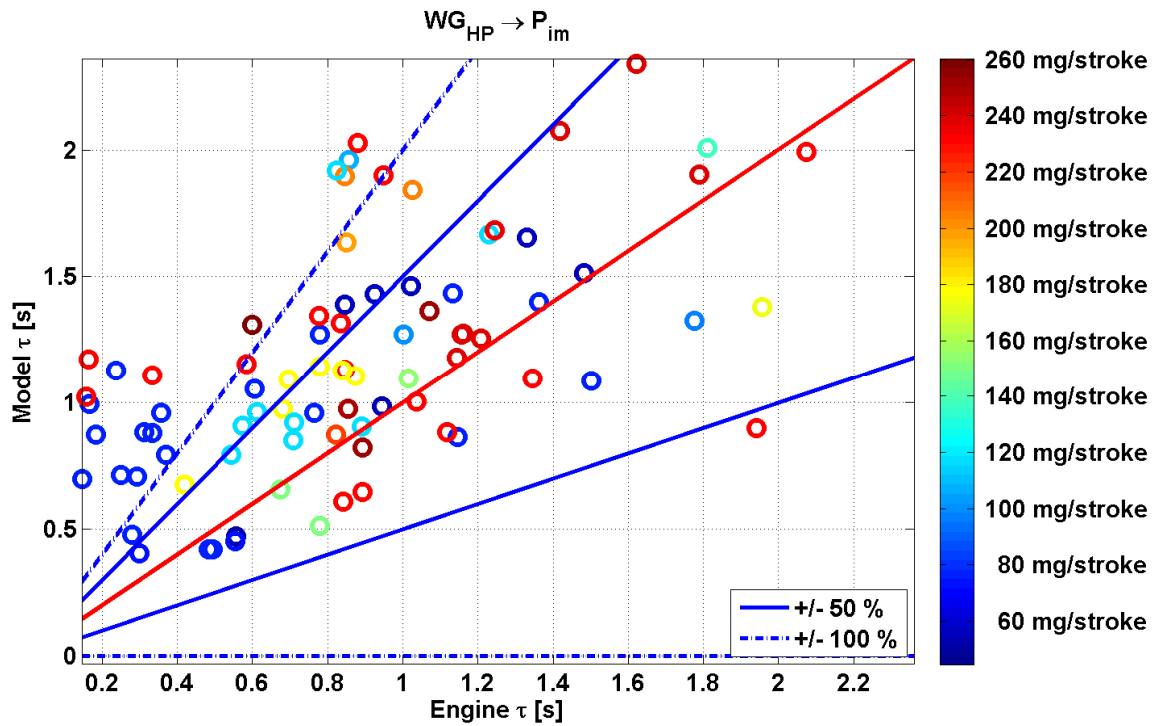


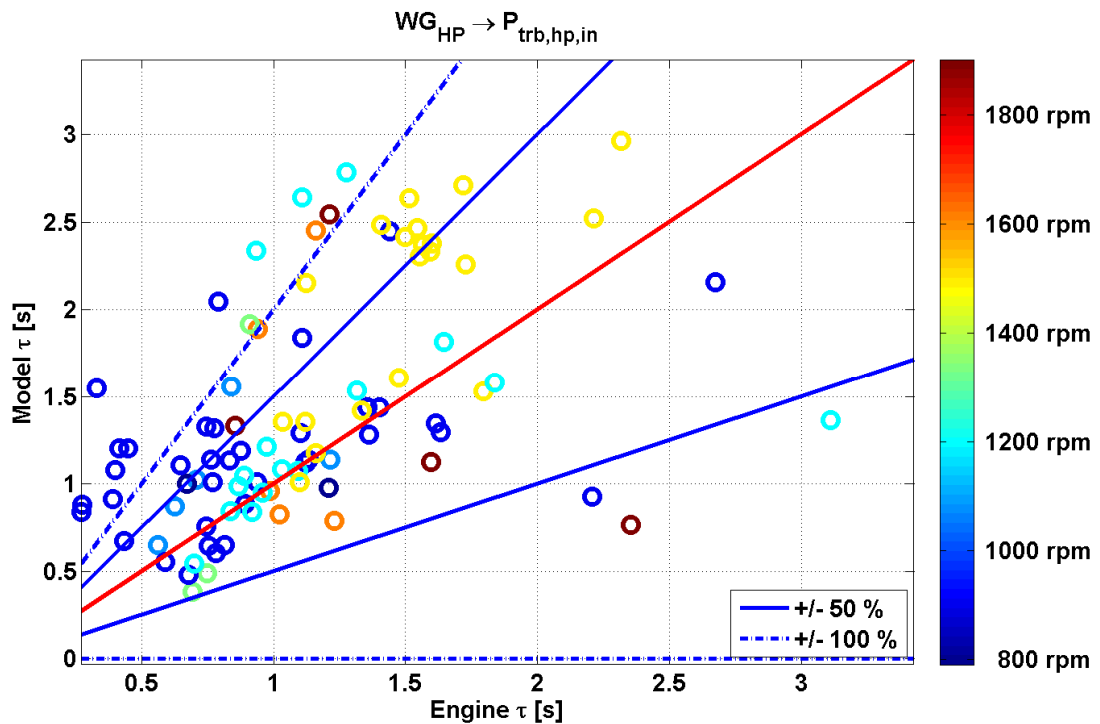
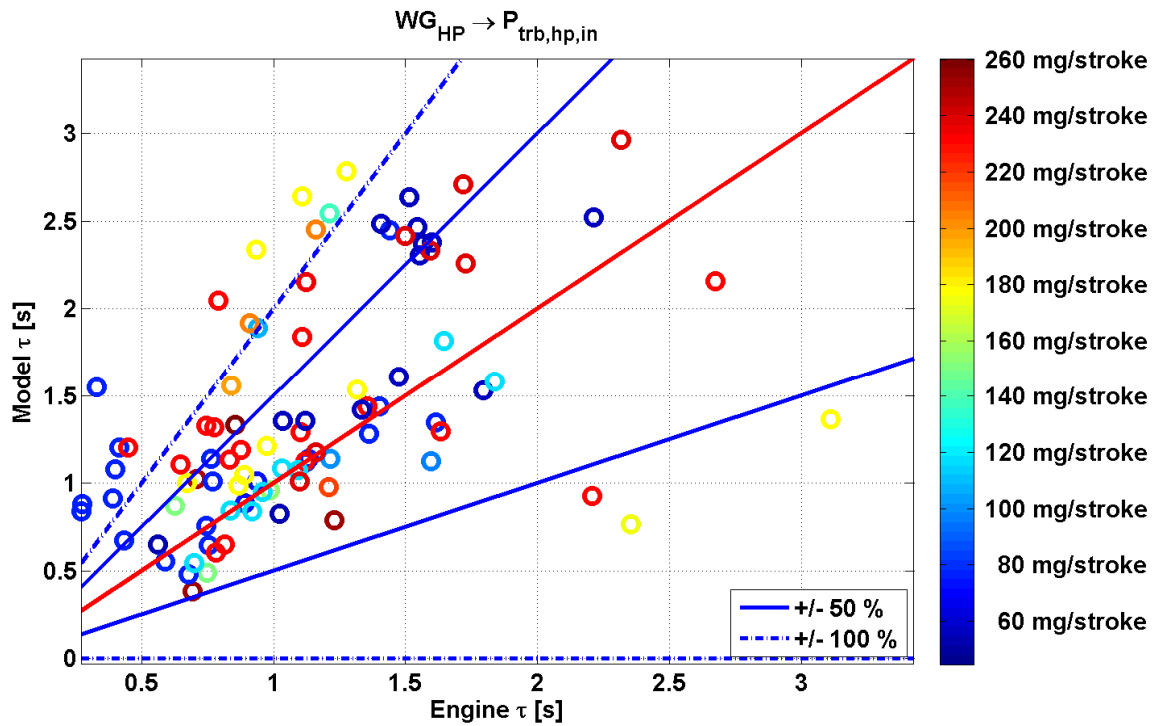


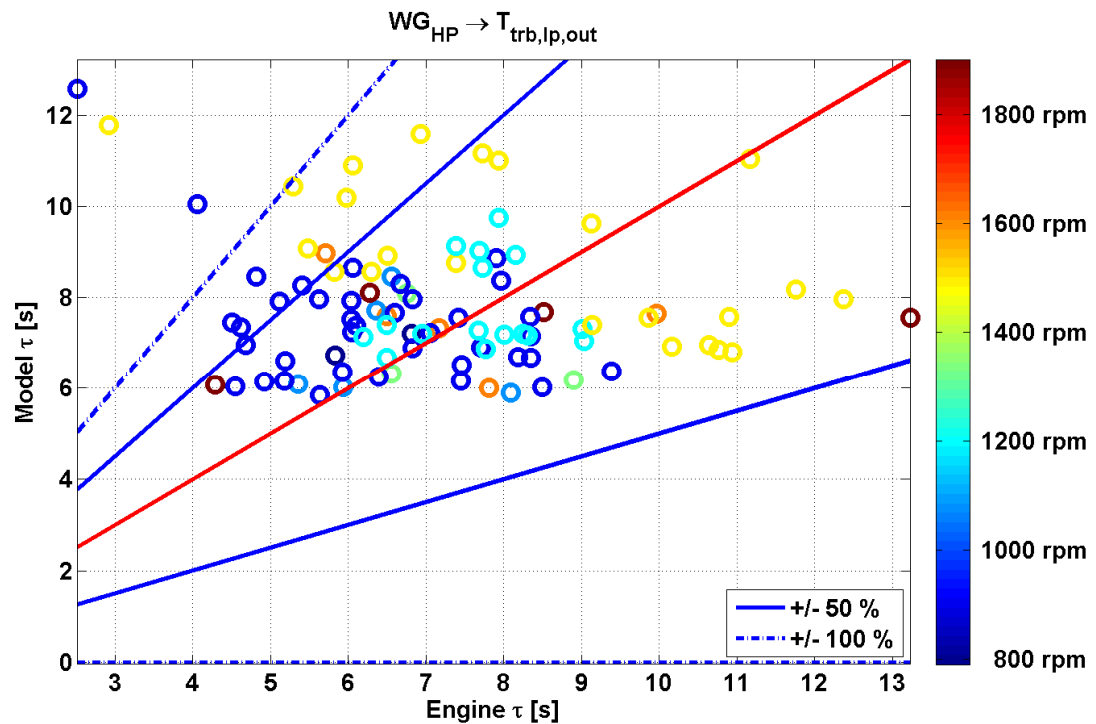
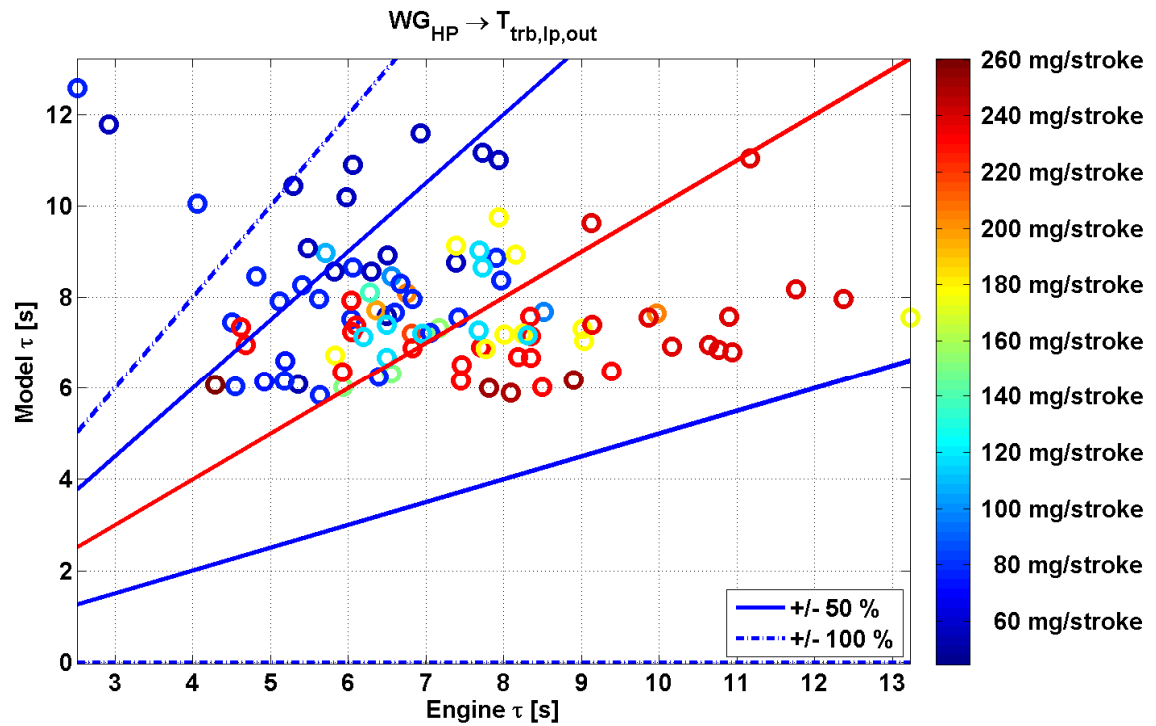








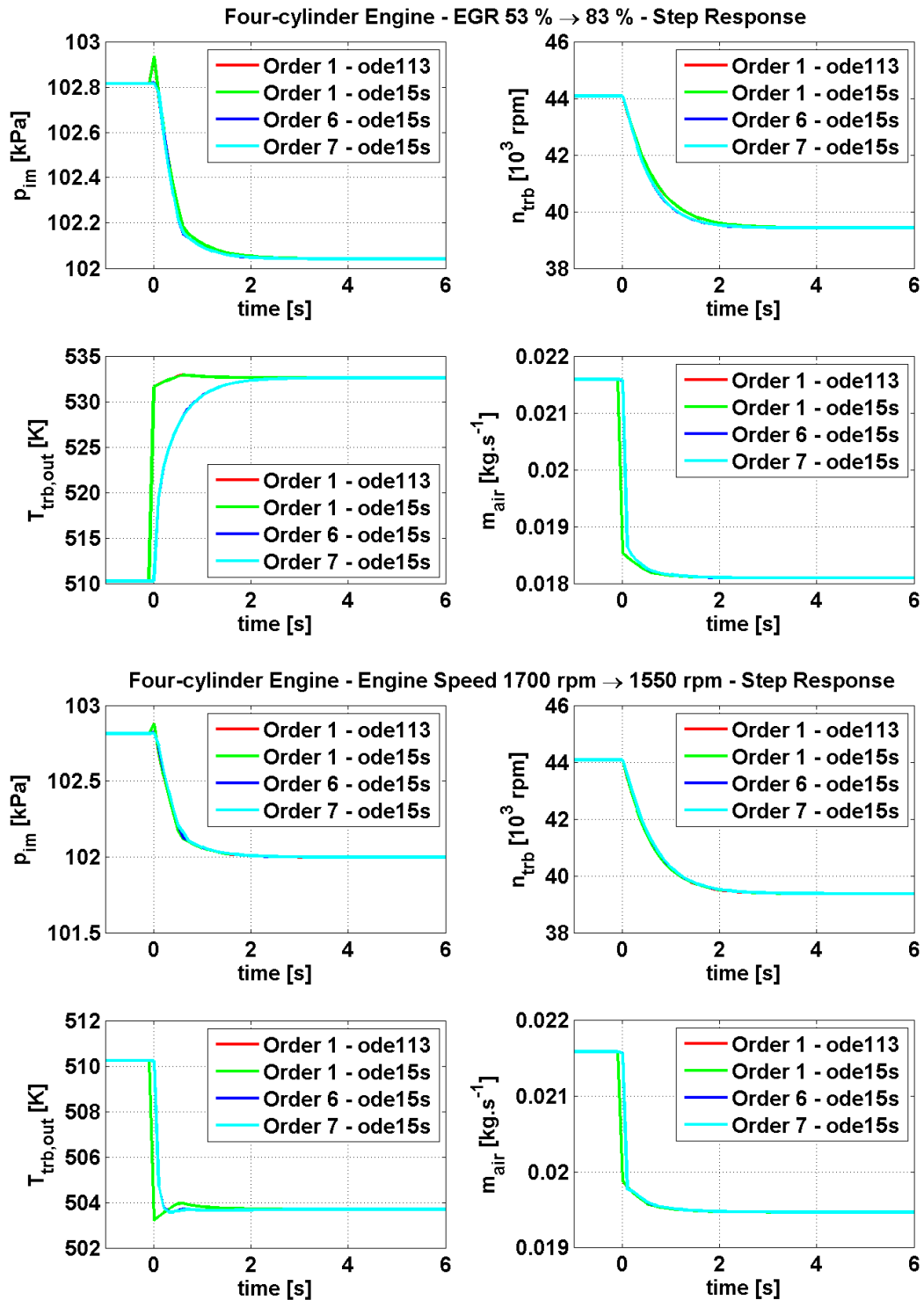




Appendix 8.1 is showing model verification results for the most important quantities with two different dependencies (engine speed and injection quantity).

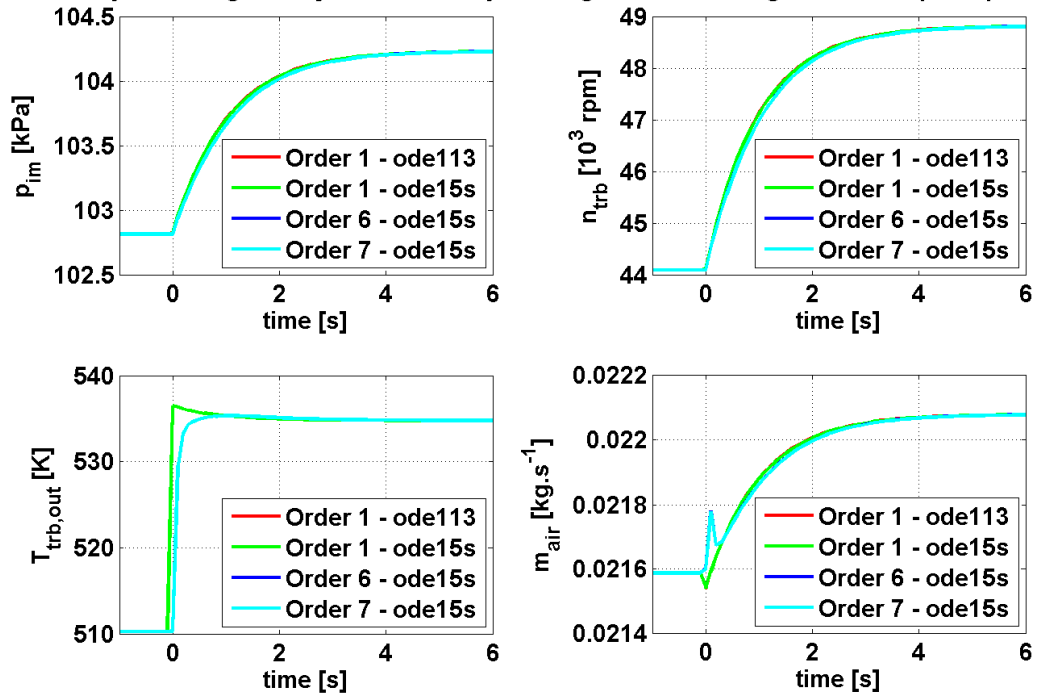


8.2. Four-cylinder Turbocharged Engine – Constrained State Reduction

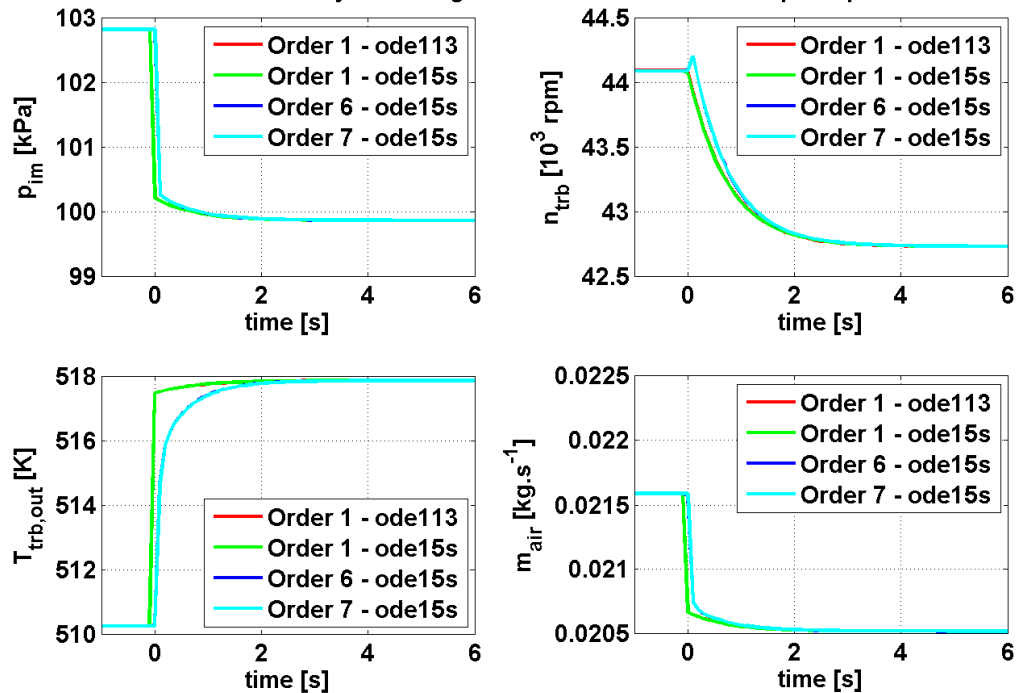


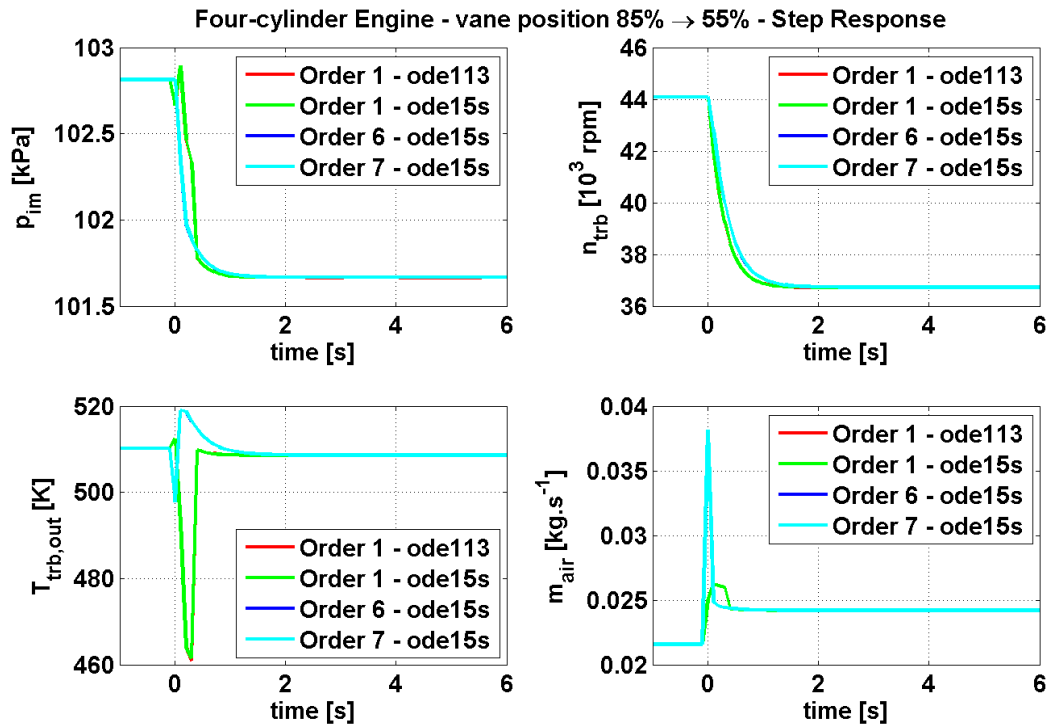


Four-cylinder Engine - Injection Quantity 13.4 mg/stroke \rightarrow 15 mg/stroke - Step Response



Four-cylinder Engine - TVA 100% \rightarrow 30% - Step Response

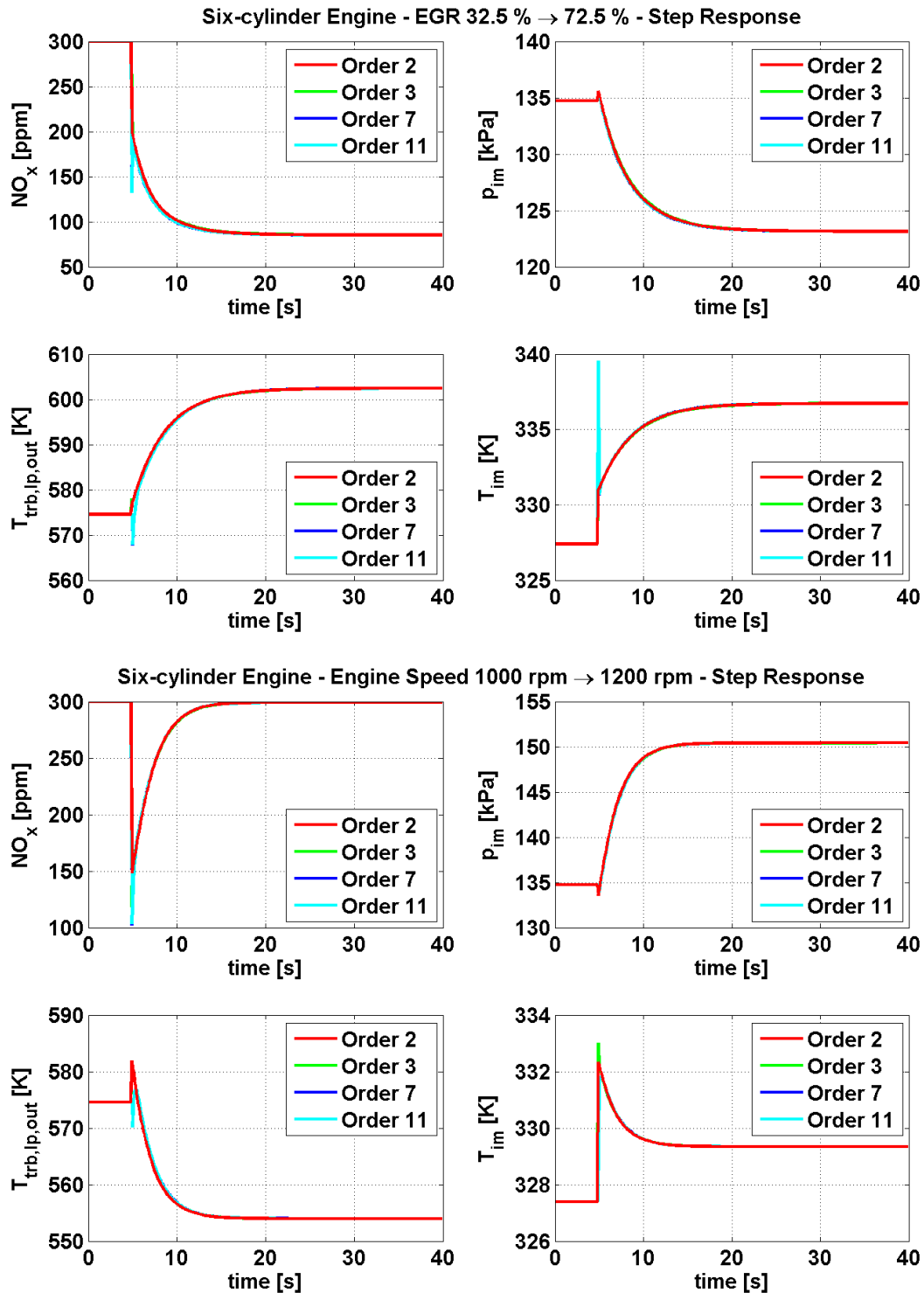


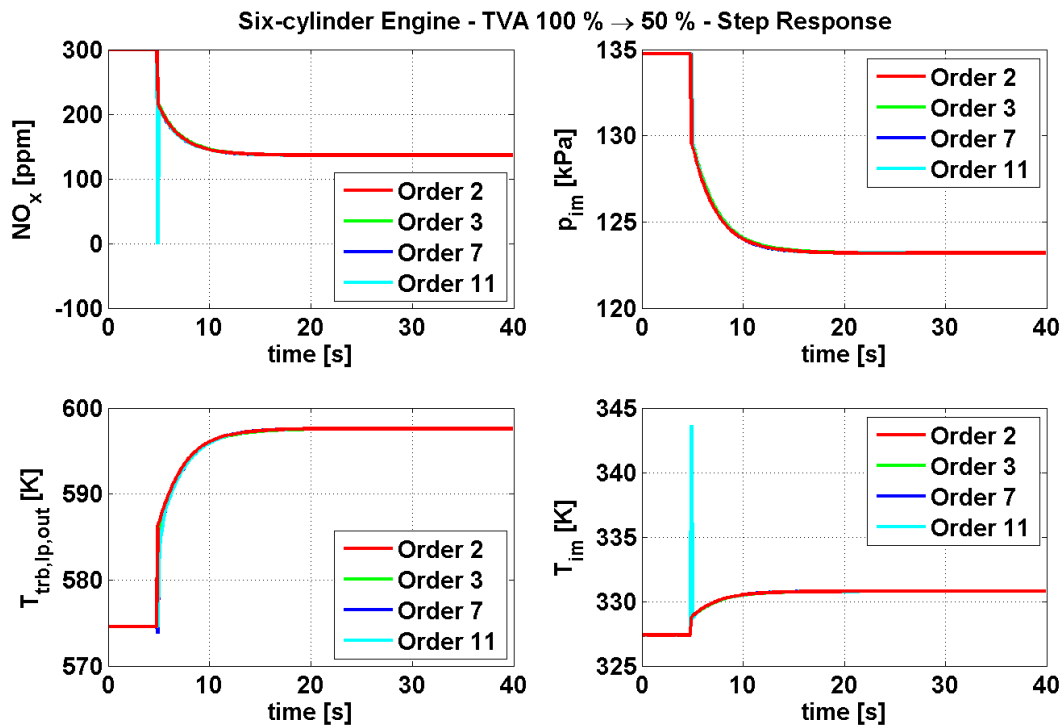
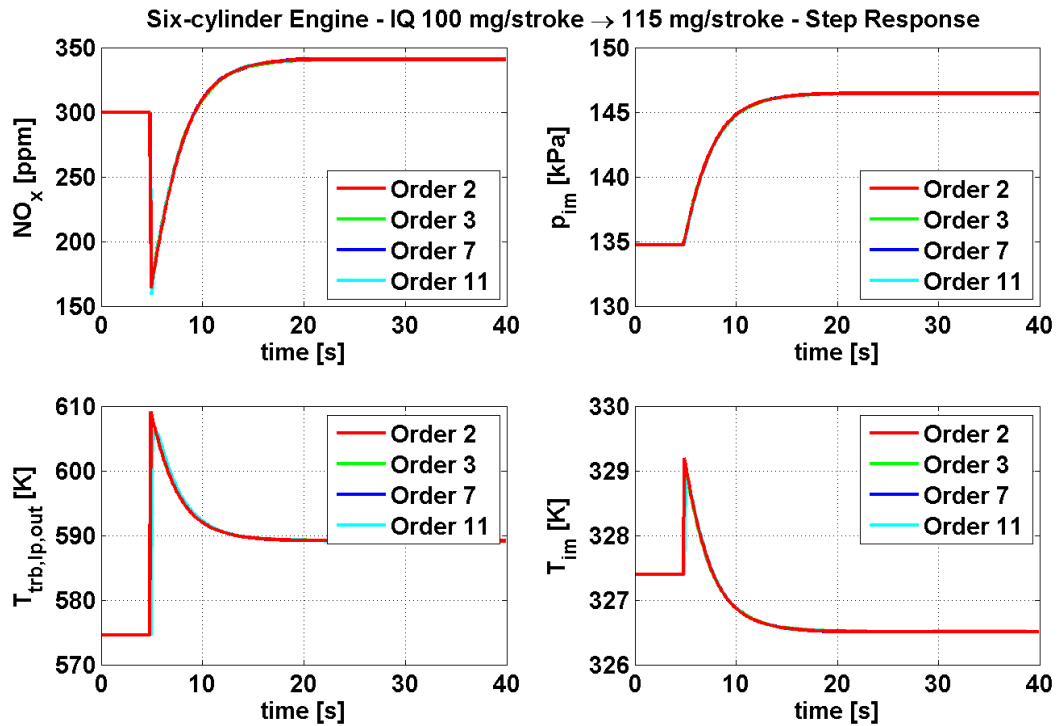


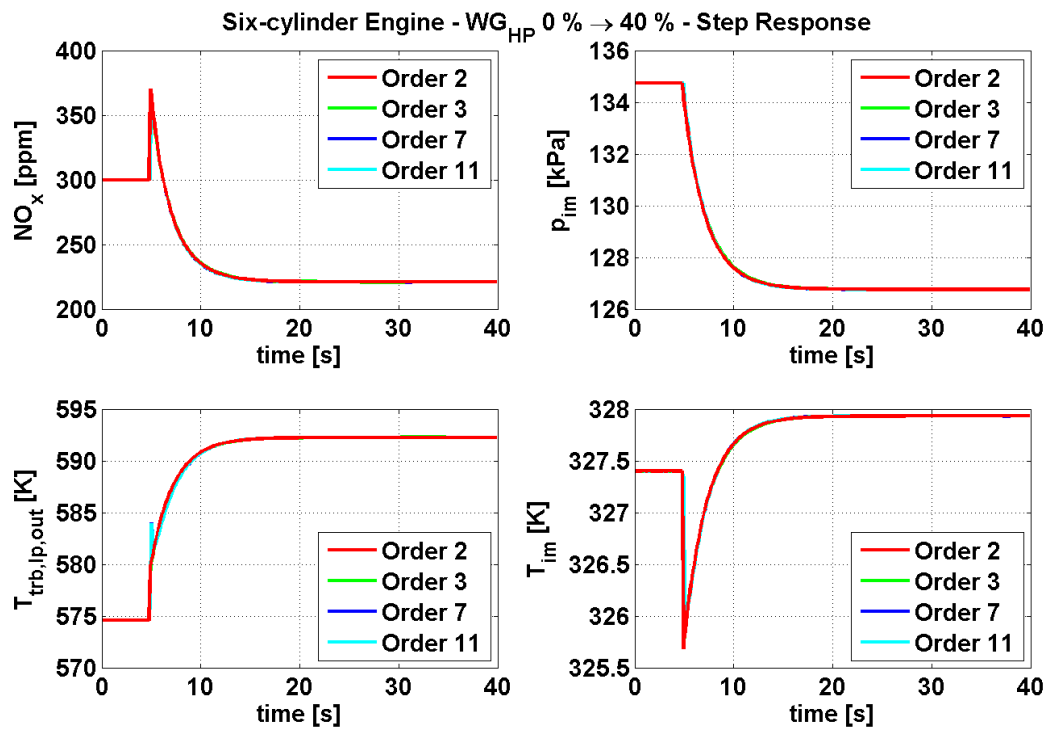
Appendix 8.2 is extending results of a constrained state reduction of the four-cylinder turbocharged engine for important step quantities. Peaks in the full order model are caused by step generation and they don't appear in the data from real engine.



8.3. Six-cylinder Bi-turbocharged Engine – Constrained State Reduction







Appendix 8.3 is extending results of a constrained state reduction of the six-cylinder bi-turbocharged engine for all important step quantities. Peaks in the full order model are caused by step generation and they don't appear in the data from real engine.